

Unfolding mechanism of soluble CLIC1

Jin-Lin, Wu

A dissertation submitted to the Faculty of Science, University of the Witwatersrand, Johannesburg, in fulfillment of the requirements for the degree of Master of Science

Johannesburg, 2012

Declaration

I declare that this dissertation is my own, unaided work. It is being submitted for the degree of Master of Science in the University of the Witwatersrand, Johannesburg. It has not been submitted for any other degree or examination at any other University.

Jin-Lin Wu

Jin-Lin, Wu

___18th___ day of ___January___, 2012

Abstract

CLIC1 is an intracellular membrane protein that has an unusual property distinct from typical membrane proteins. It is able to exist in both a soluble and membrane-bound form in cells. The membrane-insertion mechanism of soluble CLIC1 is still unknown. However, it has been proposed that soluble CLIC1 has to undergo unfolding and refolding processes to form its membrane-bound conformation. In this study, the focus is on the understanding of the unfolding mechanism of soluble CLIC1 under the pH values typical of the cytosol and the membrane surface. Equilibrium unfolding studies show that, at pH 7.0, CLIC1 unfolds via a two-state transition and the unfolding kinetics studies further confirms that there are no detectable transient intermediates. At pH 5.5, CLIC1 shows a three-state unfolding transition with a formation of an intermediate species at equilibrium in the presence of 3 ~ 4 M urea. The characterisation of this intermediate indicates that it has reduced secondary structural content and native-like tertiary structure with the exception of a more buried Trp35 when compared to the native state. Moreover, this intermediate has more exposed hydrophobic surface than the native state. The unfolding kinetics studies demonstrate that there are hidden intermediates in the native-to-unfolded transition at pH 5.5. The formation of the intermediate state involves, initially, a rapid partial unfolding followed by a slow repacking of the structure. The results from equilibrium unfolding and unfolding kinetics studies both suggest that the intermediate state is more stable than the native state at pH 5.5, indicating that under this condition, the stability of native CLIC1 is reduced and the intermediate is energetically favoured. The results from this study give information about the conformational stability and the different unfolding behaviours of soluble CLIC1 under the conditions that simulate the environments of the cytosol and the membrane surface, and further provide a possible interpretation for the *in vivo* membrane-insertion mechanism of the protein.

Acknowledgements

I wish to acknowledge my supervisor, Dr. Sylvia Fanucchi, for her support and guidance throughout my research. Her unflagging enthusiasm and dedication to the cause has been a source of strength and inspiration. In addition, special thanks are due to my co-supervisor, Professor Heini Dirr, who kept a close watch on proceedings and whose sometimes stern approach helped to keep me focused and engaged. I am also grateful to all of my colleagues in the Protein Structure Function Research Unit for their help and advice in the lab and for their great friendship.

Table of contents

Declaration.....	I
Abstract.....	II
Acknowledgements	III
Abbreviations	VI
List of figures.....	VII
List of tables.....	IX
1. Introduction.....	1
1.1. Protein folding.....	1
1.1.1. The protein folding mechanism	1
1.2. Unfolding of proteins	10
1.2.1. Equilibrium unfolding.....	10
1.2.2. Unfolding kinetics and unfolding pathways	13
1.3. Metamorphic proteins	20
1.4. Soluble proteins that insert into membranes.....	22
1.5. Chloride intracellular channels	23
1.6. Overview of CLIC1.....	24
1.6.1. Structure of soluble CLIC1	24
1.6.1.1. Primary sequence and secondary structure	24
1.6.1.2. Tertiary structure.....	26
1.6.2. The factors influencing CLIC1 membrane-insertion <i>in vitro</i>	29
1.6.2.1. Redox condition.....	29
1.6.2.2. The effect of pH.....	31
1.7. Objective	33
2. Experimental procedures	35
2.1. Materials	35
2.2. Methods.....	35
2.2.1. Expression and purification of recombinant CLIC1	35
2.2.2. Confirmation of protein purity	38
2.2.3. Determination of protein concentration	40
2.2.4. Structural characterisation of CLIC1	41
2.2.5. Urea-induced equilibrium unfolding.....	45
2.2.6. Unfolding kinetics	53
3. Results.....	56
3.1. CLIC1 expression and purification.....	56
3.2. Structural characterisation of CLIC1.....	61

3.3. Urea-induced equilibrium unfolding.....	65
3.3.1. Recovery studies.....	65
3.3.2. Effect of pH on the conformational stability of CLIC1.....	67
3.3.3. Structure of the intermediate.....	72
3.4. Unfolding kinetics	77
4. Discussion.....	86
4.1. A stable equilibrium intermediate state of CLIC1 is formed at pH 5.5	86
4.2. Unfolding of CLIC1	89
4.2.1. The appearance of hidden intermediates in the N → U transition.....	90
4.2.2. The equilibrium intermediate is more stable than the native state at pH 5.5	90
4.2.3. Formation of the equilibrium intermediate.....	91
4.2.4. Unfolding pathway of CLIC1	94
4.3. Proposed CLIC1 insertion mechanism	96
4.4 Conclusions.....	99
5. References.....	101

Abbreviations

A_{260}	Absorbance at 260 nm
A_{280}	Absorbance at 280 nm
Å	Ångström
ANS	8-anilino-1-naphthalene sulfonate
CD	Circular dichroism
CLIC	Chloride intracellular channel
C_m	The denaturant concentration at which the native and the unfolded species are equally populated
cm	centimeter
DEAE	Diethylaminoethyl
DTT	Dithiothreitol
ΔG	Change in Gibbs free energy
$\Delta G(H_2O)$	Change in Gibbs free energy between native state and unfolded state in the absence of denaturant in equilibrium unfolding studies
ϵ_{280}	Molar extinction coefficient at 280 nm
E_{222}	CD ellipticity measured at 222 nm
F_{310}	Fluorescence intensity at 310 nm
F_{345}	Fluorescence intensity at 345 nm
Far-UV CD	Far-ultraviolet circular dichroism
GSH	Reduced glutathione
GST	Glutathione transferase
I	Intermediate state
IAEW	Intensity averaged emission wavelength
IPTG	Isopropyl β -D-thiogalactopyranoside
kDa	kilodalton
M	Molar
N	Native state
OD_{600}	Optical density at 600 nm
PDB	Protein Data Bank
pI	Isoelectric point
rpm	Revolutions per minute
SDS-PAGE	Sodium dodecyl sulfate polyacrylamide gel electrophoresis
U	Unfolded state

List of figures

Figure 1: Representative protein folding funnels.....	2
Figure 2: Different states that a polypeptide chain can form	8
Figure 3: Amino acid sequence and secondary structural elements of CLIC1	25
Figure 4: Crystal structure of soluble reduced CLIC1	27
Figure 5: Structure of dimeric oxidised CLIC1	30
Figure 6: SDS-PAGE gels illustrating a representative purification process of CLIC1..	57
Figure 7: Calibration curve obtained from the SDS-PAGE gel.....	59
Figure 8: Absorbance spectrum of purified CLIC1.....	60
Figure 9: Comparison of the circular dichroism spectra of CLIC1 at pH 7.0 and pH 5.5	62
Figure 10: Comparison of the fluorescence spectra of CLIC1 at pH 7.0 and pH 5.5.....	64
Figure 11: Recovery of secondary and tertiary structure of CLIC1.....	66
Figure 12: Equilibrium unfolding of CLIC1 at pH 7.0 and pH 5.5.....	68
Figure 13: Fractional populations plot of CLIC1 as a function of urea concentrations at pH 5.5	71
Figure 14: Comparison of CD spectra of the native and the intermediate state.....	73
Figure 15: Comparison of tryptophan fluorescence spectra of the native and the intermediate state of CLIC1	74
Figure 16: ANS binds to the intermediate state of CLIC1	76

Figure 17: Representative unfolding kinetic traces for the N → U transition at pH 7.0 and pH 5.5.....	78
Figure 18: Urea dependence of the unfolding rate constants.....	79
Figure 19: Representative unfolding kinetic traces of CLIC1 from the N → I transition at pH 5.5.....	83
Figure 20: Representative unfolding kinetic traces of the I → U transition	85
Figure 21: Proposed unfolding pathway of CLIC1.....	95
Figure 22: Proposed membrane insertion model of CLIC1.....	97

List of tables

Table 1: List of diseases caused by protein misfolding and the related proteins and peptides	7
Table 2: Comparison of the thermodynamic parameters obtained from the equilibrium unfolding studies at pH 7.0 and pH 5.5	69
Table 3: Parameters of the unfolding kinetics of CLIC1 at pH 7.0 and pH 5.5	80

1. Introduction

1.1. Protein folding

Proteins are the molecules that are necessary for various biological activities and diverse physiological processes. After synthesis in the ribosomes, long polypeptide chains need to be converted into specific native three-dimensional conformations in order to conduct their functions. This process is called protein folding. Since the function of a protein is determined to a large extent by its native structure, the failure of proteins to fold correctly is often the cause of disorders. These diseases such as Alzheimer's disease are the result of misfolding and aggregation of certain proteins (reviewed by Ecroyd and Carver, 2008). Therefore, the study of protein folding is critical for getting insight into the correct folding mechanism. Only when we understand the folding mechanism, will we be able to know how a protein acquires its native structure and performs its biological function. An understanding of protein folding also allows us to reveal the pathogenic mechanism of various misfolding disorders and further to seek the cure for these diseases.

1.1.1. The protein folding mechanism

Energy landscape theory

Many different models have been used to explain the protein folding mechanism (Chan *et al.*, 1995; Dobson and Karplus, 1999; Rumbley *et al.*, 2001; Clark, 2004). Subsequently, a general theory was developed in an attempt to explain all of the current folding models (reviewed by Dobson, 2004). This theory uses an energy landscape to describe the protein folding process. An energy landscape used to indicate protein folding generally has a funnel-like shape with a wide top and a minimum point, and is therefore called a protein folding funnel (Figure 1). The x-axis of the funnel represents the conformational entropy of a polypeptide chain. The y-axis is the free energy associated with the stabilisation of the

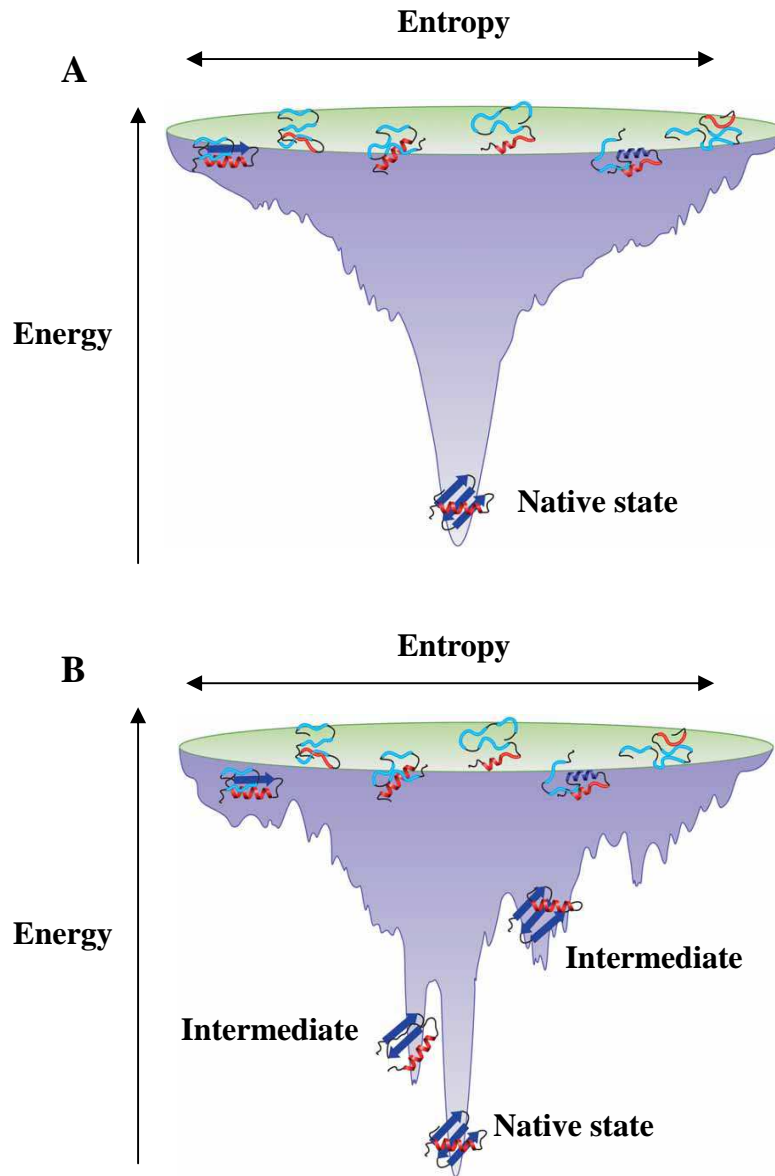


Figure 1: Representative protein folding funnels

Unfolded proteins can exist in different random structures. The width of the protein folding funnels represents the conformational entropy. The depth represents the free energy of the current structure of the polypeptide chain. As the unfolded proteins fold, they follow the landscape downwards as their structures assume lower energy conformations. This process terminates with the formation of structures with the lowest energy (the native states). **(A)** represents a smooth folding landscape without any stable intermediates. **(B)** represents a more complicated folding landscape with existence of intermediates. This figure was obtained from Bartlett and Radford, 2009.

polypeptide chain. An unfolded polypeptide chain is able to exist in a large number of different low-energy conformations that can transform between each other rapidly, and thus the top of the folding funnel is wide. The correct (native-like) interactions between residues are relatively more stable than the incorrect (non-native) interactions and thus finally lead the polypeptide chain to fold along the funnel to the structure with the lowest free energy at the minimum of the funnel (Dobson, 2004).

The presence or absence of local energy minima results in the ruggedness of energy landscapes. For some small proteins, the energy landscape might be relatively smooth (Figure 1A). However, the energy landscapes of larger proteins are often rugged and have local minima (Figure 1B). This phenomenon may explain why protein folding is so complex. Since a folding funnel is three-dimensional and polypeptide chains are able to fold along the folding funnel to the lowest energy point of the folding funnel from different start points, each protein molecule is able to follow different routes to the native state depending on environmental conditions and thus different structures can be formed from different native-like interactions among residues along the folding pathway (Szilágyi *et al.*, 2007).

Since some routes are smooth and the others are bumpy, the route which a polypeptide chain takes has an influence on its folding rate. An energy barrier, known as the transition state, is defined as the energy peak in the folding pathway between the native and unfolded states that proteins need to overcome (Onuchic *et al.*, 1996 and 1997; Onuchic and Wolynes, 2004). There can be many energy barriers along a single folding pathway, however, the transition state corresponds to the energy barrier with the highest activation energy and thus will be the main rate-limiting step of the overall reaction (Daggett and Fersht, 2000). Different obstacles along different folding routes result in local rate-limiting steps in the folding of a protein. For example, a folding protein trapped in a local energy landscape minimum has an energy

barrier to overcome before it can fold to the native state. The obstacles for protein folding do not only come from energy barriers but also from entropic barriers. For example, random search for stable interactions or structures to continue the folding process can also be rate-limiting (Dill and Chan, 1997). Proline *cis-trans* isomerisation and the formation of disulfide bonds in proteins are also causes of slow processes in protein folding. These two mechanisms will be discussed later on.

Folding intermediates

The energy landscape for small proteins (less than 100 residues) is often smoother than for large proteins and thus the small proteins often fold following a two-state process without formation of any intermediate states (Jackson, 1998). In contrast, proteins with more than 100 residues generally fold along pathways that involve the population of intermediate species under certain conditions such as high salt concentration or low pH (Dobson *et al.*, 1998; Fersht, 1999). As mentioned previously, the transition state is the main energy barrier to the overall folding process. The ensemble of all intermediate states (both transient and equilibrium intermediates) on-pathway to the native state can be seen as the transition state of the overall folding reaction (Dobson and Karplus, 1999).

It has been shown that intermediate species formation can either accelerate or slow down the protein folding processes depending on whether they are formed before or after the rate-limiting step on the folding pathway (Ellison and Cavagnero, 2006; reviewed by Udgaonkar, 2008). The intermediate states that are required to lead proteins to fold to the native state are so called “on-pathway” intermediates. If these on-pathway intermediates form after the rate-limiting step, their conformations involving critical interactions are able to facilitate protein folding by reducing the numbers of possible structures available to the folding protein (Rami and Udgaonkar, 2002). Moreover, sometimes point mutations in

proteins can block the formation of stable intermediate states and thus interrupt the normal protein folding causing diseases (Bychkova and Ptitsyn, 1995; Ptitsyn *et al.*, 1995).

A certain distinctive intermediate state has been identified in many different proteins. It has common features described as well-packed secondary structures with flexible side chains and exposed hydrophobic cores. This protein conformation was named the “molten globule” by Ohgushi and Wada in 1983 (Ohgushi and Wada, 1983). In 1985 and 1986, the molten globule state of α -lactalbumin was shown to be identical to its transient folding intermediate by Kuwajima *et al.*, 1985 and Ikeguchi *et al.*, 1986. After this, the molten globule state has been thought to be a common folding intermediate state in numerous proteins (Kuwajima, 1989; Ptitsyn, 1995; Arai and Kuwajima, 2000). However, not all the molten globule states are related exclusively to the protein folding process. Some molten globules are involved in specific biological processes such as membrane insertion (Van der Goot *et al.*, 1991), transmembrane trafficking (Hartl *et al.*, 1994) and chaperone-assisted refolding (Kuwajima and Arai, 2000)

Despite the intermediate states which lead proteins to fold, some intermediate structures which accumulate during the folding reaction are not necessary for protein folding and in many cases actually impede the process. These intermediate states are usually misfolded structures “trapped” in the local minima of the folding funnel and require complete or, at least, partial unfolding to be corrected and continue folding to the correct native state (Evan *et al.*, 2005). This kind of intermediate state is called “off-pathway”. It has been shown that these transient off-pathway intermediate species are able to cause various diseases which result from protein misfolding (reviewed by Santucci *et al.*, 2008).

Protein misfolding

As mentioned in the beginning of this chapter, it is necessary for proteins to have the correct structures, and retain the correct conformations in order to function. Furthermore, it has been shown that failures in protein folding are strongly correlated with various human diseases (Dobson, 2003 and 2004). These diseases are so-called “conformational” or “misfolding” diseases. Some of these diseases simply result from the fact that misfolded proteins cannot function properly. In other cases, the diseases are caused by the formation of misfolded aggregates that are toxic to the cell. A summary of misfolding disorders and the related proteins or peptides is shown in Table 1.

The causes of protein misfolding include amino acid composition and environmental conditions. Certain mutations are also known to induce misfolding. Protein misfolding is dependent on the environmental conditions (reviewed by Herczenik and Gebbink, 2008). Specific conditions such as extreme pH, increased temperature, agitation, elevated glucose, and oxidative agents are able to destabilise the native protein conformation and further cause the unfolding or partial unfolding of the proteins. As seen in Figure 1, the unfolded state has a high free energy and is thus thermodynamically unstable and unfavourable. Therefore, unfolded proteins are prone to form aggregates in order to lower the free energy.

The possible fates of a polypeptide chain are demonstrated in Figure 2. It is possible for a polypeptide chain to form aggregates from every structural state depending on the environment. Furthermore, there are certain factors that serve as precursors for the initiation of aggregation processes such as exposed hydrophobic segments on proteins, β -sheet content, low net charge (Linding *et al.*, 2004) and peptide segments from incomplete/incorrect proteolysis (Stix *et al.*, 2001) or partial unfolded structures such as off-pathway intermediates (Laidman *et al.*, 2006).

Table 1: List of diseases caused by protein misfolding and the related proteins and peptides

Disease	Associated proteins	Affected tissues
Amyloidosis – systemic		
Primary systemic amyloidosis	Ig light chain	Most tissues
Ig heavy-chain-associated amyloidosis	Ig heavy chain	Most tissues
Secondary (reactive) systemic amyloidosis	SAA	Most tissues
Senile systemic amyloidosis	Transthyretin	Microvasculature
Hemodialysis-related amyloidosis	β_2 – Microglobulin	Osteoarticular tissues
Hereditary systemic ApoAI amyloidosis	ApoAI	Liver, kidney, heart
Hereditary systemic ApoAII amyloidosis	ApoAII	Kidney, heart
Finnish hereditary amyloidosis	Gelsolin	Most tissues
Hereditary lysozyme amyloidosis	Lysozyme	Kidney, liver
Hereditary cystatin C amyloid angiopathy	Cystatin C	Most tissues
Amyloidosis – localised		
Injection-localised amyloidosis	Insulin	Skin, muscles
Hereditary renal amyloidosis	Fibrinogen	Kidney
Senile seminal vesicle amyloid	Lactoferrin, seminogelin	Seminal vesicles
Familial subepithelial corneal amyloidosis	Lactoferrin	Cornea
Cataract	Crystallin	Eye
Medullary thyroid carcinoma	Calcitonin	Thyroid tissues
Neurodegenerative diseases		
Alzheimer's disease	Amyloid- β , tau	Brain
Parkinson's disease	α -Synuclein	Brain
Lewy-body dementia	α -Synuclein	Brain
Huntington's disease	Huntington	Brain
Spongiform encephalopathies	Prion	Brain, peripheral nervous system
Hereditary cerebral hemorrhage with amyloidosis	Cystatin C	Cerebral vasculature
Amyotrophic lateral sclerosis	Superoxide dismutase 1	Brain
Familial British dementia	Abri	Brain
Familial Danish dementia	ADan, amyloid- β	Brain
Familial amyloidotic polyneuropathy	Transthyretin	Peripheral nervous system
Frontotemporal dementias	Tau	Brain
Other diseases		
Diabetes mellitus	IAPP, amylin	Pancreas (islet)
Atherosclerosis	Modified LDL	Arteries
Sickle cell anemia	Hemoglobin	Erythrocytes

This table was obtained from Herczenik and Gebbink, 2008.

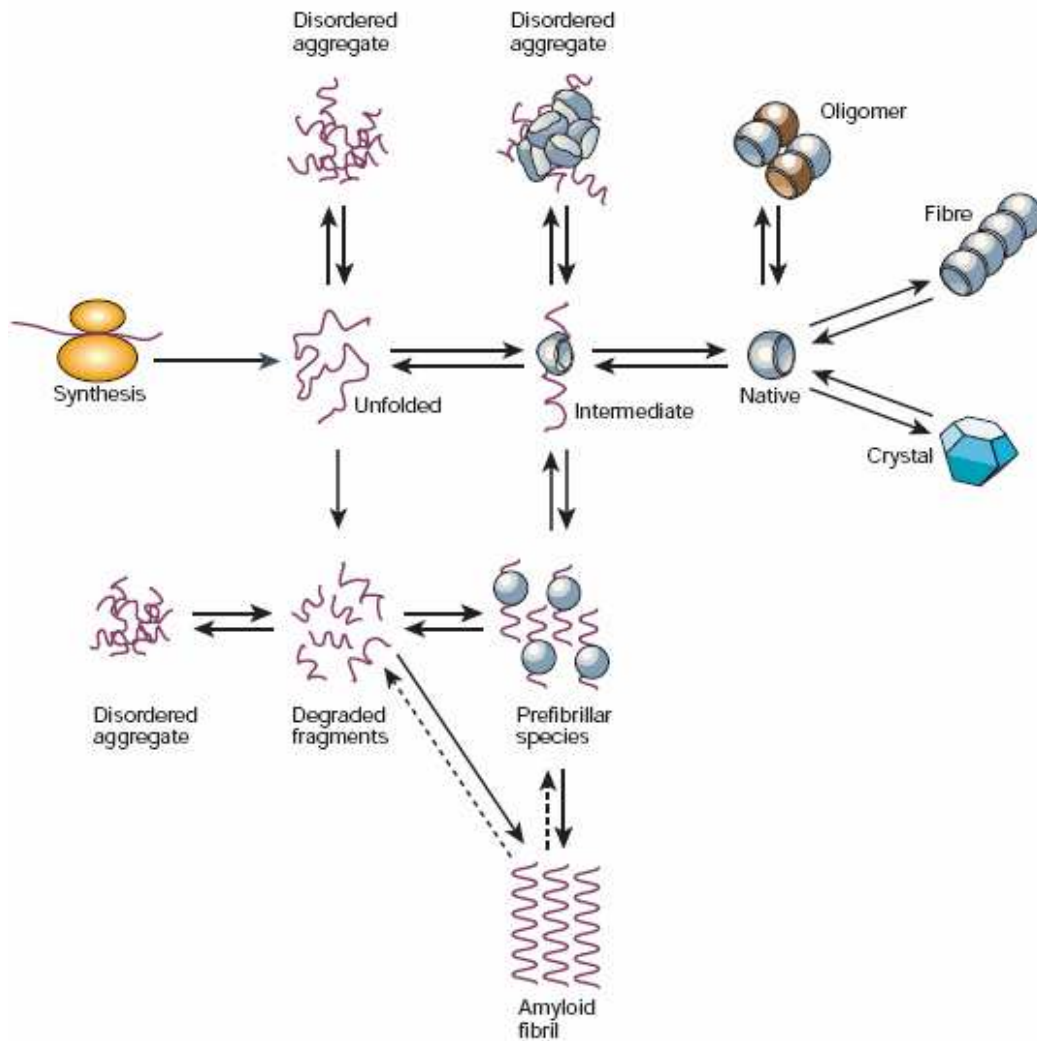


Figure 2: Different states that a polypeptide chain can form

After synthesis on ribosomes, a polypeptide chain is able to fold to its monomeric native structure, with or without involvement of partially folded intermediates. It can also experience different fates such as aggregation, amyloid formation and degradation. Native protein fibres, functional oligomers and protein crystals produced *in vitro* for X-ray diffraction structural studies are all formed by association of the monomers of native structures. The interconversion and population of different states depends on the thermodynamic and kinetic stabilities under different environmental conditions. This figure was obtained from Dobson, 2003.

There are three kinds of protein forms that are related to misfolding disorders: soluble oligomers, amorphous aggregates and amyloid fibrils. The factors that determine whether a protein forms amyloid fibrils, amorphous aggregates or soluble oligomers during the aggregation process are the amino acid sequence of the protein and the environmental conditions (reviewed by Uversky and Fink, 2004). Soluble oligomers are often precursors for the formation of amorphous aggregates and amyloid fibrils. Amorphous aggregates refer to the aggregated proteins that do not form locally ordered structure. In contrast with amorphous aggregates, amyloid fibrils have a highly organised, long unbranched structure that resembles a hollow tube. Different from other naturally occurring biological fibrils which often contain helices, amyloid fibrils formed from different proteins share a common cross- β secondary structure (Meredith, 2005; reviewed by Herczenik and Gebbink, 2008). These tubular structures are normally formed by two to six “protofilaments” twisting around one another. The formation of amyloid fibrils involves interactions between different polypeptide main chains and the whole structure is mainly stabilised by hydrogen bonds (Dobson, 2004). Although the amyloid fibril is only one of the various aggregation types, it bears a significant feature. Since the structure of amyloid fibril is highly organised, it has unique kinetic stability compared to the other kinds of aggregate (Dobson, 2003). Such aggregates are able to persist for long periods of time in cells instead of being degraded by proteosomes. This further allows the formation of additional amyloid deposit in different tissues. In fact, they can even induce the conversion of the same protein into amyloid fibrils (Dobson, 2003). Since it has unique properties and it is involved in pathogenesis of various disorders, amyloid fibrils have been the most extensively studied among the three types of aggregation.

1.2. Unfolding of proteins

Despite the fact that protein folding is essential for proteins to perform their activities, the unfolding of many proteins is also an important physiological process and may be needed for their complete function (reviewed by Fersht and Daggett, 2002). For example, unfolding is important for protein degradation via the proteasome (Baumeister *et al.*, 1998). In addition, transient unfolding is also an important process to facilitate soluble proteins that lack a leader sequence to insert into membranes post-translationally (reviewed by Zakharov and Cramer, 2002; reviewed by Matouschek, 2003). Moreover, natively unfolded proteins exist that are functional in their unfolded states because their highly flexible conformations allow a more efficient interaction between them and their several different targets (Wright and Dyson, 1999; Dunker *et al.*, 2001; reviewed by Uversky, 2002). Also, as mentioned previously, the unfolding process is sometimes related to certain protein misfolding diseases where partially unfolded intermediate states of certain proteins are the main cause of these diseases (reviewed by Dobson, 2004; Ecroyd and Carver, 2008). Since protein unfolding is involved in various important biological processes, both functional and disease-causing, the unfolding of proteins is often studied to acquire more information about the mechanism of action of these proteins or in order to understand the pathogenesis of various diseases and to develop therapies for these disorders.

The unfolding mechanism of a protein can be observed experimentally in two ways either via equilibrium unfolding or via unfolding kinetics.

1.2.1. Equilibrium unfolding

Equilibrium unfolding is a method used to study protein unfolding. The native state of a protein exists in equilibrium with the unfolded state. Simply changing in the environment to

perturb this equilibrium can cause it to shift so that one state becomes more or less populated than the other. In this method, protein can be unfolded with different concentrations of denaturant, different temperature or different pH. Since equilibrium unfolding involves thermodynamic measurements, it is essential that the unfolding reaction is allowed to reach equilibrium before measurements are taken and that the unfolding reaction is reversible (Pace *et al.*, 1989). The equilibrium unfolding of a protein is often monitored using more than one technique such as circular dichroism and fluorescence spectroscopy as probes, which allows for the detection of changes in different aspects of the structure as a function of denaturation. An unfolding curve can then be constructed by plotting the collected data from different probes against different denaturant concentrations. Generally, an unfolding curve has a single or a multiple sigmoidal shape.

Equilibrium unfolding curves can be analysed by fitting them to either a two-state or a multi-state-state model (Pace, 1986). A two-state mechanism is described as:



where N and U represent the native and the unfolded species respectively, which are populated at equilibrium during unfolding. In this mechanism, the unfolding of a protein is assumed to occur in a single step without any equilibrium intermediates. If an unfolding curve does not show a single sigmoidal transition or if data monitored using different probes do not superimpose, especially in the transition region, the unfolding reaction does not fall into the two-state category (Pace *et al.*, 1989), and the curve would be better fitted to a three-state or a multi-state model as follows:



where I^* represents one or more intermediate(s) populated at equilibrium.

From the analysis of an unfolding curve, two important thermodynamic parameters can be obtained: the free energy change in the absence of denaturant, ($\Delta G(\text{H}_2\text{O})$) and the m -value (Pace, 1986). The free energy change, ΔG , at any denaturant concentration shows a linear dependence on denaturant concentration. Therefore, $\Delta G(\text{H}_2\text{O})$ can be obtained using the linear extrapolation method (Greene and Pace, 1974) to track the ΔG back to zero denaturant concentration as shown in the following equation:

$$\Delta G = \Delta G(\text{H}_2\text{O}) - m [\text{denaturant}] \quad (1)$$

The free energy change in the absence of denaturant, $\Delta G(\text{H}_2\text{O})$, is an estimate of the conformational stability of the protein, i.e. how stable the native state of the protein is compared to the unfolded state (Pace, 1986). Comparing the conformational stability of proteins which have a slight difference in structure improves our understanding of the forces that stabilise the structure of the protein (Pace *et al.*, 1989). For example, a mutated protein (even one which only involves a single amino acid mutation) may not be able to form a certain intramolecular hydrogen bond. The equilibrium unfolding study of this mutant will show reduced conformational stability when compared to the native protein. The importance of the mutated amino acid residue in the structural stability of the protein is thereby observed. In the same way, conformational stability studies can also be used to observe the influence of environmental conditions such as pH and temperature on the stability of a protein. The m -value obtained from equilibrium unfolding studies represents the dependence of ΔG on denaturant concentration. Moreover, the m -value has been shown to be proportional to the amount of the surface area exposed to the solvent during unfolding, under the assumption that denaturant binding sites are equally distributed on the protein surface (Myers *et al.*, 1995).

In addition to the thermodynamic information, equilibrium unfolding studies can also provide information about the unfolding and folding mechanism of a protein (Pace, 1986). If the equilibrium unfolding of a protein cannot fit to a two-state unfolding mechanism, this clearly

indicates that the unfolding of that protein occurs in more than one step, that is, with the presence of intermediate(s). However, the observation of an unfolding transition without any detectable intermediates in the equilibrium unfolding studies does not definitively suggest that the protein unfolds in the absence of intermediate species. The observation only indicates that the intermediate states might not be stable enough to be detectable at equilibrium (Pace, 1986). From this point of view, although equilibrium unfolding studies are able to provide some information about protein unfolding mechanisms, this experimental method has its limitations. Therefore, in order to understand the complete mechanisms of protein unfolding, the rate of unfolding of proteins is typically also investigated via kinetics studies.

1.2.2. Unfolding kinetics and unfolding pathways

A two-state transition as detected by equilibrium unfolding studies only indicates that no intermediate states are significantly populated at equilibrium or are detectable with the probes used (Pace, 1986). This method does not give any information about the occurrence of transient intermediate species. These are intermediate states that form rapidly from the native state and are then converted into the next intermediate structure or the unfolded state during a denaturation reaction. Since these intermediates are only transiently populated, they cannot be detected in equilibrium unfolding studies. As a result, unfolding kinetics analysis is required to detect these transient intermediates in the unfolding process and to further uncover the complete unfolding pathway of a protein (Jaenicke and Rudolph, 1989).

Unfolding kinetics studies of a protein are often conducted by adding the protein into denaturant and monitoring the progress of the entire unfolding reaction. Therefore, these studies are able to monitor the kinetic events happening along the unfolding reaction and may detect those transient intermediates which do not populate at equilibrium. Similar to

equilibrium unfolding studies, unfolding kinetics is also often monitored using more than one technique as a probe.

Two-state mechanism

There are a few kinetic mechanisms which have been proposed (Utiyama and Baldwin, 1986).

The simplest mechanism is a two-state mechanism as described in the following:



where N and U represent the kinetically populated native and unfolded species of the protein as unfolding progresses. If only two species are detectable at any time in unfolding, then only one kinetic phase will be detected, indicating that the unfolding is likely to occur in accordance with the two-state mechanism (Utiyama and Baldwin, 1986).

Although a single kinetic phase often suggests a two-state unfolding mechanism, there are two exceptions suggesting the existence of intermediate species: differential results from different probes and the appearance of a burst phase. If the unfolding kinetics monitored by different probes exhibit variance, this indicates the existence of hidden intermediates even if the unfolding kinetics appears monophasic (Bhuyan and Udgaonkar, 1998). When one observes the kinetics of protein folding or unfolding using spectroscopic probes, the observed amplitude of a kinetic trace is sometimes smaller than the signal difference between the initial and final states as monitored at equilibrium. This phenomenon is called “burst phase”. In folding or unfolding kinetics studies, the appearance of burst phases often suggests that at least one additional kinetic phase exists before the kinetic events are able to be detected with the techniques used (Roder *et al.*, 2000). Therefore, a burst phase is another indication of the existence of hidden intermediates where only one kinetic phase is apparent. Generally, burst phases occur due to the rapid accumulation of folding or unfolding intermediates in the early stages of protein unfolding (Roder *et al.*, 2000).

Sequential unfolding pathways with the appearance of intermediates

If there are intermediates involved, the unfolding of a protein is naturally more complicated. When monitoring the unfolding kinetics of a protein, the appearance of more than one kinetic phase is a clear indication of the existence of species other than the folded native state and unfolded state (Utiyama and Baldwin, 1986). The unfolding pathways in the presence of intermediate species can be separated into two categories: sequential and parallel unfolding. In a sequential unfolding pathway, all the kinetic events occur in a sequence, that is, step by step. On the other hand, in a parallel unfolding pathway, the events occur in parallel, that is, at the same time. In the following, three three-state unfolding schemes are used as examples of sequential unfolding with an intermediate species:

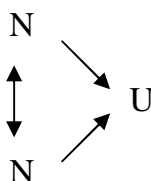


Since all three species are populated (N, I and U) during the unfolding process, two kinetic phases can be observed. Mechanism (D) represents an unfolding reaction via an on-pathway intermediate. Mechanisms (E) and (F) represent unfolding reactions with the involvement of an off-pathway intermediate. In the case of an on-pathway intermediate (mechanism D), all the native proteins need to pass through this intermediate state, and thus the formation of intermediate becomes a lag phase in the formation of the unfolded proteins (Bieri and Kiefhaber, 2000). In mechanism (E), the off-pathway intermediate is formed from U and does not lead N to U. To distinguish mechanism (D) and (E), interrupted unfolding experiments need to be performed (Bieri and Kiefhaber, 2000). From the results, the population of species can be calculated and plotted against time. Comparing the plots, the one without the expected lag phase in the formation of unfolded species indicates that the protein unfolds involving an

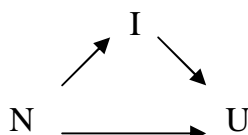
off-pathway intermediate. In mechanism (F), since an intermediate state is often less stable than the native state, it is likely to unfold faster than the native state and is thus difficult to isolate kinetically from the unfolded state under native conditions (Bai, 2003). Therefore, the unfolding reaction described by scheme (F) is generally unlikely to occur under native conditions or will only occur under a specific condition that stabilises the formation of the off-pathway intermediate.

Parallel unfolding pathways

Despite the sequential unfolding schemes mentioned above, it is also possible for unfolding to occur via a parallel pathway. The parallel unfolding can be described in the following representative schemes:



Mechanism (G)



Mechanism (H)

In scheme (G), the reaction starts with two groups of native species unfolding at the same time to the unfolded state via a parallel pathway. The parallel pathway results from the fact that the native state consists of two slowly interconverting forms with a slight difference such as a *cis*- and *trans*-proline, and the unfolding reaction is faster than the interconversion (Wallace and Matthews, 2002). As with the sequential mechanisms, there are also two kinetic phases observed in this scheme. The number of kinetic phases detected will represent the species appearing in the unfolding reaction but it cannot tell whether the unfolding reaction proceeds via a sequential or a parallel pathway. A method called the initial conditions test (ICT) is, therefore, required to distinguish whether the observed biphasic unfolding occurs

via a sequential or a parallel pathway (Wallace and Matthews, 2002). The method relies on the fact that the rate of unfolding of a protein depends only on the final denaturant concentrations while the amplitude of the observed kinetic phase is dependent on both the initial and final denaturant concentrations (Tanford, 1970; Hagerman and Baldwin, 1976). In mechanism (H), a protein unfolds through two independent pathways: one directly from the native state to the unfolded state and one from the native state through an intermediate state to the unfolded state. Since there are also three species populated during the unfolding process, two kinetic phases can be observed and this mechanism cannot be distinguished from mechanism (E) easily. However, when performing a least-squares fit to the denaturant-dependence of the two apparent rate constants, only a triangular model can be used to explain the data obtained from mechanism (H) (Wildegger and Kiefhaber, 1997).

The rate-limiting step in the unfolding reaction

There are two common rate-limiting steps in a protein unfolding process. The first one is proline *cis-trans* isomerisation of peptide bonds. The configuration of peptide bonds in a protein molecule can be either in the *cis*- or *trans*- form. However, the *cis* conformation is strongly disfavoured in non-proline dipeptides. The instability of the *cis*-form in non-proline dipeptides results from the steric hindrance between the two α -carbon atoms (Zimmerman and Scheraga, 1976). On the other hand, the *cis*-form of an Xaa-Pro dipeptide is relatively stable. A representative unfolding mechanism which involves proline *cis-trans* isomerisation can be described as follows:



where U_f represents a single unfolded population with native prolyl isomers and U_s represents one or more unfolded species of non-native isomers. In this mechanism, the unfolded form U_f is formed in the $N \leftrightarrow U_f$ transition and U_s is then formed from U_f . These two unfolded forms are both populated when the protein is completely unfolded. This phenomenon was first

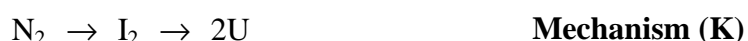
discovered by Garel and Baldwin in unfolded RNase A which consists of a heterogeneous mixture of unfolded molecules (Garel and Baldwin, 1973). Later on, Brandts and co-workers explained that the transition between the two unfolded forms is caused by proline *cis-trans* isomerisation in the protein molecule (Brandts *et al.*, 1975). Proline isomerisation is a slow reaction because it involves rotation about the whole peptide bond. Therefore, proline isomerisation results in a slow step not only in protein unfolding but also in protein folding.

In addition to proline isomerisation, the reduction of intramolecular disulfide bonds can also be a rate-limiting step in protein unfolding and folding (Creighton, 2000). The disulfide bond is a covalent bond formed between the thiol groups of two cysteine residues. Since disulfide bonds stabilise the structure of proteins, they need to be reduced before the unfolding reaction can proceed further. The formation of disulfide bonds can also be rate-limiting in the protein folding process *in vivo*. The concentration of thiolate anions and the accessibility, proximity, and reactivity of the thiol group and disulfide bonds are the four main factors which influence disulfide bond formation (reviewed by Mamathambika and Bardwell, 2008). The rate of thiol-disulfide exchange strongly depends on the concentration ratio of the reactive thiolate anions and the unreactive thiol groups (reviewed by Mamathambika and Bardwell, 2008). The pKa of cysteine residues in unfolded proteins is about 8.7. Therefore, the ideal pH for formation of disulfide bonds is above 9 where most species will be the reactive thiolate anions. Below this pH, the reaction will become progressively slower due to the decrease of the amount of the thiolate anions. In cells, the physiological pH is about 7.4 promoting slow formation of disulfide bonds. In order to solve this problem, organisms use disulfide oxidoreductase to decrease the pKa of the thiol groups and thus the thiol group can remain ionised and reactive at physiological pH (reviewed by Mamathambika and Bardwell, 2008). Moreover, because a disulfide bond forms between two cysteine residues, the number of free cysteine residues present and available for exchange also influences on the formation of

disulfide bonds and further affects the folding rate of proteins. The location of disulfide bonds also has an effect on the rate of protein unfolding. Generally, if the disulfide bonds are in or close to the folding nucleus, the protein folding will be accelerated (Abkevich and Shakhnovich, 2000). In contrast, disulfide bonds far from the folding nucleus often decelerate the folding of proteins.

Unfolding of oligomeric proteins

There are two prerequisites for all the unfolding schemes discussed above: the protein must be monomeric and the unfolding reaction must be reversible. For oligomeric proteins, over and above the general unfolding reaction discussed above, the disassociation of the subunits is also involved in the unfolding process (Jaenicke and Rudolph, 1989). For example, the overall unfolding pathway of a dimeric protein generally begins with a folded dimer (N_2) and ends with two unfolded polypeptide chains ($2U$) (Rumfeldt *et al.*, 2008). A few of the possible mechanisms are given in the following (Walters *et al.*, 2009):



The unfolding can simply follow a two-state pathway as shown in mechanism (J). If there are more species than the native state (N_2) and the unfolded state ($2U$) involved in the unfolding reaction, the pathway can be described in mechanisms (K) to (M). In mechanism (K), the intermediate is a dimeric intermediate, I_2 . If disassembly of two monomeric subunits happens prior to unfolding, the pathways are described in mechanisms (L) and (M). In these two

mechanisms, the intermediate state is either two native monomers (2N) or two monomeric intermediates (2I) (Walters *et al.*, 2009)

Irreversible unfolding

Not all protein unfolding processes are reversible. Irreversibility of unfolding reactions is a common problem in protein unfolding studies. A common sign of the irreversible unfolding process of a protein is the formation of aggregates (Eftink and Maity, 2000). The other indications include the inability to recover either the biological activity or physical properties of the native protein when the denaturing conditions are removed. The simplest representative irreversible unfolding pathway can be written as follows:



where D represents a permanent denatured state. The example here is just one of the possible aggregation pathways. As demonstrated in Figure 2, it is possible for a protein to form aggregates from any structural state. In kinetics studies, since the whole progression in the transition (such as a $N \rightarrow U$ transition) is monitored prior to the aggregation process (U to D), the events that occur along the unfolding pathway can still be detected. However, in equilibrium unfolding, the irreversible process will influence the shape of the transition and thus lead to unreliable thermodynamic data (Lepcock *et al.*, 1992). Equilibrium unfolding studies are thus unable to be performed on this kind of protein.

1.3. Metamorphic proteins

It was previously thought that proteins adopt their unique three-dimensional conformations under native physiological conditions (Anfinsen, 1973). However, more and more studies have demonstrated that some proteins have more than one native tertiary structure. These proteins are called metamorphic proteins (Murzin, 2008). Metamorphic proteins switch

between different native structures to conduct their complete functions. For the conversion between different native conformations of metamorphic proteins, unfolding of the original structures and refolding to the new configuration are essential. These structural transitions often involve secondary structural content change, appearance of new exposed surface and protein hydrophobic core repacking (Bryan and Orban, 2010). Examples of these proteins include serine protease inhibitor (Mottonen *et al.*, 1992), influenza virus hemagglutinin (Bullough *et al.*, 1994), lymphotactin (Tuinstra *et al.*, 2008), Mad2 spindle checkpoint protein (Luo *et al.*, 2004) and the chloride intracellular channel family (Littler *et al.*, 2004).

Although many different types of proteins are included in the metamorphic protein category, there are three common features needed for structural transition (Bryan and Orban, 2010). First, reduced conformational stability of proteins is necessary for fold switching. Since the native structures of proteins are known as the most stable, their location in terms of free energy is at the minimum of the energy landscape. Therefore, it is difficult for proteins in their native states to transform to a new ordered state. However, if the native state of a protein has a reduced conformational stability, that is, a more flexible structure, then this flexible structure is able to lower the energy barrier required for fold switching between the native state and the new ordered state and thus makes it easier for the protein to transit into the new conformation. Second, flexible regions are required to facilitate the configurational transition. New exposed surfaces are the last feature in protein fold switching. Sometimes these new surface areas stabilise the new alternative states through forming stable oligomeric conformations or else enable the proteins to interact with other biological molecules such as membranes and consequently form new conformations. The formation of these oligomers and new structures often lead the proteins to a new biological function.

1.4. Soluble proteins that insert into membranes

Typical membrane proteins are synthesised on ribosomes and inserted into the membrane co-translationally (reviewed by Shao and Hegde, 2010). There are, however, certain proteins with a property distinct from typical membrane proteins in that they are expressed as soluble proteins without a leader sequence for membrane targeting, but are able to insert into or associate with membranes subsequently. Because these proteins exist in both soluble and membrane-bound forms, they conform to the definition of existing in more than one native conformation and are, therefore, also classified as metamorphic proteins. These proteins include some bacterial toxins (Parker and Feil, 2005), porins (Parker and Pattus, 1993), the eukaryotic proteins Bcl-2 (Schendel *et al.*, 1997; Thuduppathy and Hill, 2005; Thuduppathy *et al.*, 2006), Bax (García-Sáez *et al.*, 2004) and the CLIC family (Ashley, 2003). Several of these proteins function as channels after membrane insertion, indicating that they not only associate with the membrane but must also completely cross the lipid bilayer and form a pore. The most interesting question about these proteins is how they change from one native state to the other.

The insertion mechanisms for some of these special proteins, such as bacterial pore-forming toxin colicin A and colicin E1, have been uncovered (Zakharov and Cramer, 2002). The polar heads of the lipid molecules which constitute biological membranes are highly negatively charged. Therefore, the negatively charged membrane surface attracts hydrogen ions and thus causes the local environment to become acidic (McLaughlin, 1989). The hydrogen ions at the membrane surface protonate the acidic residues on the surface of colicin and further increase the hydrophobicity of the protein. This reduces the activation energy barrier to conversion between soluble and membrane-bound states. The insertion of colicin also involves the formation of a molten globule-like intermediate induced by low pH at the membrane surface.

As mentioned in section 1.1.1., the molten globule state has a significant amount of exposed hydrophobic surface. Therefore, the increase in protein hydrophobicity either by protonation at the membrane surface or by formation of a molten globule-like intermediate facilitates the insertion of soluble proteins into highly hydrophobic membranes.

1.5. Chloride intracellular channels

The chloride intracellular channel (CLIC) family is a group of putative channel proteins which have different structural properties to the other known classes of channel proteins. This family consists of six members (CLIC1-6) in vertebrates (reviewed by Littler *et al.*, 2010 and Singh, 2010). The CLIC homologues have also been identified in plants (Elter *et al.*, 2007) and in invertebrates (*DmCLIC* in *Drosophila melanogaster*, and CLIC-like proteins EXC-4 and EXL1 in *Caenorhabditis elegans*) (Berry *et al.*, 2003; Littler *et al.*, 2008). A highly conserved carboxyl-terminal core segment about 240 amino acid residues long is the signature of this family. CLICs share both sequence and structural homology with the glutathione *S*-transferase (GST) proteins and thus CLICs belong to the GST superfamily (Dulhunty *et al.*, 2001; Harrop *et al.*, 2001).

Although the exact physiological function for CLIC proteins is still uncertain, the high sequence conservation of the CLICs in vertebrates suggests their functional importance. CLICs have been shown to be involved in various biological processes, including cellular division (Valenzuela *et al.*, 1997; Berryman and Goldenring, 2003), bone resorption (Schlesinger *et al.*, 1997), cell cycle regulation (Valenzuela *et al.*, 2000), p53-mediated apoptosis (Fernandez-Salas *et al.*, 1999 and 2002; Suh *et al.*, 2004 and 2005), kidney function (Berry *et al.*, 2003), and cancer-related processes such as cellular differentiation (Suh *et al.*, 2007), tubulogenesis (Berry *et al.*, 2003) and angiogenesis (Tung *et al.*, 2009; Tung and

Kitajewski, 2010). CLICs have also been implicated in Alzheimer's disease (Novarino *et al.*, 2004; Milton *et al.*, 2008).

1.6. Overview of CLIC1

CLIC1, previously called NCC27 (nuclear chloride channel 27), has been the most widely studied of the CLIC family. This protein is distributed in diverse cells and tissues (Ulmasov *et al.*, 2007) and is reported to form functional ion channels in the plasma and nuclear membranes of cells (Tulk *et al.*, 2000; Warton *et al.*, 2002). Although previous studies have shown that the expression of CLIC1 results in increased chloride channel activity in cultured cells (Valenzuela *et al.*, 1997; Tonini *et al.*, 2000), subsequent experiments have suggested that the CLIC1 channel is not only for chloride ions but also for a wider range of anions (Valenzuela *et al.*, 1997; Singh and Ashley, 2006). The anion selectivity of CLIC1 channels is thus poor and the conductance is dependent on anion concentration (Singh and Ashley, 2006; Singh *et al.*, 2007). In the following section, in order to get an insight into the CLIC1 insertion mechanism, the structure and auto-insertion controls of CLIC1 will be introduced.

1.6.1. Structure of soluble CLIC1

1.6.1.1. Primary sequence and secondary structure

CLIC1 consists of 241 amino acid residues which give it a theoretical molecular weight of 26.9 kDa and a *pI* of 4.85 (Valenzuela *et al.*, 1997; Ashley, 2003). The primary sequence and secondary structure are indicated in Figure 3. The CLIC1 monomer contains 10 α -helices and four β -strands, resulting in 47.7% α -helices and 8.3% β -strands in the secondary structure of CLIC1 according to the crystal structure (Harrop *et al.*, 2001). In CLIC1, there is only one tryptophan, Trp35 (Figure 3). Eight tyrosine and six cysteine residues are distributed throughout the protein molecule.

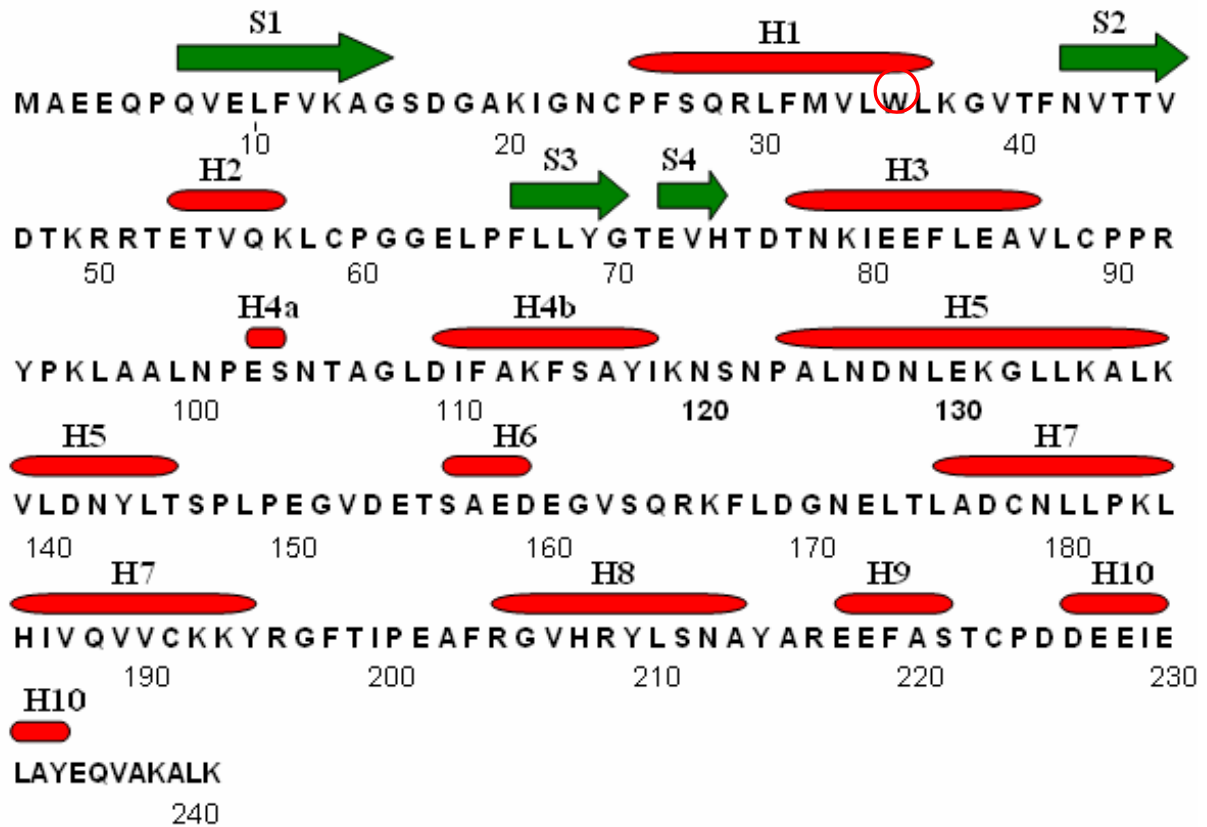


Figure 3: Amino acid sequence and secondary structural elements of CLIC1

The red bars and green arrows represent α -helices and β -strands beta strands, respectively (Harrop *et al.*, 2001). The lone tryptophan is indicated by red circle. This figure was generated using the sequence of CLIC1 obtained from NCBI using the accession code CAG46868.1.

1.6.1.2. Tertiary structure

The x-ray crystallographic structure of the soluble form of CLIC1 determined at a resolution of 1.4 Å (Harrop *et al.*, 2001) is shown in Figure 4. Soluble, reduced CLIC1 is monomeric, consisting of two domains: the N- and C-domains. The N-domain (residues 1-90) possesses a thioredoxin fold which contains a redox-active site similar to glutaredoxin. The lone tryptophan is located in this domain (Figure 4). There is a proline-rich loop (Cys89-Asn100) connecting the N- and C-domains. This proline-rich domain-connecting loop is the origin of domain interface plasticity in the structure (Harrop *et al.*, 2001). Moreover, since the N-domain is proposed to detach from the C-domain to initiate membrane insertion of CLIC1, the loop which leads to flexibility between the two domains is likely to be involved in the transition between the soluble and the transmembrane forms of CLIC1 (Harrop *et al.*, 2001).

The all-helical C-domain closely resembles that of Omega GST, but there are two distinct differences: the position of the carboxyl-terminal helix $\alpha 9$ and the existence of an acidic loop region (Pro147-Gln164) (Harrop *et al.*, 2001). This loop locates between helices $\alpha 5$ and $\alpha 6$ and consists of seven acidic residues. These acidic residues result in a highly negative net charge of -7 for CLIC1. Since this negatively charged loop is flexible and structurally close to the proline-rich loop connecting the two domains, it is assumed to play a role in protein-protein interactions (Harrop *et al.*, 2001).

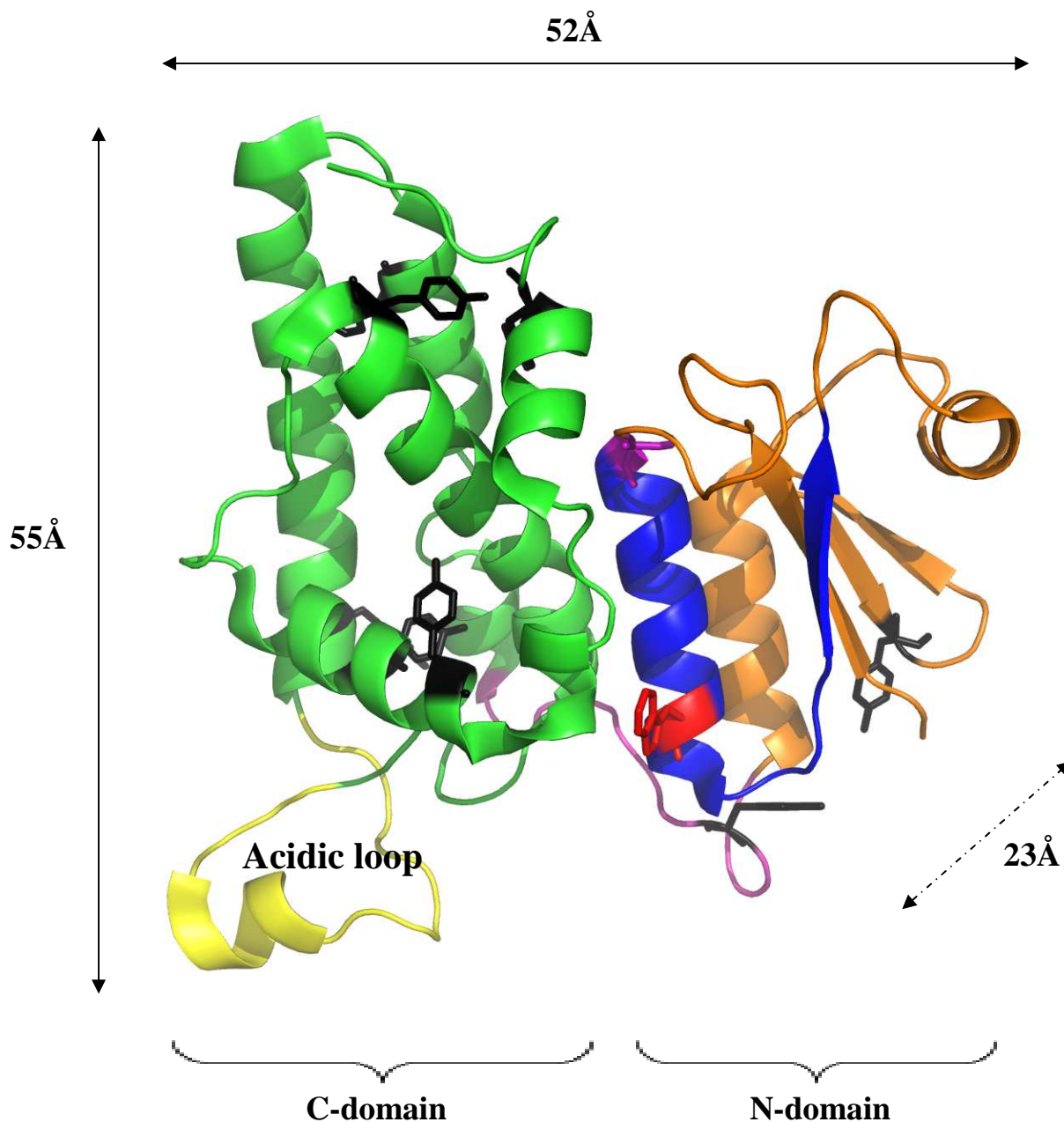


Figure 4: Crystal structure of soluble reduced CLIC1

The N-domain containing the thioredoxin fold is indicated in orange and blue. The all α -helical C-domain is shown in green and yellow. The putative transmembrane region is in blue. The proline-rich loop linking the two domains is shown in pink and the negatively charged loop is indicated in yellow. The lone tryptophan residue, Trp35 is shown in red and the eight tyrosine residues (two in the N-domain, six in the C-domain) are indicated in black. The cysteine residue (Cys24) located in the GSH binding site is shown in purple. This figure was generated using PyMOL™ (DeLano Scientific, 2006) using the PDB file 1K0M (Harrop *et al.*, 2001).

Redox effects on CLIC1

The N-domain of CLIC1 contains a glutathione (GSH) binding site. The center of the active site is a redox-active cysteine (Cys24), which is located at the beginning of helix $\alpha 2$ in the N-domain (Harrop *et al.*, 2001). CLIC1 can form both non-covalent and covalent interactions with GSH, however, CLIC1 does not bind to a GSH-Sepharose matrix. Also, GSH binding studies of CLIC1 using isothermal titration calorimetry cannot detect any noncovalent GSH binding below 10 mM GSH, which is in contrast with the strong binding between GSH and GSTs (Wilce and Parker, 1994). Therefore, non-covalent interactions between CLIC1 and GSH appear to be weak. In contrast, Cys24 forms a strong covalent interaction with GSH via a mixed disulfide bond under certain oxidising conditions (Harrop *et al.*, 2001). It has been suggested that CLIC1 may use its GSH-binding site to recognise the mixed disulfide bond of some GSH-modified proteins which may thus target the chloride channel to a specific subcellular location (Harrop *et al.*, 2001). Moreover, the mechanism for opening and closing the CLIC1 channels once inserted into membranes is also related to the redox condition (Singh and Ashley, 2006). In fact, the redox condition has been thought to be a control for membrane insertion of CLIC1. This will be discussed later on.

Putative transmembrane domain

The region from Cys24 to Val46 has been identified as the putative transmembrane domain (PTMD) for CLIC1 (Duncan *et al.*, 1997; Valenzuela *et al.*, 1997; Edwards, 1999; Fernandez-Salas *et al.*, 1999; Qian *et al.*, 1999; Berryman and Bretscher, 2000). The PTMD consists of helix $\alpha 1$ and strand $\beta 2$ in the N-domain. In the PTMD of CLIC1, there are two conserved phenylalanines (Phe26 and Phe41). Ten non-polar residues (Leu30 to Val39) are located between these two conserved phenylalanine residues. The remaining places are filled in with six to seven polar residues. This sequence of the PTMD matches a typical pattern for transmembrane helices (Sakai and Tsukihara, 1998). The non-polar residues in the PTMD

form a hydrophobic surface patch exposed on one side of the protein molecule (Harrop *et al.*, 2001). This surface in the proteins that are closely related to the CLICs in terms of sequence similarity contains several additional charged residues and thus is not hydrophobic. Therefore, the hydrophobicity of helix $\alpha 1$ and strand $\beta 2$ makes CLIC1 unique in the GST superfamily (Harrop *et al.*, 2001). It is hypothesised that the transmembrane region detaches from the C-domain, unfolds, and refolds into its membrane-bound conformation (Fanucchi *et al.*, 2008). However, the exact mechanism of this process as well as the role that the C-terminal domain plays in this process is still unknown.

1.6.2. The factors influencing CLIC1 membrane-insertion *in vitro*

The mechanism of CLIC1 membrane-insertion remains unknown. However, previous studies have proposed some factors which are able to influence CLIC1 insertion *in vitro*. These factors include pH and redox status.

1.6.2.1. Redox condition

It has been shown that the insertion of CLIC1 into membranes is under redox control (Singh and Ashley, 2006; Goodchild *et al.*, 2009; Littler *et al.*, 2004 and 2010). Under oxidising conditions, insertion and channel activity of CLIC1 are enhanced in artificial membranes. Cys24 is involved in this reaction. Although the CLIC1 C24A mutant is still able to insert into membranes, the redox control of insertion is removed (Singh and Ashley, 2006). Upon oxidation, it has been shown that CLIC1 forms a reversible non-covalent dimer with an intramolecular disulfide bond between Cys24 and Cys59 (Figure 5) (Littler *et al.*, 2004). Dimeric CLIC1 undergoes a dramatic structural rearrangement when compared to monomeric CLIC1. Instead of the four β -strands, α -helices and loops emerge in the N-domain and form a hydrophobic dimer interface non-covalently interacting with the other subunit of the CLIC1

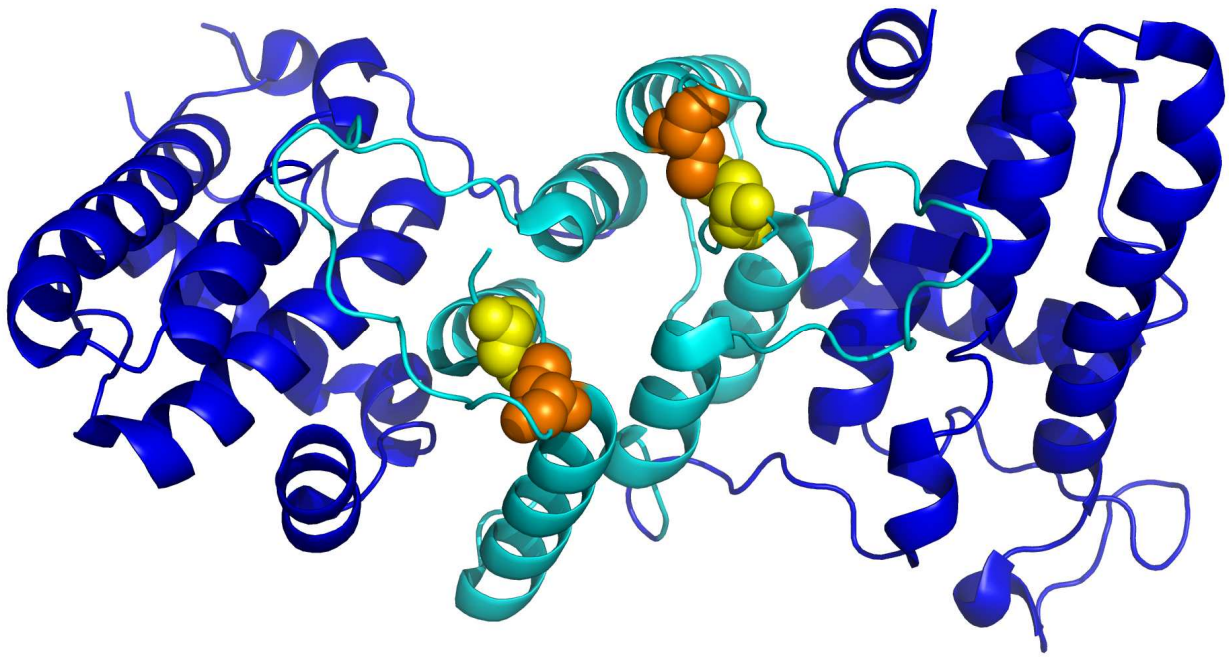


Figure 5: Structure of dimeric oxidised CLIC1

Upon oxidation, CLIC1 undergoes a dramatic structural transition to form a homodimer. In this dimeric structure, an intramolecular disulfide bond forms between Cys24 (yellow) and Cys59 (orange). The all-helical C-domain (blue) retains the original structure whereas the N-domain (cyan) rearranges from three α -helices and four β -strands to an all α -helical structure. This figure is generated by PyMOL™ (DeLano Scientific, 2006) using PDB entry 1RK4 (Littler *et al.*, 2004).

dimer (Figure 5). It is proposed that CLIC1 might use a structure similar to this hydrophobic dimer interface to dock it on the membranes (Littler *et al.*, 2010). However, it has been demonstrated that both monomeric and dimeric CLIC1 have the ability to insert into and form functional ion channels in artificial membranes (Littler *et al.*, 2004). Moreover, oxidation of monomer promotes insertion better than oxidation of dimer (Goodchild *et al.*, 2009). Therefore, the CLIC1 dimerisation process is not necessary for membrane docking and insertion (Goodchild *et al.*, 2009). Furthermore, the discrete dimer formed by the strong interaction between the hydrophobic interfaces may even cause steric hinderance for CLIC1 in terms of membrane docking and insertion (Goodchild *et al.*, 2009). In addition, Cys59 is not conserved in other CLICs and thus it is difficult to conclude the role of the intramolecular disulfide bond in membrane insertion of the CLIC family.

1.6.2.2. The effect of pH

CLIC1 channel formation and activity have been reported to be highly pH-dependent (Tulk *et al.*, 2002; Warton *et al.*, 2002). The activity at neutral pH is lowest while it rises at both acidic and basic pH (Tulk *et al.*, 2002; Warton *et al.*, 2002). It has been demonstrated that, in the absence of denaturant or membranes, the core structure and size of CLIC1 do not show any significant changes at different pH values (Fanucchi *et al.*, 2008). However, hydrogen-deuterium exchange studies do show that the PTMD in the N-domain is more flexible at acidic pH than at neutral pH (Stoychev *et al.*, 2009). Equilibrium unfolding studies of CLIC1 show a two- and three-state transition at pH 7.0 and pH 5.5, respectively. A stable equilibrium intermediate forms in the presence of mild urea concentrations at pH 5.5 (Fanucchi *et al.*, 2008), which corresponds roughly to the pH value at the surface of membranes (McLaughlin, 1989), and the intermediate does not appear at pH 7.0 (roughly the pH value in cytosol). This equilibrium intermediate retains approximately 50% of the native secondary structure and has a well-packed tertiary structure similar to the native CLIC1

(Fanucchi *et al.*, 2008). Despite overall similar tertiary structure, the lone CLIC1 tryptophan residue which is located in the PTMD becomes more buried in the intermediate state compared to the native state (Fanucchi *et al.*, 2008). The hydrophobic fluorescent dye ANS binds to the intermediate more strongly than to the native and unfolded states, indicating that the intermediate has more hydrophobic surfaces exposed than the native and unfolded states (Fanucchi *et al.*, 2008). As proposed by Littler *et al.* (2010), the membrane-docking form of CLIC1 is likely to possess exposed hydrophobic surfaces in order to interact with membranes. Therefore, this equilibrium intermediate which has exposed hydrophobic areas may be significant in CLIC1 membrane-docking.

1.7. Objective

Since it has been suggested that CLIC1 needs to unfold partially prior to membrane insertion, the main objective of this study is to determine the unfolding mechanism of CLIC1. This objective can be divided into three aims.

Aims:

1. Characterise the structure of CLIC1 under different pH values corresponding to the pH in cytosol and at the membrane surface (pH 7.0 and pH 5.5, respectively) and different urea concentrations where the native, intermediate, and unfolded states of CLIC1 are populated.
2. Perform equilibrium unfolding studies to detect the conformational stability of CLIC1 at pH 7.0 and pH 5.5 to investigate the influence of pH on the stability of the protein. CLIC1 has been shown to form a stable equilibrium intermediate under mild denaturing conditions at pH 5.5 (Fanucchi *et al.*, 2008). This intermediate has structural properties that are similar to the proposed CLIC1 membrane-docking form. Therefore, the exact conditions at which the intermediate state is stable need to be determined for the subsequent kinetic experiments.
3. Measure the unfolding kinetics of CLIC1 from the native state to the unfolded state ($N \rightarrow U$), from the native state to the intermediate state ($N \rightarrow I$), and from the intermediate state to the unfolded state ($I \rightarrow U$) at pH 7.0 and pH 5.5. This aim forms the largest part of this study. Unfolding kinetics studies have never been done before on CLIC1. First, unfolding of $N \rightarrow U$ will be measured at both pH 7.0 and pH 5.5 in order to compare the different unfolding behaviours of CLIC1 in the environments which are similar to the

cytosol and membrane surface. Since the equilibrium intermediate only appears at pH 5.5, the unfolding of the $N \rightarrow I$ and $I \rightarrow U$ transitions will only be monitored at this pH. The most important part of this study is to observe the kinetic mechanism of the formation of the equilibrium intermediate. This novel study has the potential to improve the knowledge of the membrane insertion mechanism of CLIC1.

2. Experimental procedures

2.1. Materials

The pGEX-4T-1 plasmid encoding the cDNA for recombinant GST-CLIC1 fusion protein was a gift from S. N. Breit, Centre for Immunology, St. Vincent's Hospital and University of New South Wales, Sydney, Australia. Isopropyl- β -D-thiogalactopyranoside (IPTG) and dithiothreitol (DTT) were obtained from Melford Laboratories Ltd (Suffolk, UK). Thrombin from human plasma (1 KU) was purchased from Sigma-Aldrich (St. Louis, MO, USA). Reduced glutathione (GSH), 8-anilino-1-naphthalene sulfonate (ANS) and ultrapure urea were acquired from Merck laboratory supplies (Darmstadt, Germany). SDS-PAGE molecular weight markers were purchased from Fermentas (Ontario, Canada). All the other chemicals used in this study were of standard analytical grade.

2.2. Methods

2.2.1. Expression and purification of recombinant CLIC1

Expression

CLIC1 was expressed and purified following the methods used by Fanucchi *et al.* (2008) with a few modifications. First of all, *Escherichia coli* BL21(DE3) pLysS cells were transformed with the pGEX-4T-1 plasmid containing the GST-CLIC1 fusion protein. A glycerol stock was prepared by adding transformed *E. coli* cells at mid-log phase to sterile glycerol in a 1 : 1 ratio and stored at -80°C. Two hundred microlitres of BL21 cells from the glycerol stock were added into a sterile 200 ml 2X YT medium (1.6% tryptone, 1% yeast extract and 0.5% NaCl). All the sterile media were inoculated with 100 μ g/ml ampicillin before use. The cells were then incubated overnight at 37°C with shaking at 250 rpm. The next day, each overnight culture was poured into a 2L sterile 2X YT medium and incubated at 37°C with shaking at

250 rpm for approximately 2.5 hours until the OD₆₀₀ reached 0.6 ~ 0.8. The overexpression of the fusion protein was induced by adding IPTG to a final concentration of 1 mM and the cells were allowed to grow for another 4 ~ 5 hours. The cells were then centrifuged at 5000 rpm for 15 minutes at 5 ~ 20°C in a Sorvall RC5C centrifuge using a SLA3000 rotor. The pellet was resuspended in 3 ml resuspension buffer, pH 8.0 (10 mM Tris-HCl, 100 mM NaCl, 1 mM EDTA, 0.02% NaN₃) and stored at -20°C.

The frozen cells were defrosted with rotating at 4°C. After thawing, 50 µl DNase (0.1 g/ml), 500 µl MgCl₂ (0.095 g/ml) and 250 µl lysozyme (0.1 g/ml) were added to each 25 ml cell solution and mixed properly. The cells were then sonicated on ice for 5 cycles of 30 seconds, pulsed (intensity 4, pulsed 0.5 sec) on a Sonicator™ Ultrasonic Processor XL (Misonix Inc.). The lysed cells were centrifuged at 15 000 rpm, for 30 minutes, at 4 ~15°C using a SS34 rotor and the supernatant was collected.

Glutathione-Sepharose affinity chromatography

Before use, a 10 ml GSH-Sepharose column was equilibrated at 4°C with 150 ~ 200 ml GSH-equilibration buffer, pH 8.0 (10 mM Tris-HCl, 150 mM NaCl, 1 mM EDTA, 1 mM DTT added fresh). The supernatant obtained from the lysed cells was diluted 5X with GSH-equilibration buffer and loaded onto the GSH-Sepharose column. This method is based on the strong affinity between CLIC1-fused GST and GSH. The GST-CLIC1 fusion protein can thus be retained in the column and separated from the contaminating proteins in the supernatant. To improve the quantity of bound GST-CLIC1 fusion protein to the resin of the GSH-Sepharose column, the flow-through was collected and reloaded. After the supernatant was reloaded, the column was washed with 300 ml GSH-equilibration buffer in order to wash off all the unbound fusion protein and contaminants. Then the column was equilibrated with five column volumes of thrombin cleavage buffer, pH 8.4 (200 mM Tris-HCl, 1.5 M NaCl,

25 mM CaCl₂, 0.8 mM DTT added fresh). To separate CLIC1 from resin-bound GST, two column volumes of thrombin cleavage buffer containing human plasma thrombin (80 µl per litre cell culture) was loaded on the column. The cleavage reaction was allowed to continue for 16 hours at 20°C on a rotator. The next day, after digestion, the GSH-Sepharose resin was allowed to settle before the CLIC1 and thrombin mixture was collected.

Anion-exchange chromatography

A 40 ml DEAE-Sepharose column was equilibrated with 400 ml DEAE-equilibration buffer, pH 6.5 (20 mM Tris-HCl, 0.02% NaN₃) before use. DEAE is a positively charged group covalently linked to the Sepharose beads and has the ability to bind and retain negatively charged particles. Increasing the ionic strength or varying the pH value of the elution buffer are common methods used to elute bound particles. CLIC1 and thrombin are able to be separated due to the difference in their *pI* values. At pH 6.5, human thrombin with a *pI* value of 7.0 ~ 7.6 (Fenton *et al.*, 1977) is positively charged and does not bind to the DEAE resin whilst CLIC1 with a *pI* value of 4.85 (Ashley, 2003) becomes negatively charged and binds to the resin. The solution containing CLIC1 and thrombin from the GSH-Sepharose column was loaded onto the DEAE-Sepharose column and the column was washed with 150 ml DEAE-equilibration buffer to ensure that all the thrombin was removed. CLIC1 was then eluted with an increased salt concentration (DEAE-equilibration buffer containing 300 mM NaCl) and the fractions were collected for every 3 ml. The high concentration of salt results in an enhanced competition between the anions in the buffer and the negatively charged CLIC1 for the positively charged DEAE groups on the resin, and hence it reduces the interaction between the resin and CLIC1 molecules, and thus causes the protein to elute. CLIC1 was successfully eluted between 30 ml and 60 ml.

2.2.2. Confirmation of protein purity

SDS-PAGE is a technique used to separate and characterise complex mixtures of proteins (reviewed by Makowski and Ramsby, 1997). The basic principle for the method is that charged particles in an electric field move toward the electrode of opposite sign. SDS is an anionic detergent that is able to denature secondary and non-disulfide linked tertiary structures of proteins. SDS generally binds to protein molecules in a ratio of 1.4 g/g protein. Since the negative charge of the bound SDS is large, it has ability to mask the net charge of the protein effectively, giving all the proteins in the sample a uniform charge:mass ratio. Therefore, the coated negative charge is in proportion to the mass of the protein molecule so that the distance of migration of the protein through the gel is only related to the size of the protein (reviewed by Makowski and Ramsby, 1997). The different proteins in the sample are thus able to be separated according to their size.

In this study, the discontinuous system (Laemmli, 1970) was used for SDS-PAGE analysis. Discontinuous systems divide the gel into two parts: an upper part called the stacking gel with large pore size and low pH (pH 6.8) and a lower part called the resolving gel with smaller pores and higher pH (pH 8.8). The electrode buffer contains glycine anions while both gels use chloride ions as the main mobile anions. In the stacking gel with a pH value of 6.8, glycines are mainly zwitterions without net charge and thus move very slowly in the electric field. On the other hand, the strongly charged, smaller chloride ions move relatively faster in the electric field and cause the formation of an ion front. The faster-moving chloride ions followed by the slower-moving glycine zwitterions result in two separated fronts of migrating ions and thus creates a narrow zone between the two fronts. All the proteins in the gel have an intermediate mobility between the glycine and chloride ions. Therefore, when the two fronts pass through the sample wells, the proteins will be concentrated in the narrow zone

between the chloride and glycine ion fronts. When the glycine front reaches the running gel which has a pH of 8.8, the increase in pH makes the glycine molecules ionised and then increases their mobility. The proteins are, therefore, left behind and stack in the narrow band at the interface between the stacking and running gels. The function of the protein stacking is to improve band sharpness and resolution. The proteins are now allowed to separate according to the difference in their molecular weight in the resolving gel.

For all SDS-PAGE experiments in this study, the stacking gels (4%) used were composed of 1.3 ml 30% acrylamide/bis (acrylamide : bis = 37.5 : 1), 2.5 ml 0.5 M Tris-HCl, pH 6.8, 0.1 ml 10% SDS, 50 µl 10% ammonium persulfate, 10 µl TEMED and 6.1 ml dH₂O. The separating gels (15%) used consisted of 5 ml 30% acrylamide/bis (acrylamide : bis = 37.5 : 1), 2.5 ml 1.5 M Tris-HCl, pH 8.8, 0.1 ml 10% SDS, 50 µl 10% ammonium persulfate, 5 µl TEMED and 2.4 ml dH₂O. Sample buffer was composed of 0.5 ml 2% bromophenol blue, 2.5 ml 0.5 M Tris-HCl (pH 6.8), 8 ml 100% glycerol, 4 ml 10% SDS, 1 ml 2-mercaptoethanol and 3.5 ml dH₂O and was added to each sample in a 1:1 sample buffer to sample ratio. Samples were then boiled for 5 minutes and 10 ~ 15 µl of each sample was loaded on the gels. The electrode buffer, pH 8.3, consists of 14.4% glycine, 3% Tris-HCl and 1% SDS in 1 L. The electrophoresis was performed at 200 V until the dye front reached 0.5 cm from the bottom of the gels. The gels were stained for 2~16 hours in Coomassie Blue stain solution made up of 0.25% (w/v) Coomassie Brilliant Blue R250, 45% (v/v) methanol and 10% (v/v) glacial acetic acid. Then gels were destained in the destain solution consisting of 25% (v/v) ethanol and 10% (v/v) glacial acetic acid for 3 ~ 16 hours.

In this study, samples for the gels included the protein complement of *Escherichia coli* cells before and after induction with IPTG, the pellet and supernatant of the lysed cells, the flow-through from the GSH-Sepharose column, the CLIC1-thrombin mixture from thrombin

cleavage, thrombin separated from the CLIC1 and thrombin mixing solution, cleaved GST and purified CLIC1. The molecular mass markers used were β -galactosidase (116 kDa), bovine serum albumin (66.2 kDa), ovalbumin (45 kDa), lactate dehydrogenase (35 kDa), restriction endonuclease *Bsp98I* (25 kDa), β -lactoglobulin (18.4 kDa) and lysozyme (14.4 kDa).

After confirming the purity, CLIC1 was dialysed into CLIC1 storage buffer, pH 7.0 (50 mM sodium phosphate, 0.02% NaN_3 , 1 mM DTT) using Snakeskin™ Pleated dialysis tubing MWCO 10 000 (Pierce). The purified protein used for all subsequent experiments was either snap-frozen with liquid nitrogen and stored at -80°C or dialysed every week against a storage buffer containing 1 mM fresh DTT in order to maintain the protein under reducing conditions. Depending on the experiments, CLIC1 was also dialysed into acetate buffer (50 mM sodium acetate, 0.02% NaN_3 , 1 mM DTT, pH 5.5) for the studies performed at pH 5.5.

2.2.3. Determination of protein concentration

The concentration of purified CLIC1 was determined with ultraviolet (UV) absorbance spectroscopy before each experiment in order to ensure the integrity of the results. The Beer-Lambert law, $A = \epsilon cl$, was used. For a protein solution, A represents the absorbance at 280 nm; ϵ is the molar extinction coefficient of the protein at 280 nm in $\text{M}^{-1}\text{cm}^{-1}$; c is the concentration of the protein solution in M and l is the path length of the cuvette in cm. The molar extinction coefficient of CLIC1 was determined based on the numbers of tryptophan, tyrosine and cysteine residues (Perkins, 1986):

$$\begin{aligned}\epsilon_{280} (\text{M}^{-1}\text{cm}^{-1}) &= 5550 \Sigma \text{Trp} + 1340 \Sigma \text{Tyr} + 150 \Sigma \text{Cys} \\ &= 5550(1) + 1340(8) + 150(6) \\ &= 17170 \text{ M}^{-1}\text{cm}^{-1}\end{aligned}$$

The 280 nm absorbance readings of five serial dilutions (4X, 5X, 6X, 8X and 10X) of CLIC1 stock were collected to construct a dilution curve. The absorbance at 340 nm that indicates the existence of aggregation was also collected for correction purposes. The absorbance at 280 nm was corrected using the following equation (Reed *et al.*, 2003):

$$A_{280 \text{ (corrected)}} = A_{280 \text{ (protein)}} - A_{280 \text{ (buffer)}} - (A_{340 \text{ (protein)}} - A_{340 \text{ (buffer)}})(A_{280 \text{ (buffer)}}/A_{340 \text{ (buffer)}}) \quad (2)$$

By fitting a linear regression analysis to the standard curve, the molar concentration of CLIC1 can then be calculated. Furthermore, an absorbance spectrum of purified CLIC1 was also collected over a wavelength range of 190 to 360 nm. DNA has a maximum absorbance at 260 nm while proteins absorb UV light mainly at 280 nm. The A_{280}/A_{260} ratio of CLIC1 was therefore used to assess DNA contamination. A ratio close to 1.8 generally indicates a pure protein with low DNA contamination. All absorbance measurements were performed on a Jasco V-550 UV/VIS spectrophotometer at 20°C.

2.2.4. Structural characterisation of CLIC1

Far-UV circular dichroism spectroscopy

Circular dichroism (CD) spectroscopy is a technique which is often used to characterise the structures of various biological molecules such as nucleic acids and proteins. The principle of this technique relies on the fact that optically active chromophores absorb right and left circularly polarised radiation components differently. When an equal amount of right and left polarised components of radiation pass through a sample at a given wavelength, an asymmetric chromophore does not absorb the two components equally. The differential absorption of two polarised components from the chromophore then gives the dichroism at the specific wavelength which is often expressed as either the ellipticity in degrees or the

difference in absorbance of two components (reviewed by Kelly and Price, 1997). In proteins, the optically active chromophores are the peptide backbone, aromatic residues and disulfide groups (Woody, 1995). Far-UV CD is performed over a wavelength range of 190 ~ 250 nm to assess the content of global secondary structure of a protein. In this region, the main absorbing group is peptide bonds linking amino acid residues (Woody, 1995). It has been known that different regular secondary structures give different specific far-UV CD spectra (Woody, 1995). Therefore, far-UV CD is able to indicate characteristics of the secondary structural content of proteins. A predominantly α -helical protein has a specific spectrum with a strongly positive ellipticity near 190 nm and two dominant minima near 208 nm and 222 nm (Woody, 1995).

In this study, to characterise the secondary structures of CLIC1 in the native, intermediate and unfolded states, far-UV CD was performed. For far-UV CD spectra, each protein sample was made up with 10 μ M CLIC1, CLIC1 storage buffer, pH 7.0 (50 mM sodium phosphate, 0.02% NaN₃, 1 mM DTT) or pH 5.5 (50 mM sodium acetate, 0.02% NaN₃, 1 mM DTT) and different concentrations of urea (0 M and 7 M, which populate the native and unfolded state of CLIC1, respectively). Since the intermediate state of CLIC1 has exposed hydrophobic surface, it is prone to form aggregates while the protein concentration is high. Therefore, in order to prevent the formation of aggregates, the samples of intermediate state were made up with 2 μ M CLIC1, in CLIC1 storage buffer (pH 7.0 or pH 5.5) and in the presence of 3.4 M urea (which populates the intermediate state of CLIC1 mostly). The spectra were obtained on a Jasco J-810 spectropolarimeter at 20°C. The scan speed was 200 nm/min over a wavelength range of 190 ~ 250 nm, with a cuvette of path length 2 mm. The spectra were the result of 10 accumulations.

For all the far-UV CD measurements, the unit, ellipticity, obtained from CD was converted into the mean residue ellipticity $[\Phi]$ ($\text{deg.cm}^2.\text{dmol}^{-1}.\text{residue}^{-1}$) using the following equation:

$$[\Phi] = 100\theta/cnl \quad (3)$$

where θ is the ellipticity (mdeg); c represents the protein concentration in mM; n is the number of residues in the protein and l is the path length (cm) of the cuvette. All the CD spectra were smoothed using the negative exponential methodology (SigmaPlot[®] v11.0).

Fluorescence spectroscopy

Fluorescence spectroscopy is a type of electromagnetic spectroscopy that analyses the fluorescence of a sample (Lakowicz, 2006). When a fluorophore absorbs light of a specific wavelength, the electrons in the molecule which are in their ground state can be excited to a higher energy state. These electrons then fall back from the excited state to the ground state by losing electronic energy in the way of emitted light (that is, fluorescence). A common phenomenon known as Stoke's shift is the explanation for the bathochromic (red) shift in the emission spectra compared to the excitation wavelength. In proteins, the amino acid residues which contribute to the fluorescence are mainly tyrosine and tryptophan. Tryptophan is the one which absorbs light at the longest wavelength and its extinction coefficient is the largest. Therefore, the energy from tyrosine is often transferred to tryptophan and thus the fluorescence of most proteins is dominated by tryptophan. In addition, tryptophan residues can be selectively excited at 295 nm in order to avoid the effect from tyrosine residues and make the fluorescence specific to that of the tryptophan residues rather than of Tyr-to-Trp energy transfer.

The indole group of tryptophan is very sensitive to changes in environment polarity (Lakowicz, 2006). The wavelength at which tryptophan residues emit light depends on the

polarity of the environment to which they are exposed. Since the polar solvent molecules lower the energy of the excited state, when a more polar environment surrounds the tryptophan residues, the spectrum will display a red shifted maximum emission wavelength toward a longer wavelength (Lakowicz, 2006). In contrast, if the environment is more nonpolar, the maximum emission wavelength shows a blue shift toward to a shorter wavelength. Therefore, the location of tryptophan residues in the protein can be inferred and fluorescence spectroscopy can be used as a probe to monitor the change in tertiary structure of a protein, specifically in the microenvironment surrounding the tryptophan residues.

For the fluorescence spectroscopy measurements, each protein sample was made up with 10 μ M CLIC1, in CLIC1 storage buffer, pH 7.0 (50 mM sodium phosphate, 0.02% NaN_3 , 1 mM DTT) or pH 5.5 (50 mM sodium acetate, 0.02% NaN_3 , 1 mM DTT) and different concentrations of urea (0 M and 7.M, which populate the native and unfolded state of CLIC1, respectively). As mentioned in the far-UV CD section, in order to avoid the formation of aggregation, the representative samples of the intermediate state of CLIC1 were made up with 2 μ M CLIC1, in CLIC1 storage buffer, pH 7.0 or pH 5.5 and in the presence of 3.4 M urea (where the intermediate populates mostly). The spectra were measured on a Perkin-Elmer Luminescence Spectrometer LS50B at 20°C. The scan speed was 100 nm/min over a wavelength range of 280 ~ 450 nm using a cuvette of path length 10 mm. The excitation wavelengths were 280 nm and 295 nm to excite both tyrosine and tryptophan residues and to selectively excite only the tryptophan residue, respectively. The spectra were the result of 10 accumulations. All the fluorescence spectra were smoothed using the negative exponential methodology (SigmaPlot[®] v11.0).

2.2.5. Urea-induced equilibrium unfolding

Equilibrium unfolding is a process of unfolding a protein by gradually changing its environment with a chemical denaturant, temperature change or pH change. The functions of denaturation curves include comparing conformational stability among proteins, observing equilibrium unfolding intermediates and further indicating unfolding and folding pathway of proteins (see Section 1.2.1.). Since the existence of unfolding intermediates often indicates that the protein has more than one domain and that it unfolds following a more complex pathway, denaturation curves are also able to give information about the structure (number of domains) of a protein. For equilibrium unfolding studies, two important thermodynamic parameters can be obtained: $\Delta G(\text{H}_2\text{O})$ and m -value. The $\Delta G(\text{H}_2\text{O})$ of an unfolding reaction is defined as the change in free energy between the native and the unfolded state in the absence of denaturant. It serves as an indication of the conformational stability of proteins. The m -value is the slope of the transition region of unfolding curves. It has been shown that m -values are related to the surface area of proteins exposed to solvent during unfolding (Myers *et al.*, 1995). Equilibrium unfolding of CLIC1 has been previously studied (Fanucchi *et al.*, 2008). However, in order to determine the precise conditions which are required for the subsequent kinetics experiments, the equilibrium unfolding of CLIC1 was repeated.

Recovery studies

Since the equilibrium constant of the unfolding reaction is required for calculating the free energy change between the native and the unfolded state, it is essential to make sure that the unfolding reaction is at equilibrium and hence reversible (Pace, 1986). The recovery and reversibility of wild type CLIC1 have both been previously demonstrated (McIntyre PhD thesis 2008; Fanucchi *et al.*, 2008). Therefore, in this study, recovery studies of native CLIC1 were just performed to demonstrate the CLIC1 unfolding process is reversible.

Recovery studies were conducted by unfolding 20 μ M CLIC1 in 7 M urea at pH 7.0 (50 mM sodium phosphate, 0.02% NaN₃, 1 mM DTT) or pH 5.5 (50 mM sodium acetate, 0.02% NaN₃, 1 mM DTT) at 20°C for 2 hours or 1 hour to reach equilibrium, respectively. Unfolded CLIC1 was then diluted 10X to a final concentration of 2 μ M protein in 0.7 M urea and allowed to refold for 1 hour. Far-UV CD and fluorescence spectroscopy were used as probes to detect changes in secondary and tertiary structure. The spectra of 2 μ M native and unfolded CLIC1 (in 0.7 M and 7 M urea, respectively) were used as controls. The CD and fluorescence spectra were collected over wavelength ranges of 190 ~ 250 nm and 280 ~ 450 nm, respectively. The excitation wavelength for fluorescence measurements was 280 nm.

Sample preparation

Equilibrium unfolding of CLIC1 was performed using urea as the denaturant. Samples and urea stock (10 M) were made up with CLIC1 storage buffer, pH 7.0 (50 mM sodium phosphate, 0.02% NaN₃, 1 mM DTT) or pH 5.5 (50 mM sodium acetate, 0.02% NaN₃, 1 mM DTT). Samples of 2 μ M CLIC1 were prepared in urea concentrations ranging from 0 to 8 M at both pH 7.0 and pH 5.5. After sample preparation, unfolding at pH 5.5 and pH 7.0 were allowed to unfold at 20°C for one and two hours, respectively, in order to reach equilibrium. Far-UV CD and fluorescence spectroscopy were used as probes to monitor structural changes of CLIC1 in the equilibrium unfolding studies.

Far-UV CD measurements

As mentioned previously, since CLIC1 is a predominantly α -helical protein, the CD spectra for CLIC1 show a specific signature of two minima at 208 nm and 222 nm, respectively. Furthermore, the signal at 222 nm of a native helical-protein is relatively larger when compared to the low signal at 222 nm from its unfolded structure. Therefore, the ellipticity at

222 nm was chosen as a probe to detect any change in secondary structure of CLIC1 in the equilibrium unfolding studies as the denaturant concentration increases. The ellipticity at 222 nm was recorded over a urea concentration range of 0 to 8 M. The CD measurement was conducted over 60 seconds with 0.5 second interval for each sample and then averaged. For each urea concentration, the final result was obtained from the average of three experiments.

Fluorescence measurements

When excited at either 280 nm or 295 nm, CLIC1 has a maximum fluorescence emission wavelength at 345 nm. However, excitation at 295 nm resulted in a rather small quantum yield compared to excitation at 280 nm. Therefore, 280 nm was chosen to be the excitation wavelength for the equilibrium unfolding studies of CLIC1. For fluorescence measurements of equilibrium unfolding, the emission spectrum was recorded over a wavelength range of 280 ~ 450 nm for each sample over a urea concentration range of 0 to 8 M. The excitation wavelength was 280 nm. The scan speed was 350 nm/min. The path length of cuvette was 10 mm. Each spectrum was the result of 3 accumulations.

Since tryptophan fluorescence spectroscopy is sensitive to environmental polarity, the maximal emission wavelength is usually used as a probe to monitor any change in the microenvironment of tryptophan residues (Lakowicz, 2006). However, tryptophan fluorescence spectroscopy is also sensitive to changes in protein concentration. Change in protein sample concentration can lead to change of the emission intensity. Therefore, intensity-averaged emission wavelength (IAEW) is a better way to measure any change in the spectral shift or in the shape of spectra than the emission maximum wavelength because it takes both intensity and wavelength of an entire spectrum into account (Royer *et al.*, 1993). In addition, IAEW is also an integral measurement and thus it is able to avoid instrumental noise. IAEWs $\langle\lambda\rangle$ of fluorescence-monitored equilibrium unfolding data were calculated

using the following equation:

$$\langle \lambda \rangle = \sum_i^N (I_i \lambda_i) / \sum_i^N (I_i) \quad (4)$$

where I_i is the intensity at wavelength λ_i and i represents any point along entire spectrum.

ANS binding

ANS, a hydrophobic fluorescent dye, is often used as a probe to examine the nonpolar character of macromolecules such as membranes and proteins. ANS is an amphipathic molecule with a hydrophobic naphthalene part and a negatively charged sulfonate group. Binding of ANS to proteins is mainly initiated through the electrostatic interaction between the cationic groups on proteins and the ANS sulfonate group (Matulis and Lovrien, 1998). Therefore, the cationic charge of a protein and the pH of the protein solution are both able to influence the binding of ANS. However, the most important property of this dye is that the hydrophobic naphthalene moiety of ANS is able to bind to the hydrophobic clusters on macromolecules. When ANS is excited alone in water, the emission maximum is above 500 nm with a very small quantum yield (Lakowicz, 2006). Once ANS binds to the nonpolar clusters on a protein, the maximum emission wavelength of the fluorescence spectrum will display a blue shift (shift to a lower wavelength) and the quantum yield increases largely (Lakowicz, 2006). Since unfolding intermediates usually have exposed hydrophobic surface, ANS is often used to detect the existence of intermediates in protein unfolding reactions in both equilibrium unfolding and unfolding kinetics studies (Stryer, 1965; Kuwajima *et al.*, 1991; Semisotnov *et al.*, 1991).

ANS binding was conducted along with equilibrium unfolding experiments of CLIC1 at pH 7.0 and pH 5.5 to detect the formation of the intermediate. ANS stock was prepared to 2 mM. After the protein was allowed to unfold to reach equilibrium at different urea

concentrations, ANS was added from the stock to each sample to a final concentration of 200 μ M and allowed to bind for one hour. The spectrum (390 ~ 600 nm) for each sample was recorded on the fluorimeter with an excitation wavelength of 390 nm. The scan speed was 500 nm/min. A cuvette of path length 10 mm was used. Each final spectrum was the result of 3 accumulations. After ANS binds to the intermediate state of CLIC1, the ANS spectrum displays a maximum emission wavelength of ~460 nm. Therefore, the ANS binding as a function of urea was plotted using the fluorescence intensity at 460 nm. All the spectra of ANS binding were corrected with blank controls (free ANS + urea at different concentrations).

Data analysis

The data chosen to construct unfolding curves were CD ellipticity at 222 nm and fluorescence intensity at 310 nm and 345 nm. The spectra of native CLIC1 show a maximum emission wavelength at ~345 nm. The maximum emission wavelength of unfolded CLIC1 shifts to ~356 nm. Like CD ellipticity at 222 nm, the fluorescence intensity at 345 nm displays a relatively large difference between the spectra of native and unfolded CLIC1. It can, therefore, serve as a good probe to monitor changes in tertiary structure of CLIC1. Previous equilibrium unfolding studies at pH 5.5 have shown that, when plotted using emission intensity at 310 nm, the unfolding curve of CLIC1 does not display a single sigmoidal transition (Fanucchi *et al.*, 2008). Therefore, fluorescence intensity at 310 nm was selected as a probe to demonstrate the appearance of the intermediate. In addition, the IAEW of CLIC1 was also plotted against urea concentration of 0 ~ 8 M to create unfolding curves as an indication of the intermediate.

The unfolding curves (F_{310} , F_{345} , and E_{222}) obtained from equilibrium unfolding studies at pH 7.0 and at pH 5.5 were globally fit to a two-state model or a three-state model, respectively. Global analyses of data involve the simultaneous analysis of multiple data sets

from different experiments with reference to internally unified sets of fitting parameters (Beechem, 1992). The advantage of global analysis is that using consistent parameters to analyse all sets of data gives more precise results than the separate fits. All the data fitting were performed using a nonlinear least-squares programme, Savuka 6.2.26 (Zitzewitz *et al.*, 1995; Bilsel *et al.*, 1999).

Two-state monomer unfolding mechanism:

A two-state equilibrium unfolding mechanism for a monomeric protein is presented as $N \leftrightarrow U$, where N and U represent the native and the unfolded states, respectively. This mechanism assumes that the protein can only be in the native state or in the unfolded state along the unfolding transition. Therefore, if we sum up the fraction of the native protein (f_N) and the fraction of the unfolded protein (f_U), the value is 1.

$$f_N + f_U = 1 \quad (5)$$

The observed values (y) using CD or fluorescence as a probe at any point along the unfolding transition will be:

$$y = y_N f_N + y_U f_U \quad (6)$$

where y is the recorded value obtained from CD or fluorescence; y_N and y_U are the values of y of the native and unfolded protein, respectively. Then, combining equation 5 and 6 leads to:

$$f_U = (y_N - y) / (y_N - y_U) \quad (7)$$

$$f_N = (y_U - y) / (y_U - y_N) \quad (8)$$

An equilibrium constant between the native protein and the unfolded protein, K_{eq} , can be calculated using the following equation:

$$\begin{aligned} K_{eq} &= f_U / f_N \\ &= (y_N - y) / (y - y_U) \end{aligned} \quad (9)$$

The free energy change, ΔG , is a measure of stability of a protein in the unfolding reaction. ΔG will be:

$$\begin{aligned}\Delta G &= -RT \ln K_{eq} \\ &= -RT \ln \left[(y_N - y) / (y - y_U) \right]\end{aligned}\quad (10)$$

where R represents the universal gas constant ($1.987 \text{ cal. mol}^{-1} \cdot \text{K}^{-1}$); T is the temperature in kelvin.

Two important parameters, $\Delta G(\text{H}_2\text{O})$ and the m -value, can be obtained from equilibrium unfolding curves using the linear extrapolation method (Greene and Pace, 1974). This method is based on the assumption that ΔG has a linear dependence on denaturant concentration in the transition region and can be tracked back to zero denaturant concentration to obtain the ΔG values in the absence of denaturant ($\Delta G(\text{H}_2\text{O})$) using the following equation:

$$\Delta G = \Delta G(\text{H}_2\text{O}) - m[\text{denaturant}] \quad (11)$$

In a two-state unfolding mechanism, the C_m value represents the midpoint of the unfolding curves and is defined as the denaturant concentration at which the native and the unfolded species are equally populated at equilibrium. The C_m value was obtained using the equation:

$$C_m = \Delta G(\text{H}_2\text{O}) / m \quad (12)$$

Three-state monomer unfolding mechanism:

A three-state equilibrium unfolding mechanism for a monomeric protein is presented as $N \leftrightarrow I \leftrightarrow U$, where I represents the intermediate detected at equilibrium. This mechanism states that the protein can be in the native, intermediate or the unfolded state. Therefore, the sum of fraction of the native, intermediate and unfolded protein can be written as:

$$f_N + f_I + f_U = 1 \quad (13)$$

where f_N , f_I and f_U represents the fraction of the native, intermediate and unfolded protein,

respectively. In this model, there are two equilibrium constants: K_1 for the $N \leftrightarrow I$ transition and K_2 for the $I \leftrightarrow U$ transition. The equilibrium constants K_1 and K_2 can be written as:

$$K_1 = f_I / f_N \quad (14)$$

$$K_2 = f_U / f_I \quad (15)$$

Therefore, the equilibrium constant for the whole reaction ($N \leftrightarrow U$ transition) is:

$$K_U = K_1 K_2 \quad (16)$$

The observed signal, y , can be written as:

$$y = y_N f_N + y_I f_I + y_U f_U \quad (17)$$

In terms of K_1 and K_2 , equation 13 can be described as:

$$f_U + (f_U / K_1 K_2) + (f_U / K_1) = 1 \quad (18)$$

Therefore, we can get:

$$f_U = K_1 K_2 / (K_1 K_2 + 1 + K_1) \quad (19)$$

$$f_I = K_1 / (K_1 K_2 + 1 + K_1) \quad (20)$$

$$f_N = 1 / [(K_1 K_2 + 1 + K_1) / (K_1 K_2)] \quad (21)$$

The $\Delta G(H_2O)_I$ and $\Delta G(H_2O)_{II}$ can be obtained from equation 22 and 23:

$$\Delta G(H_2O)_I = -RT \ln K_1 \quad (22)$$

$$\Delta G(H_2O)_{II} = -RT \ln K_2 \quad (23)$$

Also,

$$\Delta G_I = \Delta G(H_2O)_I - m_I [\text{denaturant}] \quad (24)$$

$$\Delta G_{II} = \Delta G(H_2O)_{II} - m_{II} [\text{denaturant}] \quad (25)$$

where subscript I and II represent the $N \leftrightarrow I$ and $I \leftrightarrow U$ transitions, respectively.

Therefore,

$$K_1 = e^{(m_I [\text{denaturant}] - \Delta G(H_2O)_I) / RT} \quad (26)$$

$$K_2 = e^{(m_{II} [\text{denaturant}] - \Delta G(H_2O)_{II}) / RT} \quad (27)$$

Combining equations 19 ~ 27 with equation 17, the final fit is obtained as:

$$y = \left[y_N + y_I K_1 + y_U K_1 K_2 \right] / \left[1 + K_1 + K_1 K_2 \right] \quad (28)$$

where K_1 is $e^{(m_I [\text{denaturant}] - \Delta G(\text{H}_2\text{O})_I) / RT}$ and K_2 is $e^{(m_{II} [\text{denaturant}] - \Delta G(\text{H}_2\text{O})_{II}) / RT}$.

From the three-state global fit, $\Delta G(\text{H}_2\text{O})_I$ and $\Delta G(\text{H}_2\text{O})_{II}$ were obtained. The fractional population of the native, the intermediate and the unfolded protein was calculated from K_1 and K_2 using equation 19 to 21.

2.2.6. Unfolding kinetics

Equilibrium unfolding studies provide information about conformational stability of proteins while unfolding kinetics studies are used to detect the presence of transient intermediates that emerge during the unfolding process and enable the construction of the specific unfolding pathway. In this study, the kinetics of CLIC1 unfolding was separated into three sections: unfolding from the native state (N) to the unfolded state (U), from N to the intermediate state (I), and from I to U. All the unfolding experiments were conducted with a final concentration of 2 μM CLIC1 at 20°C using a manual mixing method. The CD ellipticity at 222 nm (E_{222}) and fluorescence intensity at 345 nm (F_{345}) with an excitation wavelength of 280 nm were used as probes to monitor any change in structure of the protein over time. To prevent the separation of urea from the buffer, a stirring apparatus was used for all fluorescence-monitored unfolding kinetic experiments.

For unfolding kinetics of the N \rightarrow U transition, native CLIC1 was added to a solution of a final concentration of 5.5 M to 8 M urea (which represents the posttransition region in the equilibrium unfolding studies) at pH 7.0 and pH 5.5 to produce unfolded protein. The data recording time ranges using fluorescence and CD as probes for the N \rightarrow U transitions at

pH 7.0 and pH 5.5 were at most 2 hours and 10 minutes, respectively. Since the intermediate state is only detectable at pH 5.5, the unfolding experiments of the N→I and the I→U transitions were only performed at pH 5.5. For the unfolding experiments of the N→I transition, native CLIC1 was added to a solution of a final concentration of 3 to 4 M urea (which corresponds to the condition where the intermediate appears in the equilibrium unfolding studies). The unfolding traces of the N→I transition were recorded using both probes over at most 1 hour. For the I→U transition, CLIC1 was incubated in the presence of 3.4 M urea (the condition where the intermediate is most populated) for one hour to obtain the equilibrium intermediate. The intermediate was then unfolded in the presence of 5.5 to 7 M urea and the unfolding traces were recorded over at most 20 minutes.

The native baselines (the N→U transition and the N→I transition) were obtained from the signal of native protein at both pH values. The intermediate baselines for the N→I and the I→U transition were constructed by measuring the signal of native protein incubated in the presence of 3 ~ 4 M or 3.4 M urea for at least one hour, respectively. The unfolded baselines (the N→U and the I→U transition) were acquired from the signal of native protein incubated in the presence of 5 to 7 M urea (depending on the experiments) for at most 2 hours. All the measurements were repeated three times. The data analysis was done on all of the three recorded kinetic traces from each experiment using SigmaPlot® v11.0 and the results of analysis were then averaged.

Data analysis

In this study, all the kinetics data were fit to the exponential decay model. Depending on the data, the kinetics trace was fitted to either a single or double exponential model. However, there was an exception: the N → I transition. For this transition, all the fluorescence-monitored traces were fitted to two separate single exponential models using the

minimum of each trace as a boundary. The single and double exponential models can be described using the general equation shown in the following:

$$A_{(t)} = y_0 + \sum A_i e^{-K_i t} \quad (29)$$

$A_{(t)}$ represents the observed ellipticity from circular dichroism or the observed fluorescence intensity, t is time, y_0 is the amplitude from the beginning to the end of each kinetic trace at given time, K_i and A_i are the apparent rate constant and the amplitude of the phase i , respectively. The residuals for each plot were computed to facilitate better choice of the two models and presented to indicate the quality of each fitting. The obtained apparent unfolding rate constants for each trace were then plotted against different final urea concentrations to construct chevron plots. To obtain the unfolding rate constant in the absence of denaturant, every chevron plot was fit to linear regression using the following equation:

$$\log(k_u) = \log(k_u(\text{H}_2\text{O})) + m_u [\text{denaturant}] \quad (30)$$

where k_u is the apparent rate constant for unfolding at different urea concentrations, $k_u(\text{H}_2\text{O})$ is the value of apparent unfolding rate in the absence of denaturant, and m_u represents the amount of exposed surface area to the solvent at different denaturant concentrations during unfolding.

3. Results

3.1. CLIC1 expression and purification

SDS-PAGE (Figure 6) was utilised to demonstrate the process of the purification and to confirm the purity of purified CLIC1. IPTG (final concentration 1 mM) was confirmed to induce the overexpression of GST-CLIC1 fusion protein (Figure 6A, lanes 2 and 3). The GST-CLIC1 fusion protein demonstrates a molecular weight of approximately 58 kDa on the SDS-PAGE gel. After harvesting, the fusion protein appeared to be soluble and was mainly present in the supernatant compared to the small fraction of insoluble protein, which remained in the pellet (Figure 6A, lanes 4 and 5). The fusion protein was separated from all other cellular proteins by using the affinity between the GST fusion protein and a GSH-coated resin, GSH-Sepharose. The supernatant of the lysed cells was loaded on the GSH-Sepharose column and the flow-through was collected once the fusion protein bound to the column. Comparing the much smaller band representing the fusion protein in the flow-through with the larger band of the fusion protein in the supernatant indicates that most of the fusion protein was captured and retained on the GSH-Sepharose column (Figure 6A, lanes 4 and 6).

Thrombin was used to separate fused GST and CLIC1. After thrombin cleavage on the GSH-Sepharose column for 16 hours, CLIC1 and thrombin were recovered from the GSH-Sepharose column (Figure 6B, lane 2). The GST remained bound to the column and was then eluted with a high concentration of GSH. The eluted GST is displayed on the gel along with a band at 58 kDa representing uncleaved fusion protein (Figure 6B, lane 3). Since the band of uncleaved fusion protein is tiny when compared to the thick band of the cleaved GST, the cleavage was relatively efficient.

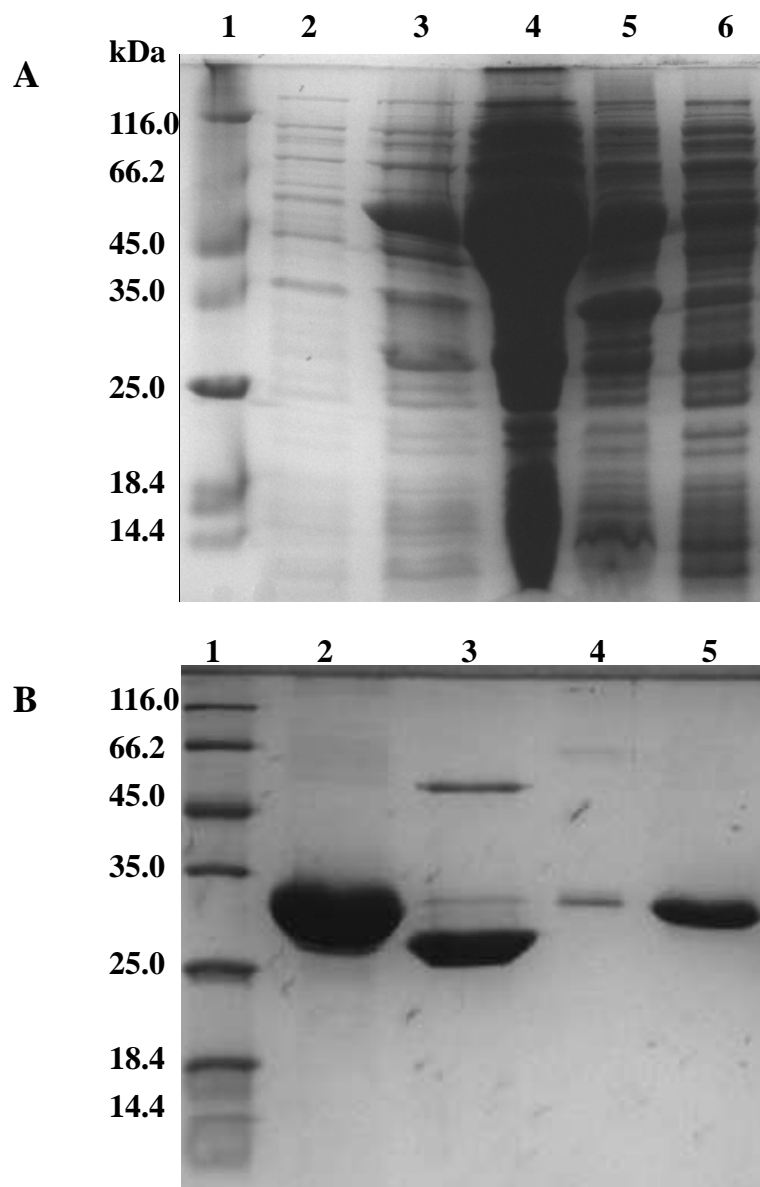


Figure 6: SDS-PAGE gels illustrating a representative purification process of CLIC1

(A) Lane 1 contains molecular weight markers; lanes 2 and 3 contain whole *E. coli* cell extract before and after induction with 1 mM IPTG, respectively; lanes 4 and 5 contain supernatant and pellet of the lysed cells, respectively. Lane 6 shows the flow-through from the GSH-sepharose column indicating that most of the fusion protein bound. The GST-CLIC1 fusion protein is displayed on the gel with a molecular mass of approximately 58 kDa. (B) Lane 1 contains a molecular weight marker. Lane 2 shows CLIC1 and thrombin mixture recovered from the GSH-Sepharose column. Lane 3 displays the cleaved GST with a small amount of uncleaved fusion protein from the GSH-sepharose column. Lane 4 contains the separated thrombin. Purified CLIC1 with an apparent molecular mass of approximately 32 kDa is shown in lane 5.

CLIC1 has a *pI* value of 4.85, and thus it is negatively charged at pH 6.5 and binds to the positively charged DEAE-Sepharose resin. Thrombin, in contrast, with a *pI* value of 7~7.6 (Fenton *et al.*, 1977) is positively charged and does not bind to the DEAE-Sepharose resin at pH 6.5. Therefore, the CLIC1 recovered from the GSH-Sepharose column was able to be separated from thrombin by DEAE anion exchange chromatography at pH 6.5. Human thrombin demonstrates a molecular weight of 36.6 kDa on SDS-PAGE gels (Fenton *et al.*, 1977). In this study, the eluted thrombin migrates a distance which corresponds to a molecular size of approximately 34 kDa (Figure 6B, lane 4) on the SDS-PAGE gel, which is slightly smaller when compared to the result shown by Fenton *et al.*, 1977. The DEAE-bound CLIC1 was then eluted with an increased salt concentration of 300 mM NaCl at pH 6.5. Purified CLIC1 demonstrates a molecular weight of approximately 32 kDa (Figure 6B, lane 5 and Figure 7). The theoretical molecular weight of CLIC1 is 26.9 kDa. It has been demonstrated that CLICs, on SDS-PAGE gels, display a higher molecular weight than their theoretical molecular weights (Tulk and Edwards, 1998; Berryman and Bretsher, 2000; Tulk *et al.*, 2000; Board *et al.*, 2004). A possible reason for this unusual migration is that the acidic nature of CLIC1 has an influence on SDS binding (Lehtovaara, 1978). The negative charge of CLIC1 might reduce the SDS:protein ratio and further lower the mobility of the protein. To conclude, the lone band of the CLIC1 sample indicates that CLIC1 was purified successfully.

For protein concentration determination of CLIC1, the Beer-Lambert law was used. The yield of CLIC1 from 4 litres of cell culture was calculated to be approximately 80 mg. The $A_{280}:A_{260}$ ratio was close to 1.8, indicating that there was no significant DNA contamination (Figure 8).

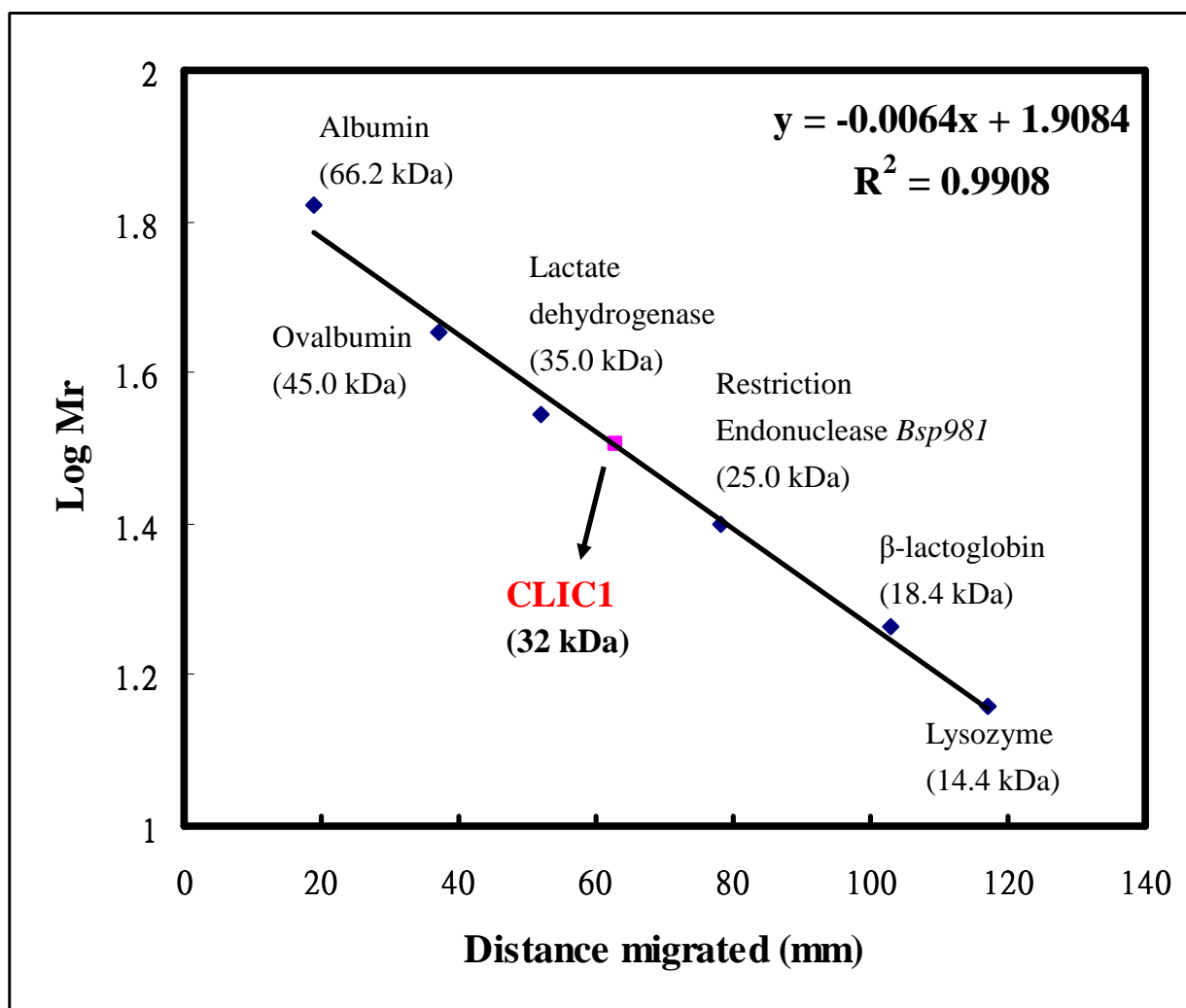


Figure 7: Calibration curve obtained from the SDS-PAGE gel

The curve was constructed from the log values of the molecular weight (in kDa) of molecular weight marker against their migrated distances on the gel. The molecular weight of CLIC1 was calculated as 32 kDa.

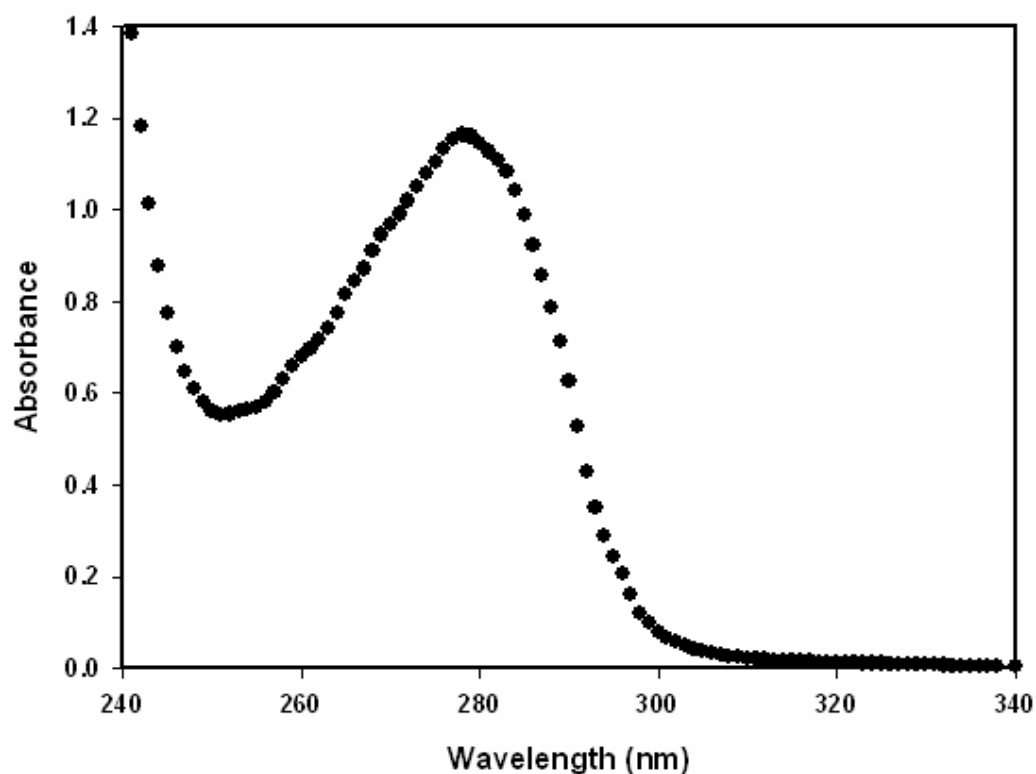


Figure 8: Absorbance spectrum of purified CLIC1

The absorbance of CLIC1 at 280 nm is 1.14, this corresponds to a protein concentration of 66 μ M. There is no significant DNA contamination detectable in the purified protein since the $A_{280}:A_{260}$ ratio is close to 1.8. The negligible absorbance at 340 nm indicates that the level of aggregation is negligible.

3.2. Structural characterisation of CLIC1

Secondary structure

Far-UV CD (190-250 nm) was performed to study the secondary structural content of the native and unfolded states of CLIC1 at pH 7.0 and pH 5.5. Two minima at 208 and 222 nm are shown in the spectra of native CLIC1 at both pH values (Figure 9), which is typical for α -helical proteins (Woody, 1995).

The CD spectra of native CLIC1 at pH 5.5 shows about 18% reduction in the CD signal compared to at pH 7.0 (Figure 9). This indicates a lower secondary structural content under this condition (at pH 5.5). However, the two clear minima demonstrate that the entire secondary structure is still mainly α -helical and not significantly different from the one at pH 7.0. The result suggests that the pH level only has a small effect on the secondary structure of the native state of CLIC1.

The spectra of unfolded CLIC1 at pH 7.0 and pH 5.5 both display a spectral signature of random coil structures (Woody, 1995), suggesting that CLIC1 is unfolded in the presence of 8 M urea at either pH 7.0 or pH 5.5 and most of the predominantly α -helical secondary structure is disrupted (Figure 9).

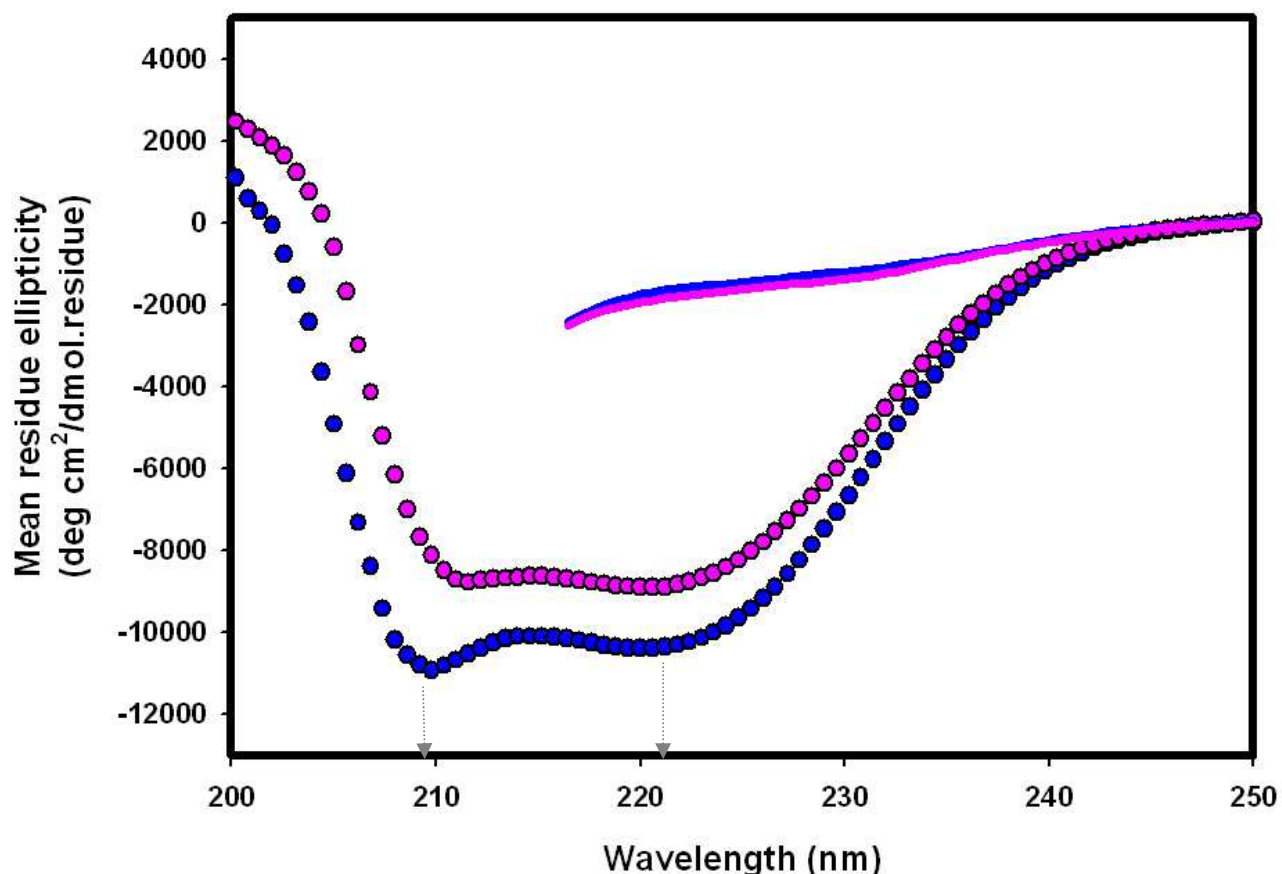


Figure 9: Comparison of the circular dichroism spectra of CLIC1 at pH 7.0 and pH 5.5

Far-UV CD spectra of 10 μ M CLIC1 at pH 7.0 (blue) and pH 5.5 (pink) recorded at 20°C. The buffers used: pH 7.0 (50 mM sodium phosphate, 0.02% NaN₃, 1 mM DTT) and pH 5.5 (50 mM sodium acetate, 0.02% NaN₃, 1 mM DTT). Two minima, one at 208 nm and one at 222 nm in the spectra of native CLIC1 (closed circles) are indicated by arrows. In the presence of 8 M urea, the spectra of unfolded CLIC1 at both pH 7.0 and pH 5.5 display a spectral pattern typical for random coil (solid lines). The spectra were smoothed using the negative exponential methodology (SigmaPlot® v11.0).

Tertiary structure

The tertiary structure of CLIC1 was monitored using fluorescence spectroscopy. This technique demonstrates specifically the environment surrounding tryptophan residues (Lakowicz, 2006). Fluorescence resonance energy transfer (FRET) is a mechanism of energy transfer between a donor chromophore in its excited state and an acceptor chromophore. In a protein, the chromophores are mainly tyrosine and tryptophan residues. When a protein is excited at 280 nm, both tyrosine and tryptophan residues are excited resulting in FRET to the final acceptor, the tryptophan residues (Lakowicz, 2006). CLIC1 has only one tryptophan, Trp35, which is located in the putative transmembrane region in the N-domain (see Figure 4) (Harrop *et al.*, 2001). In the case of CLIC1 which has one tryptophan and eight tyrosine residues, excitation at 280 nm results in a higher quantum yield than excitation at 295 nm which only excites the tryptophan residue (Figure 10).

The fluorescence spectra of native CLIC1 at both pH 7.0 and pH 5.5 show a maximum emission wavelength of 345 nm (Figure 10). The intensities of the spectra are also similar at both pH values. The maximum emission wavelength shifts when tryptophan residues are exposed to environments of different polarity (Lakowicz, 2006). The fact that the maximum emission wavelengths of the spectra at pH 7.0 and pH 5.5 are identical indicates that the location of the lone tryptophan residue of native CLIC1 at both pH values is similar. This suggests that the tertiary structure, specifically around Trp35, is not influenced by changes in pH. In the presence of 8 M urea, the maximum emission wavelength of unfolded CLIC1 shows a red shift to 356 nm (Figure 10), which indicates the exposure of the tryptophan residue to the polar solvent. The unfolding of CLIC1 also increases the distance between the lone tryptophan and the tyrosine residues, resulting in the FRET from the tyrosine to the tryptophan being disrupted. Therefore, the quantum yields of the spectra of unfolded CLIC1 are reduced and the emission from the tyrosine residues can be seen as a shoulder at 310 nm.

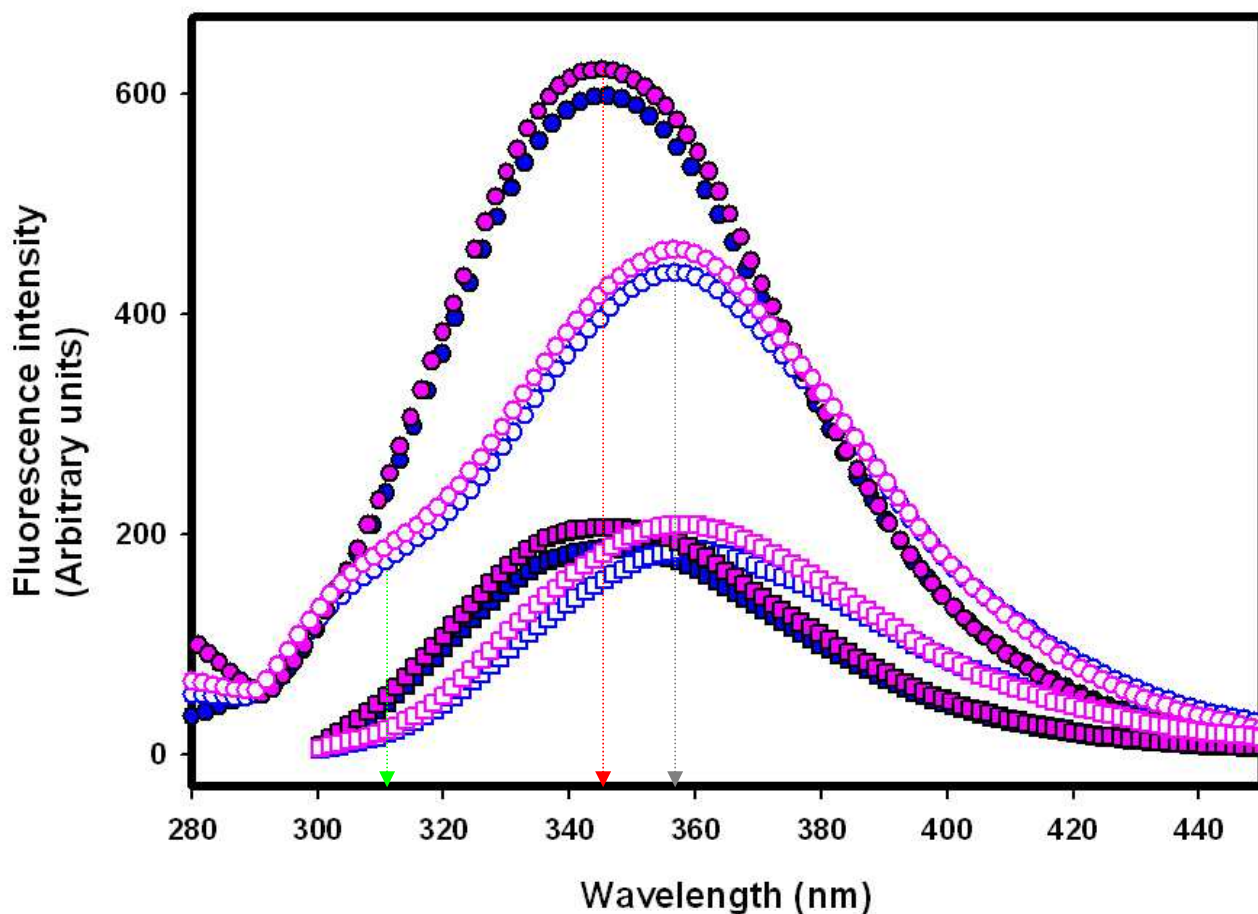


Figure 10: Comparison of the fluorescence spectra of CLIC1 at pH 7.0 and pH 5.5

Fluorescence emission spectra of 10 μ M CLIC1 at pH 7.0 (blue) and pH 5.5 (pink) when excited at 280 nm (circles) or 295 nm (squares) recorded at 20°C. Native CLIC1 (closed symbols) has a maximum emission wavelength of 345 nm (indicated by the red arrow) when excited at either 280 nm or 295 nm. Unfolded CLIC1 (open symbols) shows a red-shifted emission wavelength of 356 nm (indicated by the grey arrow) when excited at 280 nm and has a shoulder at 310 nm (indicated by the green arrow). When unfolded CLIC1 is excited at 295 nm, the spectra peak at 360 nm. The buffers used: pH 7.0 (50 mM sodium phosphate, 0.02% NaN₃, 1 mM DTT) and pH 5.5 (50 mM sodium acetate, 0.02% NaN₃, 1 mM DTT). All the spectra were smoothed using the negative exponential methodology (SigmaPlot[®] v11.0).

3.3. Urea-induced equilibrium unfolding

3.3.1. Recovery studies

It is very important for equilibrium unfolding data analysis that the unfolding reaction is at equilibrium and is reversible (Pace, 1986). Therefore, the reversibility of unfolding of a protein needs to be established in order to enable the analysis of its thermodynamic parameters obtained from equilibrium unfolding studies (Pace, 1986). Recovery and reversibility studies of CLIC1 have been previously demonstrated by Fanucchi *et al.*, 2008. The recovery of the secondary and tertiary structure of CLIC1 was conducted by denaturing native CLIC1 in the presence of 7 M urea then diluting it ten times so as to refold it. Both circular dichroism and tryptophan fluorescence were used as probes to detect any change in secondary and tertiary structure. In this study, the recovery monitored by CD at pH 7.0 and pH 5.5 is 93% and 91%, respectively (Figure 11A). The fluorescence-monitored recovery at pH 7.0 and pH 5.5 is 96% and 97%, respectively (Figure 11B). The high recovery of the native structure at pH 7.0 and pH 5.5 indicates that the unfolding of CLIC1 is reversible after denaturation in the presence of 7 M urea at both pH values. Therefore, the equilibrium unfolding curves of CLIC1 can be analysed in terms of the thermodynamic parameters.

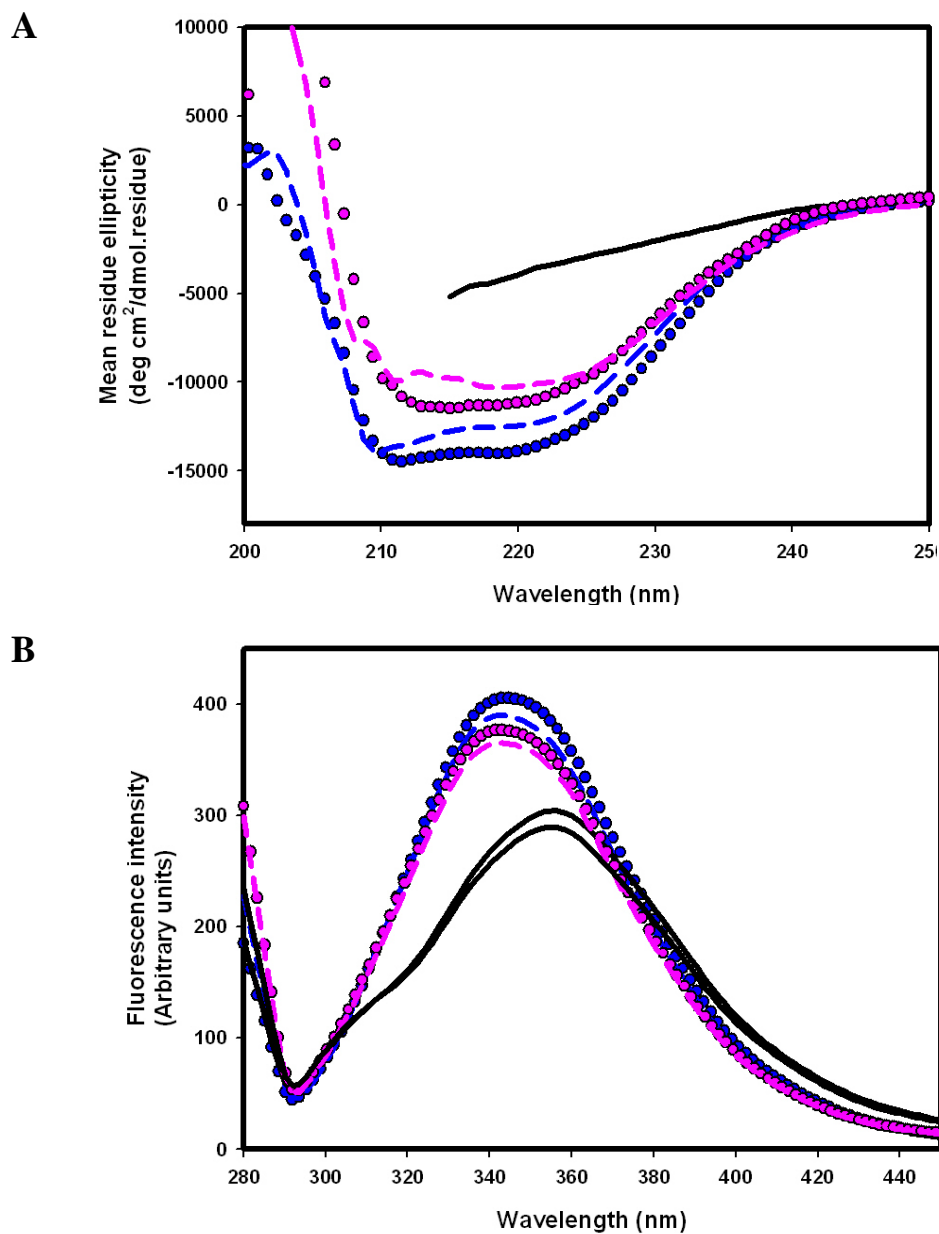


Figure 11: Recovery of secondary and tertiary structure of CLIC1

Recovery of secondary (**A**) and tertiary (**B**) structure of CLIC1 at pH 7.0 (blue) and pH 5.5 (pink). Twenty microlitres of CLIC1 was unfolded in the presence of 7 M urea and diluted 10X to refold to a concentration of 2 μ M protein in 0.7 M urea. The spectra of native and unfolded CLIC1 (7 M urea) are shown as references and are indicated with closed circles and solid lines, respectively. The spectra of refolded CLIC1 are given by dashed lines. All the spectra were smoothed using the negative exponential methodology (SigmaPlot[®] v11.0).

3.3.2. Effect of pH on the conformational stability of CLIC1

Equilibrium unfolding studies were performed using CD and fluorescence spectroscopy as probes to monitor changes in secondary and tertiary structure, respectively. The influence of pH on the equilibrium unfolding of CLIC1 is shown in Figure 12. At pH 7.0, the CD- and fluorescence-monitored unfolding curves, especially in the transition region, coincide within error and show a monophasic transition (Figure 12A). This behaviour suggests a cooperative two-state unfolding process, $N \leftrightarrow U$, where N and U represent the native and the unfolded states, respectively. Therefore, a two-state model was used to globally fit the unfolding data at pH 7.0. The global fit of the CD- and fluorescence-monitored data at pH 7.0 gives a $\Delta G(H_2O)$ of 7.9 ± 0.46 kcal/mol and a m -value of 1.8 ± 0.11 kcal/mol/M urea (Table 2).

At pH 5.5, the F_{345} -monitored curve also shows a single sigmoidal transition. However, the F_{310} - and E_{222} -monitored curves display more than one transition (Figure 12B). This suggests that the unfolding of CLIC1 at pH 5.5 cannot be described using a two-state mechanism. Therefore, the unfolding data monitored at pH 5.5 were globally fit to a three-state model, $N \leftrightarrow I \leftrightarrow U$, where I represents an intermediate. The $\Delta G(H_2O)$ and m -value for forming the intermediate species (the $N \leftrightarrow I$ transition) are 6.7 ± 1 kcal/mol and 2.5 ± 0.45 kcal/mol/M urea, respectively (Table 2). The $\Delta G(H_2O)$ and m -value for unfolding the intermediate (the $I \leftrightarrow U$ transition) are 13.7 ± 2.1 kcal/mol and 3.5 ± 0.5 kcal/mol/M urea, respectively. The $\Delta G(H_2O)$ of the $N \leftrightarrow I$ transition is smaller than the one of the $I \leftrightarrow U$ transition, suggesting that these conditions are conducive to the formation of the intermediate of CLIC1.

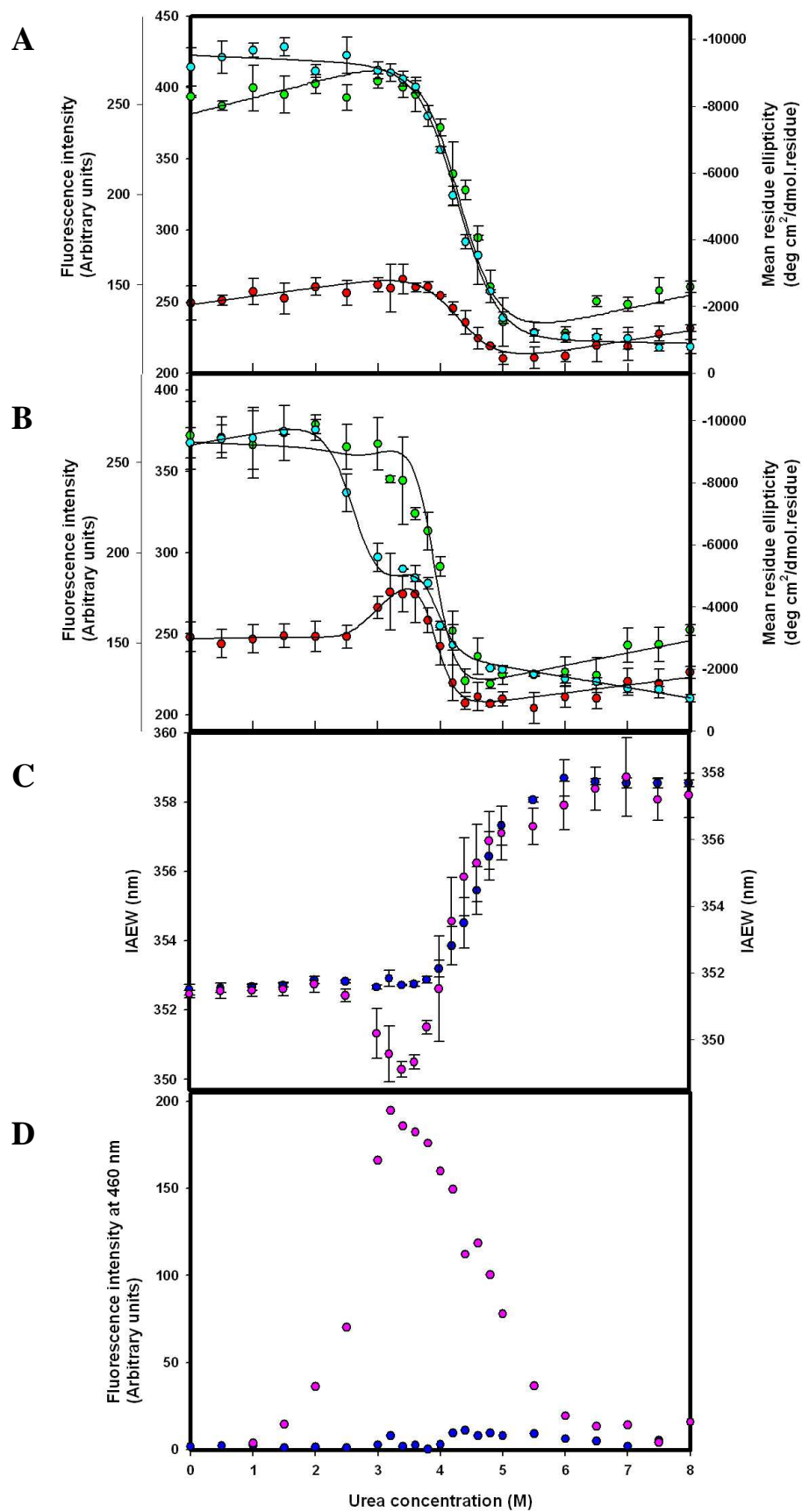


Figure 12: Equilibrium unfolding of CLIC1 at pH 7.0 and pH 5.5

Equilibrium unfolding experiments conducted on 2 μ M CLIC1 at 20°C as a function of urea at pH 7.0 (**A**) and pH 5.5 (**B**). In (**A**) and (**B**), the ellipticity at 222 nm (blue) and the fluorescence emission intensity at 310 nm and 345 nm (red and green, respectively) were used as probes. The solid lines represent the global fit of a two-state (**A**) and a three-state (**B**) model to the data. The IAEW and ANS binding as a function of urea are shown in (**C**) and (**D**), respectively, where data monitored at pH 7.0 and pH 5.5 are indicated in blue and pink, respectively. The buffers used: pH 7.0 (50 mM sodium phosphate, 0.02% NaN₃, 1 mM DTT) and pH 5.5 (50 mM sodium acetate, 0.02% NaN₃, 1 mM DTT).

Table 2: Comparison of the thermodynamic parameters obtained from the equilibrium unfolding studies at pH 7.0 and pH 5.5

	pH 7.0	pH 5.5	
	N \leftrightarrow U	N \leftrightarrow I	I \leftrightarrow U
$\Delta G(H_2O)$ (kcal/mol)	7.9 \pm 0.46	6.7 \pm 1	13.7 \pm 2.1
<i>m</i>-value (kcal/mol/M urea)	1.8 \pm 0.11	2.5 \pm 0.45	3.5 \pm 0.5
<i>C</i>_m (M urea)	4.2	2.7	3.9

The existence of the intermediate is further confirmed by intensity-averaged emission wavelength (IAEW) changes along the equilibrium unfolding transition and ANS binding studies (Figure 12 panel C and D). At pH 7.0, the IAEW curve of the fluorescence-monitored unfolding shows a single transition. At pH 5.5, a minimum at 3.4 M urea of the IAEW curve indicates that the unfolding does not follow a two-state mechanism. This transition occurs at the same urea concentrations that the peak of the F_{310} -monitored unfolding curve occurs. Furthermore, the decrease in IAEW at 2.5 ~ 4 M urea suggests that the location of the lone tryptophan moves to a more nonpolar environment than the native state under this condition.

ANS is a fluorescent dye which binds to hydrophobic patches on proteins and is often used to detect unfolding intermediates (Stryer, 1965; Semisotnov *et al.*, 1991). ANS does not bind to CLIC1 in the native and unfolded state or at any point along the unfolding transition at pH 7.0 (Figure 12D). At pH 5.5, the binding of ANS increases from 2 to 5.5 M urea and peaks at 3.4 M urea which corresponds to the condition where the decrease in IAEW and the peak in the F_{310} -monitored curve occur (Figure 12 C and D).

In addition, the population plot calculated from the global fitting shows that the intermediate is most highly populated in the presence of 3.4 M urea. Approximately 91% of species are in the intermediate state under this condition (Figure 13). The high intermediate population is significant for the feasibility of the subsequent kinetics studies (the $N \rightarrow I$ and $I \rightarrow U$ transitions).

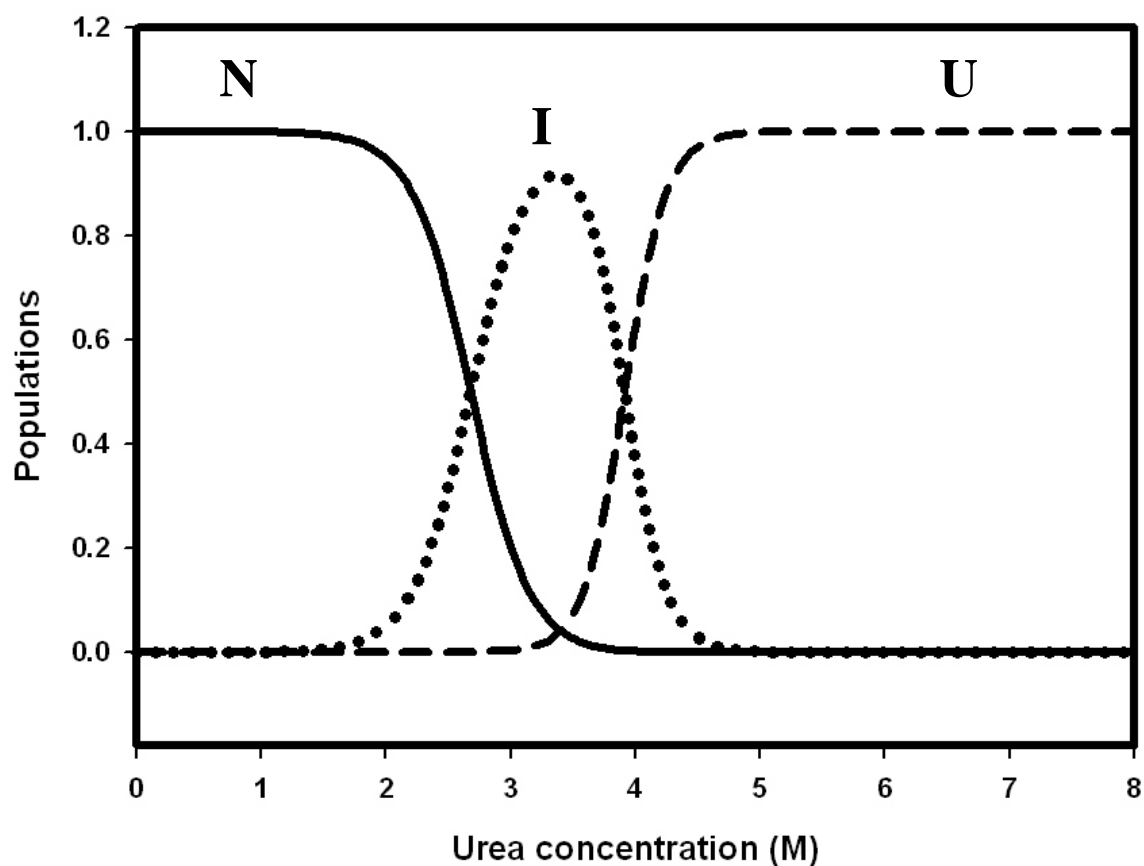


Figure 13: Fractional populations plot of CLIC1 as a function of urea concentrations at pH 5.5

The populations were obtained from the global fitting of the equilibrium unfolding to a three-state model. The native (N), unfolded (U) and intermediate (I) populations are indicated in solid, dashed and dotted lines, respectively.

3.3.3. Structure of the intermediate

The equilibrium unfolding studies of CLIC1 at pH 5.5 indicate the appearance of an intermediate species that is stable at equilibrium under mild denaturing conditions (Figure 12). In order to obtain the intermediate species, CLIC1 was incubated in the presence of 3.4 M urea at pH 5.5, which corresponds to the highest population of the intermediate relative to the native and unfolded state. The secondary and tertiary structure of the intermediate state of CLIC1 were then further characterised using far-UV circular dichroism and intrinsic tryptophan fluorescence spectroscopy, respectively. ANS binding was also performed to establish the hydrophobicity of this intermediate species.

Secondary structure

The far-UV CD spectra of the native and the intermediate states of CLIC1 are shown in Figure 14. For comparison, CLIC1 was also incubated in 3.4 M urea at pH 7.0. When CLIC1 is exposed to 3.4 M urea at pH 7.0, the secondary structure does not change significantly compared to native CLIC1 at pH 7.0 (Figure 14). This result is consistent with the fact that there is no detectable intermediate species under these conditions. At pH 5.5, however, CLIC1 intermediate displays an approximate 40% loss in secondary structure from that of the native state at pH 5.5 (Figure 14).

Tertiary structure

The fluorescence spectra of the native and the intermediate states of CLIC1 are shown in Figure 15. At both pH 7.0 and pH 5.5, the fluorescence emission intensities between the spectra of native CLIC1 and CLIC1 in the presence of 3.4 M urea do not show a significant difference (Figure 15). The maximum emission wavelengths of the spectra of native CLIC1 and CLIC1 at 3.4 M urea both locate at 345 nm at pH 7.0. However, the maximum emission

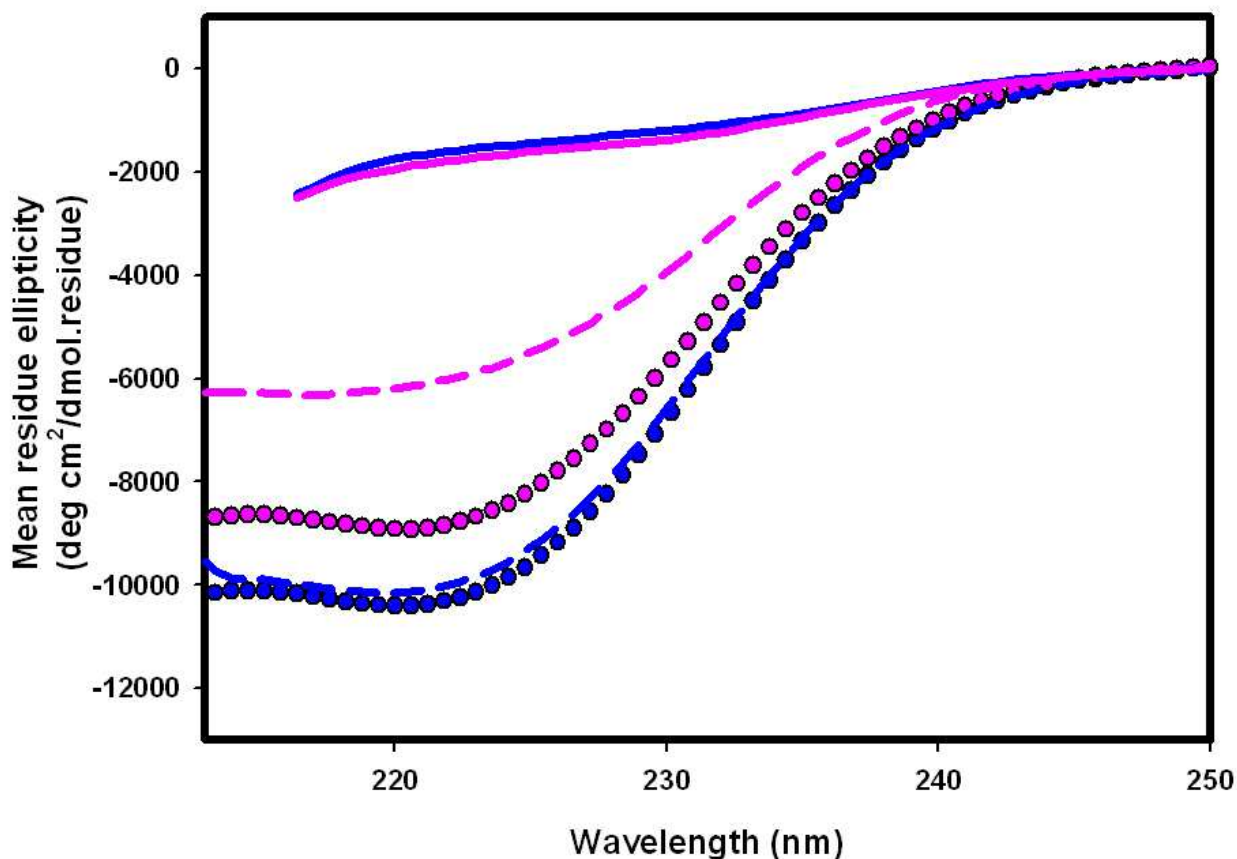


Figure 14: Comparison of CD spectra of the native and the intermediate state

Far-UV CD spectra of 2 μ M CLIC1 at pH 7.0 (blue) and pH 5.5 (pink) recorded at 20°C. The buffers used: pH 7.0 (50 mM sodium phosphate, 0.02% NaN₃, 1 mM DTT) and pH 5.5 (50 mM sodium acetate, 0.02% NaN₃, 1 mM DTT). At pH 7.0, CD spectra of CLIC1 in the native state (closed circles) and in the presence of 3.4 M urea (dashed lines) do not display a significant difference, indicating a similar secondary structural content. At pH 5.5, the intermediate state of CLIC1 at 3.4 M urea only retains approximately 60 % of the secondary structure compared to the native state. The spectra of unfolded CLIC1 are indicated with solid lines. The spectra were smoothed using the negative exponential methodology (SigmaPlot[®] v11.0).

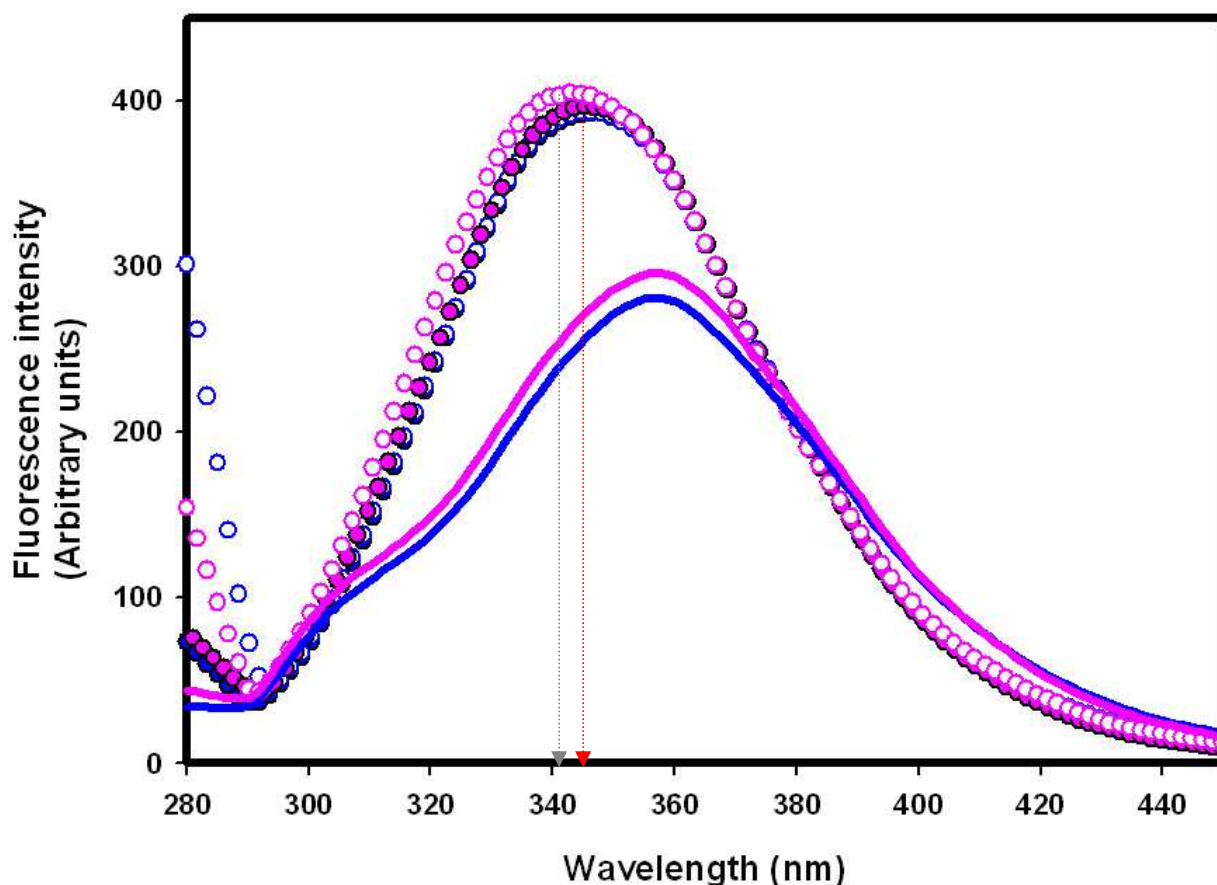


Figure 15: Comparison of tryptophan fluorescence spectra of the native and the intermediate state of CLIC1

Fluorescence spectra of 2 μ M CLIC1 at pH 7.0 (blue) and pH 5.5 (pink) recorded at 20°C. The excitation wavelength of the measurements was 280 nm. The buffers used: pH 7.0 (50 mM sodium phosphate, 0.02% NaN₃, 1 mM DTT) and pH 5.5 (50 mM sodium acetate, 0.02% NaN₃, 1 mM DTT). At pH 7.0, CLIC1 in the native state (closed symbols) and in the presence of 3.4 M urea (open symbols) do not show a significant difference in either intensity or maximum emission wavelength. The spectrum of the intermediate state exhibits a blue shift from 345 nm (indicated by the red arrow) to about 340 nm (indicated by the grey arrow) at pH 5.5, which indicates a more embedded tryptophan. The spectra of unfolded CLIC1 are shown with solid lines. All the spectra were smoothed using the negative exponential methodology (SigmaPlot[®] v11.0).

wavelength of the spectra at pH 5.5 shifts from 345 nm in the native state to approximately 340 nm in the intermediate state (in the presence of 3.4 M urea). This blue shift indicates that CLIC1 in the intermediate state has a more embedded tryptophan in the tertiary structure when compared to the native state.

ANS binding

Free ANS in the absence of protein produces a fluorescent peak at 510 nm when excited at 390 nm. Once ANS binds to hydrophobic clusters on a protein, the maximum emission will show a blue shift toward lower wavelength and the intensity will increase largely (Lakowicz, 2006). Representative spectra of CLIC1 in the presence of ANS at pH 7.0 and pH 5.5 are shown in Figure 16. The spectra of CLIC1 show that ANS does not bind to native CLIC1 at both pH 7.0 and pH 5.5. Furthermore, ANS does not bind to CLIC1 when in the presence of 3.4 M urea at pH 7.0 either. This is consistent with the results obtained from the equilibrium unfolding studies showing that ANS does not bind to CLIC1 over the entire unfolding transition at pH 7.0 (Figure 12D). At pH 5.5, however, the maximum emission wavelength of the ANS spectra of the CLIC1 intermediate shifts to 465 nm and the intensity of the emission increases significantly, indicating that ANS binds to hydrophobic patches on the surface of the CLIC1 intermediate (Figure 16). To conclude, CLIC1 in the intermediate state, which forms in the presence of 3.4 M urea at pH 5.5, has far more exposed hydrophobic patches on its surface than in the native or the unfolded state at both pH 7.0 and pH 5.5.

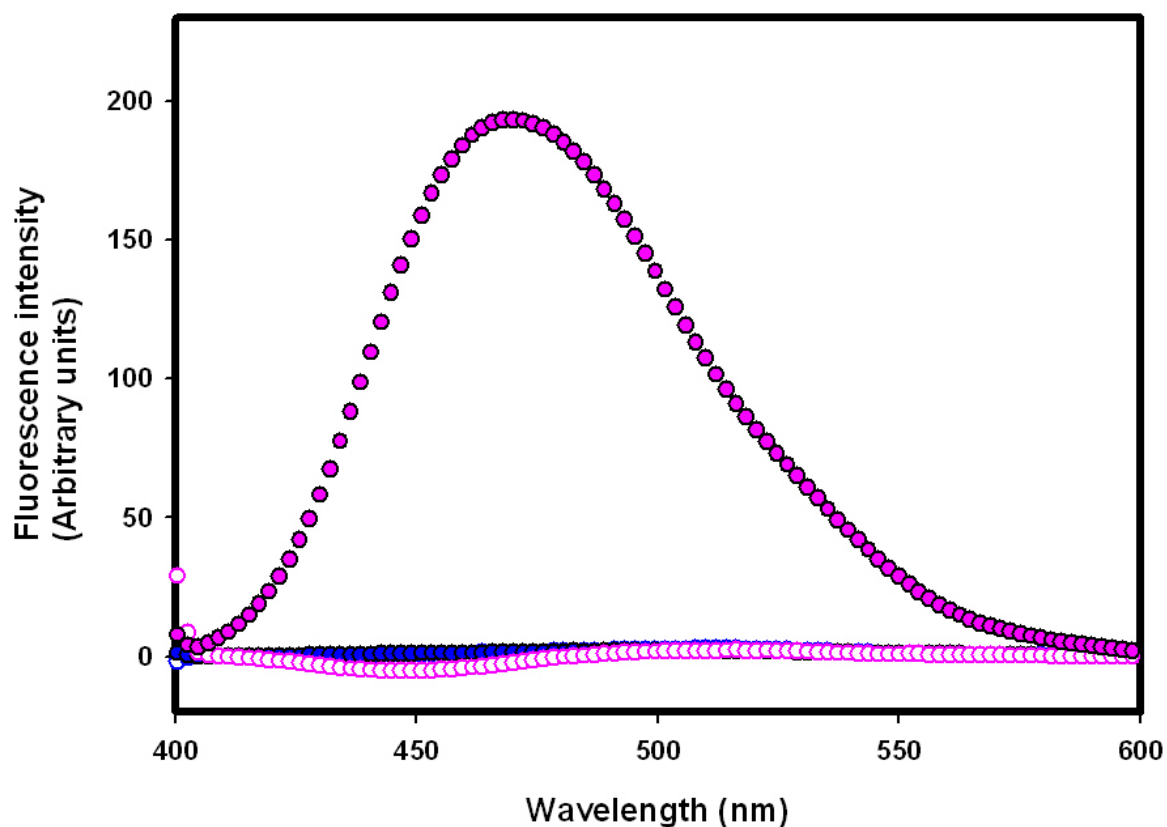


Figure 16: ANS binds to the intermediate state of CLIC1

The ANS binding spectra of 2 μM CLIC1 in the native state (open symbols) and in the presence of 3.4 M urea (closed symbols) at pH 7.0 (blue) and pH 5.5 (pink) after incubation with 200 μM ANS for one hour. Only the spectrum of the CLIC1 intermediate (pH 5.5 and 3.4 M urea) displays a significant quantum yield when compared to the protein in the native state at both pH and in the presence of 3.4 M urea at pH 7.0, indicating that ANS only binds to the intermediate state. The excitation wavelength of the spectra is 390 nm. All the spectra were corrected for free ANS. The spectra were smoothed using the negative exponential methodology (SigmaPlot[®] v11.0).

3.4. Unfolding kinetics

Unfolding kinetics studies were performed to uncover the unfolding pathway of CLIC1. In the equilibrium unfolding studies, CLIC1 follows a two-state unfolding transition at pH 7.0 while at pH 5.5 it forms an intermediate in the presence of 2.5 ~ 4 M urea (see section 3.3.2.). Therefore, the unfolding kinetics studies were divided into three transitions: $N \rightarrow U$, $N \rightarrow I$ and $I \rightarrow U$, where N, I and U represent the native, the equilibrium intermediate and the unfolded states of CLIC1, respectively. CD ellipticity at 222 nm (E_{222}) and fluorescence intensity at 345 nm (F_{345}) were used to monitor the rate of unfolding of the secondary and tertiary structure, respectively. Since the signals of E_{222} and F_{345} show the largest difference between native and unfolded CLIC1, these two probes were chosen for clear indication of change in structure.

The $N \rightarrow U$ transition

CLIC1 was denatured from the native state (N) to the unfolded state (U) by adding the protein into urea with a concentration ranging from 5.5 M to 8 M which represents the post-transition region of the equilibrium unfolding curves (Figure 12). Representative unfolding traces for CLIC1 at pH 7.0 and pH 5.5 at a final urea concentration of 7 M urea are shown in Figure 17. For the $N \rightarrow U$ transition, all the unfolding traces fit to a single exponential model without any detectable burst phase at both pH 7.0 and pH 5.5. The urea dependence of the unfolding rate constants at pH 7.0 and pH 5.5 was plotted to obtain the $k_u(\text{H}_2\text{O})$ and m_u values (Figure 18). All the parameters obtained from unfolding kinetic studies are shown in Table 3. The unfolding rate in the absence of denaturant, $k_u(\text{H}_2\text{O})$, is an estimate of the *in vivo* unfolding rate of a protein. The m_u value gives a measure of the amount of surface area exposed in the transition state as a protein unfolds (Myers *et al.*, 1995).

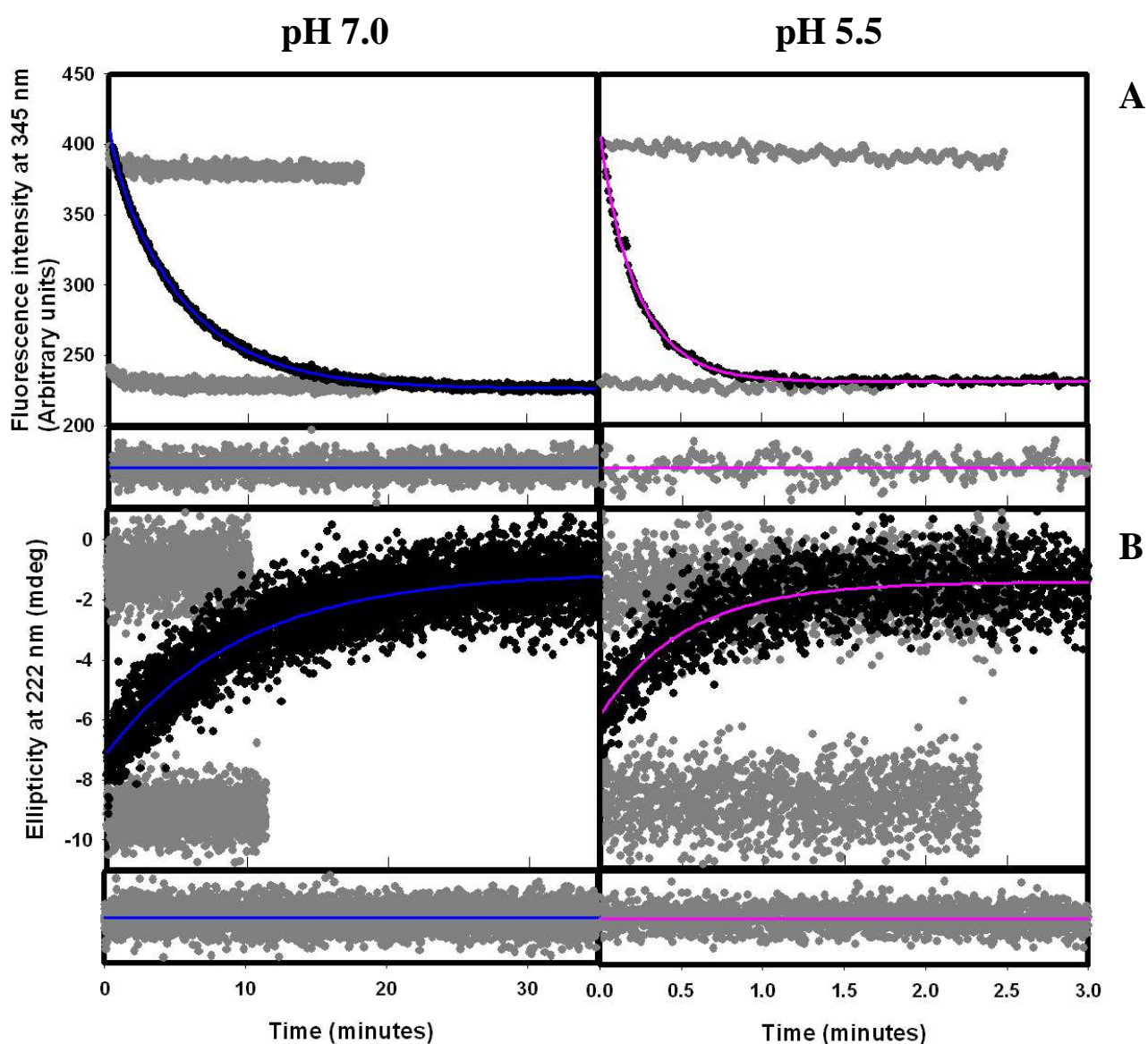


Figure 17: Representative unfolding kinetic traces for the N \rightarrow U transition at pH 7.0 and pH 5.5

The protein was unfolded in the presence of urea at a final concentration of 7 M and the structural changes were monitored by F₃₄₅ (A) and E₂₂₂ (B) as probes. The solid lines represent the fit to a single exponential model at pH 7.0 (blue) and pH 5.5 (pink) and the residuals from the fit are also plotted in the panels beneath each figure. The baselines of native and unfolded (7 M urea) CLIC1 are indicated in grey and show that no burst phase is present.

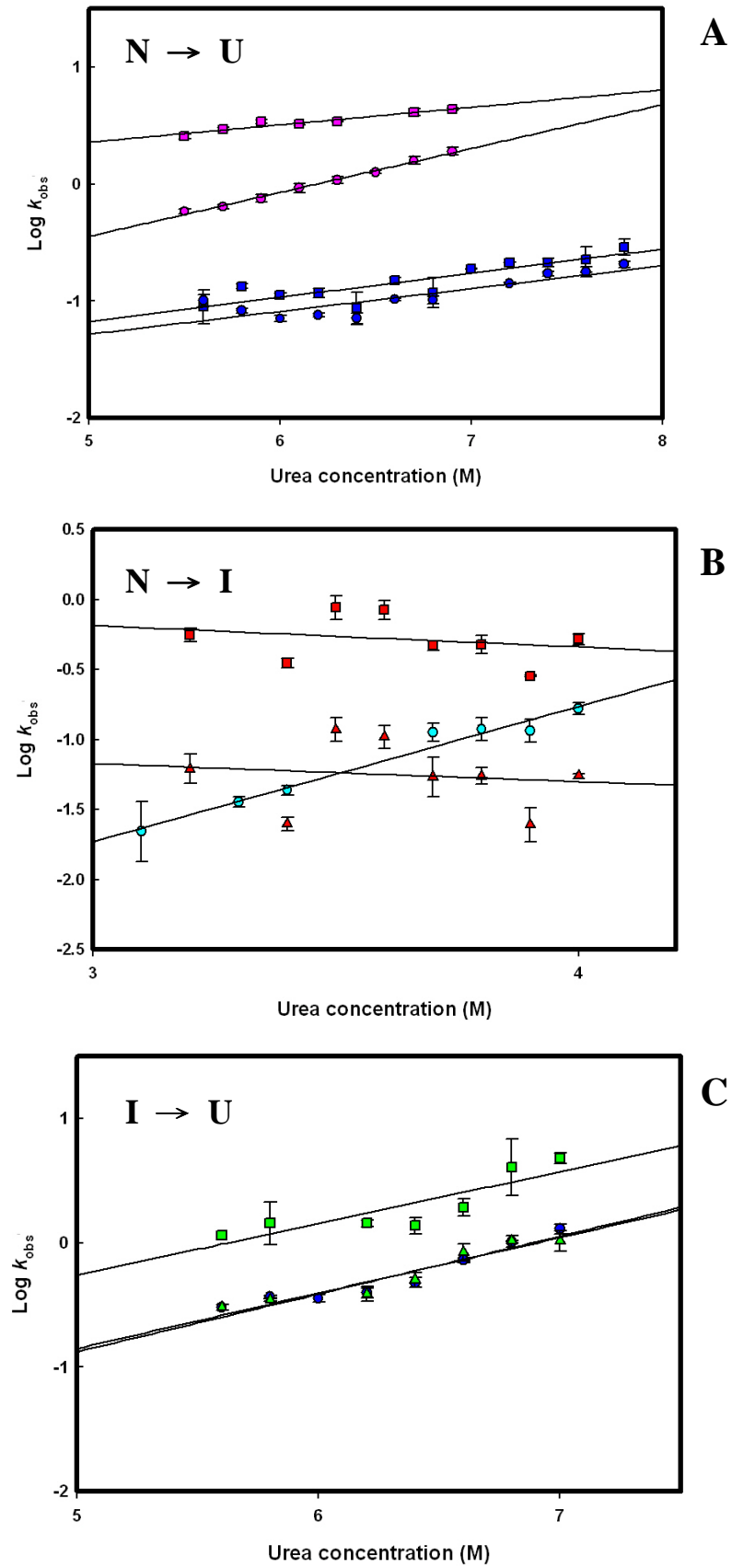


Figure 18: Urea dependence of the unfolding rate constants

Unfolding kinetics experiments were performed at 20°C using circular dichroism ellipticity at 222 nm (circles) and fluorescence emission at 345 nm (squares as single or fast phase and triangles as slow phase) as probes. All the kinetic traces were fitted to either a single or a double exponential model. The urea dependence of the unfolding rate constants (k_{obs}) were plotted and fitted to a linear regression to acquire the slope (m_u values) and apparent unfolding rate in the absence of denaturant, $k_u(\text{H}_2\text{O})$. **(A)** Unfolding of the N \rightarrow U transition at pH 7.0 (blue) and pH 5.5 (pink). **(B)** Unfolding of the N \rightarrow I transition. **(C)** Unfolding of the I \rightarrow U transition.

Table 3: Parameters for the unfolding kinetics of CLIC1 at pH 7.0 and pH 5.5

		m_u (kcal/mol/M urea)		$k_u(\text{H}_2\text{O})$ (min^{-1})	
		CD	Fluorescence	CD	Fluorescence
pH 7.0	N \rightarrow U	0.19 ± 0.02	0.21 ± 0.03	5.6×10^{-3} ($\pm 1.8 \times 10^{-3}$)	6.1×10^{-3} ($\pm 2.4 \times 10^{-3}$)
pH 5.5	N \rightarrow U	0.37 ± 0.01	0.15 ± 0.01	4.8×10^{-3} ($\pm 8.8 \times 10^{-4}$)	0.4 (± 0.08)
	N \rightarrow I	0.97 ± 0.07	Fast phase: -0.13 ± 0.22 Slow phase: -0.15 ± 0.14	2.3×10^{-5} ($\pm 1.3 \times 10^{-5}$)	First phase: 1.9 ± 2.2 Second phase: 0.17 ± 0.31
	I \rightarrow U	0.47 ± 0.03	Fast phase: 0.42 ± 0.09 Slow phase: 0.45 ± 0.04	6.3×10^{-4} ($\pm 3.1 \times 10^{-4}$)	Fast phase: 4.6×10^{-3} ($\pm 6.3 \times 10^{-3}$) Slow phase: 7.9×10^{-4} ($\pm 5.1 \times 10^{-4}$)

At pH 7.0, the $k_u(\text{H}_2\text{O})$ and m_u values of CD- and fluorescence-monitored unfolding are similar indicating that the secondary and tertiary structure of CLIC1 unfold at a similar rate (Table 3), although the CD-monitored unfolding is slightly slower. This phenomenon might result from the fact that CD at 222 nm monitors global changes of an entire protein while fluorescence monitors local environmental changes near the lone tryptophan.

At pH 5.5, if only comparing the $k_u(\text{H}_2\text{O})$ of the fluorescence-monitored unfolding with the $k_u(\text{H}_2\text{O})$ of both the CD and fluorescence data at pH 7.0, the unfolding rate of CLIC1 is much faster than at pH 7.0. However, the $k_u(\text{H}_2\text{O})$ from the CD data at pH 5.5 shows a very similar value to the values obtained at pH 7.0 (Table 3). CLIC1 is a predominantly α -helical protein and the far-UV CD spectra of CLIC1 show a pattern typical of α -helical proteins with two minima at 208 and 222 nm. CLIC1 has two domains: the smaller N-domain with mixture of α -helices and β -strands and the bigger all-helical C-domain. Therefore, the majority of E_{222} -monitored signals comes from the bigger all-helical C-domain. Hydrogen-deuterium exchange has demonstrated that at pH 5.5 the N-domain becomes more flexible than at pH 7.0 (Stoychev *et al.*, 2009). In contrast, the C-domain is not really influenced by the low pH. In unfolding kinetics, the similar $k_u(\text{H}_2\text{O})$ of the CD-monitored unfolding at both pH values might suggest that in the absence of denaturant, the stability of the C-domain is not influenced by pH. The large m_u value of the CD-monitored data at pH 5.5 indicates a large increase in solvent accessibility of CLIC1 upon unfolding. This result might suggest C-domain is more compact than the N-domain in the absence of urea at pH 5.5. On the other hand, the fluorescence monitors the changes in local tertiary structure where the tryptophan residues are located. In the case of CLIC1, the lone tryptophan, Trp35, locates in the N-domain and thus the fluorescence is able to monitor changes specifically in the N-domain. In contrast with the large m_u value obtained from CD-monitored data, the smaller m_u value obtained from fluorescence-monitored unfolding might suggest that the conformation of the

N-domain is less compact at pH 5.5 and thus the N-domain exposes less solvent accessible area compared to the C-domain upon unfolding. Moreover, this significant difference between the m_u values of CD and fluorescence-monitored unfolding is only detected at pH 5.5. Although the CD- and fluorescence-monitored unfolding traces at pH 5.5 both show a single-phasic transition, this m_u value difference suggests the existence of hidden intermediate species appearing in the unfolding reaction at this pH which is confirmed by the equilibrium work (Bhuyan and Udgaonkar, 1998).

The N \rightarrow I transition

CLIC1 was denatured from the native state (N) to the intermediate state (I) by adding the protein into buffers with a final urea concentration ranging from 3 M to 4 M at pH 5.5 which represents the condition that the intermediate state forms at equilibrium (Figure 12). Representative unfolding traces are shown in Figure 19. The CD-monitored traces fit well to a single exponential model. However, the fluorescence-monitored unfolding kinetics of the N \rightarrow I transition is no longer monophasic. Hypofluorescence is initially detected and separates the unfolding traces into a clear biphasic transition as the protein unfolds (Figure 19). Therefore, the fluorescence-monitored kinetic traces were fit to two separate single exponential models. The $k_u(\text{H}_2\text{O})$ values of the first and second detected phase show that the first phase proceeds at a faster rate when compared to the second phase (Figure 18 and Table 3). The m_u value of the CD-monitored data is large (Figure 18 and Table 3), indicating that the structure of CLIC1 in the N \rightarrow I transition is very sensitive to urea concentration. Moreover, the large m_u value of the CD-monitored data indicates that the global structure of the intermediate has a much more exposed surface area compared to native CLIC1. However, the m_u values of both fluorescence-monitored phases show negative trends (Figure 18), suggesting that the local tertiary structure (where Trp35 locates) of the intermediate is changed and Trp35 becomes more embedded compared to that of the native state of CLIC1.

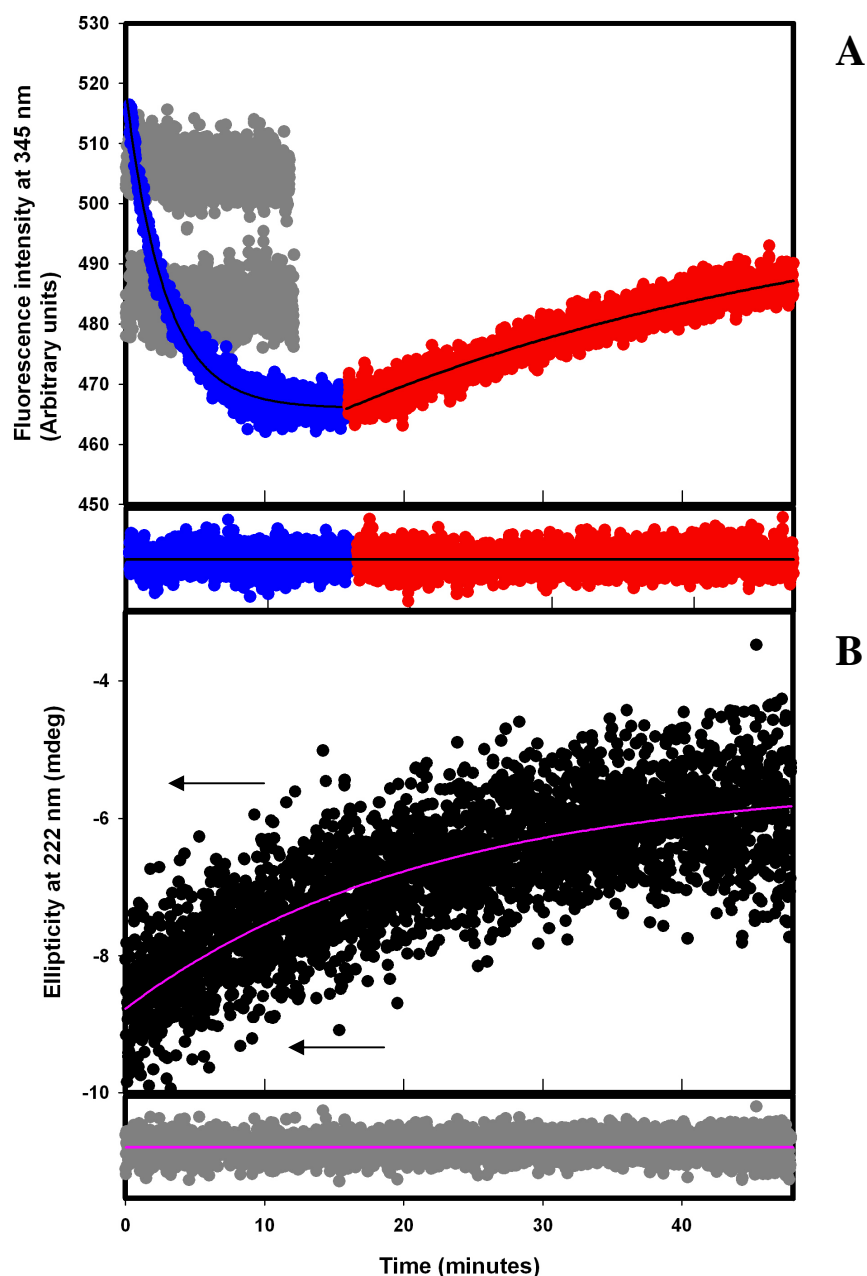


Figure 19: Representative unfolding kinetic traces of CLIC1 from the N → I transition at pH 5.5

CLIC1 (2 μ M) was unfolded from the native state to a final concentration of 3.4 M urea. The traces were monitored using both F₃₄₅ (A) and E₂₂₂ (B) as probes. The solid lines represent the fit to a single (B) or two separate single (A) exponential models and the residuals are plotted in the panels beneath each figure. The baselines of the native and the intermediate states are indicated in grey (A) and by arrows (B).

This observation is consistent with the fluorescence spectra that show that CLIC1 has a more buried tryptophan in the intermediate state (Figure 15).

The I → U transition

For this study, CLIC1 was firstly incubated in the presence of 3.4 M urea at pH 5.5 which corresponds to the condition that the most intermediate species accumulates (Figure 13) for 1 hour in order to obtain the stable equilibrium intermediate species. The intermediate was then unfolded in the presence of a final concentration of 5.6 M to 7 M urea. Representative unfolding traces are shown in Figure 20. The CD-monitored traces fit to a single exponential model without any detectable burst phase. However, the fluorescence-monitored traces fit to a double exponential model, indicating that there are two kinetic phases. The two phases monitored by fluorescence are similar in their m_u values (Figure 18 and Table 3), indicating a similar amount of surface area exposed as the protein unfolds in the two phases. Both the fluorescence-monitored phases have similar urea-dependence on the rate constants to the CD-monitored data. The $k_u(\text{H}_2\text{O})$ of the CD-monitored unfolding, however, is only similar to the one from the fluorescence-monitored slow phase. This suggests that CD is only able to record this slow phase.

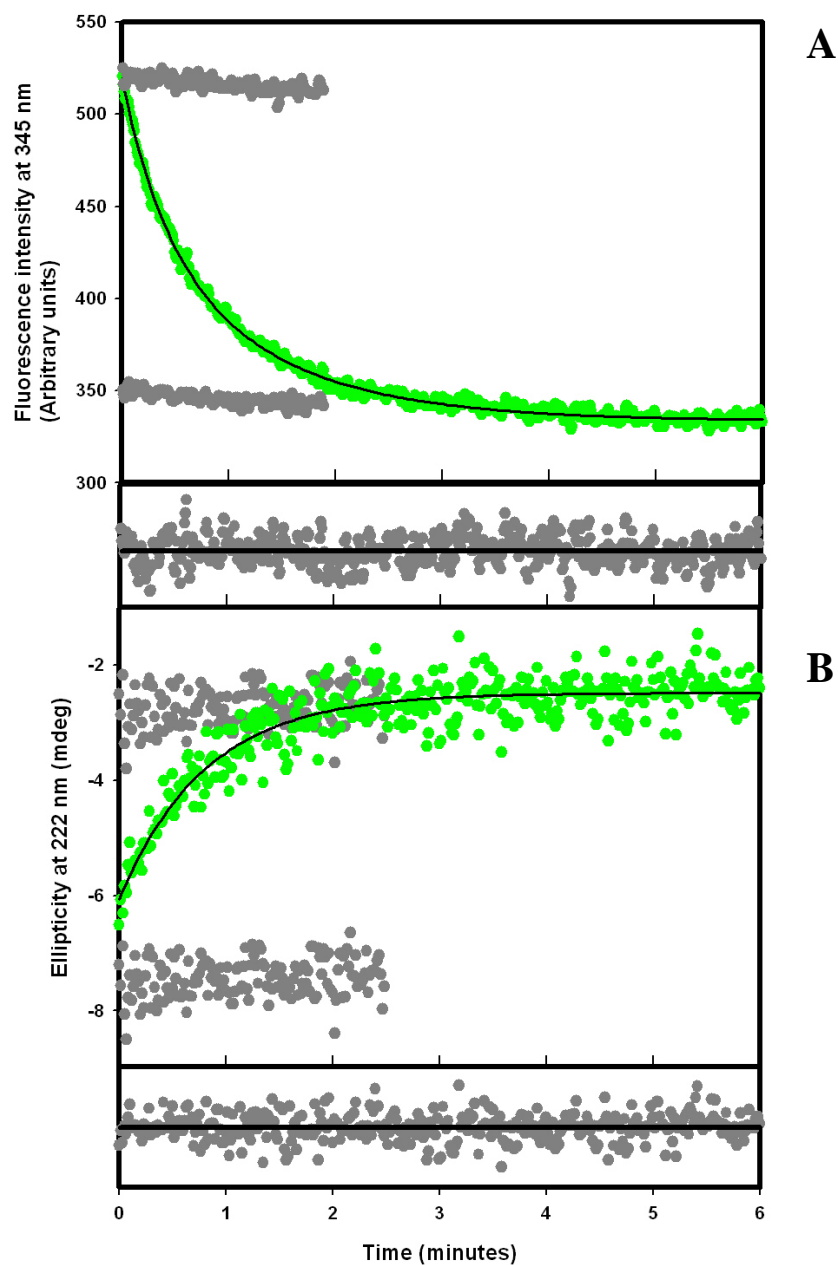


Figure 20: Representative unfolding kinetic traces of the I \rightarrow U transition

CLIC1 (2 μ M) was incubated in the presence of 3.4 M urea at pH 5.5, then unfolded in the presence of a final concentration of 7 M urea. The traces were monitored using both F_{345} (**A**) and E_{222} (**B**) as probes. The solid lines represent the fit to a single (B) or a double (A) exponential model and the residuals are plotted in the panels beneath each figure. The baselines of the intermediate (3.4 M urea) and the unfolded CLIC1 (7 M urea) are indicated in grey.

4. Discussion

CLICs are channel proteins which have distinct properties from traditional channel proteins. The most unusual one is that, unlike typical channel proteins, they do not insert into membranes cotranslationally. Instead, CLIC proteins are translated as soluble proteins in the cytosol without leader sequences to direct them to insert into membranes (reviewed by Singh, 2010). An as yet unknown signal directs the protein from the cytosol to the membrane where it changes conformation from a soluble form to a transmembrane protein. The main question that puzzles many scientists is how CLIC1 converts between soluble and membrane-bound forms. In its transition from a fully folded soluble protein to a membrane-bound protein, CLIC1 has been hypothesised to unfold or at least partially unfold in order to insert into the membrane (Littler *et al.*, 2010). However, the exact mechanism of this conversion is still unknown. Therefore, in an attempt to get insight into the conversion between CLIC1 soluble and membrane-bound states, the unfolding mechanism of soluble CLIC1 was investigated at the pH values typical of the cytosol and the membrane surface.

4.1. A stable equilibrium intermediate state of CLIC1 is formed at pH 5.5

The equilibrium unfolding studies of CLIC1 were conducted at pH 7.0 and pH 5.5 which correspond to the pH values in cytosol and near the surface of membranes (McLaughlin, 1989), respectively. At pH 5.5, under mild denaturing conditions, CLIC1 forms a stable equilibrium intermediate species which is unlike its native state or unfolded state, while there is no intermediate formed at pH 7.0 (Figure 12).

At low pH (pH 4.0 or lower), the channel peptide of the bacterial channel-forming toxin, colicin E1, has been shown to transit into an insertion-competent state (Merrill *et al.*, 1990;

Merrill *et al.*, 1993; Schendel and Cramer, 1994). These toxins have a similar property to CLIC1: they are also translated as soluble forms and transform into their membrane-bound forms once they reach their targets (Parker and Feil, 2005). The insertion-competent state of colicin E1 increases the exposure of the peptide's hydrophobic core due to structural rearrangements. Moreover, it has been reported that low pH acts as a general trigger to activate the membrane-insertion mechanism for these bacterial pore-forming toxins (Musse and Merrill, 2003). The mechanism starts with the structures of the toxins becoming destabilised at low pH (corresponding to the pH level at the membrane surface) and forming molten globule-like intermediate states. The "molten globule" is characterised by native-like secondary structure with a poorly defined tertiary structure (Ptitsyn, 1995) and binds to the hydrophobic dye ANS which is how it can be detected (Banerjee and Kishore, 2005). Since the structure of these molten globule-like intermediates is more flexible and hydrophobic, it also lowers energy barriers needed for exposure of the buried hydrophobic helices and for interaction with membranes in order to facilitate membrane-insertion (Parker and Feil, 2005).

Is the equilibrium intermediate of CLIC1 a "molten globule" state?

In the case of CLIC1, an intermediate state is formed at pH 5.5 in the presence of 3 ~ 4 M urea. Moreover, ANS is also able to bind to this intermediate state of CLIC1 (Figure 16). Therefore, since the intermediate state forms under mild denaturing conditions and it has exposed hydrophobic surface, it is suspected to be in a molten globule-like state. The CLIC1 intermediate state has approximately 60% secondary structure when compared to the native CLIC1 (Figure 14). The fluorescence spectra of the CLIC1 intermediate show neither increased nor decreased fluorescence intensity when compared to the native state. This suggests that the compactness of CLIC1 tertiary structure in the intermediate state does not change significantly compared to the native state. The only difference in the spectra between the native and intermediate state is that, the maximum emission wavelength of the

intermediate shows a slight blue shift from 345 nm to 340 nm, indicating that the single tryptophan, Trp35, is more embedded in the protein than it is in the native state. The observations from fluorescence spectra indicate that the CLIC1 intermediate still has a well-defined tertiary structure and is even more compact in the environment around the lone tryptophan residue than in the native state. The reduced secondary and the well-packed tertiary structure of the intermediate state make it fall out of the definition of “molten globule”. Therefore, CLIC1 does not form a molten globule-like equilibrium intermediate state that is true to the definition as the colicins do.

The hydrophobicity of the intermediate

Previous studies have proposed that it is likely that the membrane-docking form of CLIC1 has exposed hydrophobic surface area (Littler *et al.*, 2010). In this study, ANS binding studies show that the intermediate state of CLIC1 also has more hydrophobic area on its surface than in the native state (Figure 16). Whether this equilibrium intermediate of CLIC1 is a membrane-competent form or not, still remains to be determined. However, the hydrophobicity of the intermediate clearly has potential to enable the protein to interact with highly hydrophobic biological membranes when in this state.

The low pH-induced destabilisation of CLIC1

Even though CLIC1 does not form an intermediate that is true to the definition of “molten globule”, it is likely that the structural transition between soluble and membrane-insertable CLIC1 might involve intermediate states and might also be induced by low pH in a similar way to the colicins. It has been demonstrated that the pH-activated membrane-insertion mechanism of colicin E1 involves protonation of some acidic residues which form a pH-sensitive motif, resulting in disruption of some critical hydrogen bonds and salt bridges which further loosen the tertiary structure for membrane-insertion (Musse and Merrill, 2003).

In the N-domain of CLIC1, there are two salt bridges (Arg29-Glu81 and Lys37-Glu85), and one formed across the domain interface (Lys20-Asp225). Arg29 in helix $\alpha 1$ forms a salt bridge and a hydrogen bond with Glu81 in helix $\alpha 3$ while Asn78 forms hydrogen bonds with both Arg29 and Glu81. It has been reported that, at acidic pH, the N-domain of CLIC1, especially in the putative transmembrane region, becomes more flexible than at neutral pH (Stoychev *et al.*, 2009). Also, breaking the salt bridge between Arg29 and Glu81 via R29M and E81M single mutants as well as the R29M/E81M double mutant, has been shown to decrease the conformational stability of the N-domain (Legg E'Silva PhD thesis, 2011), indicating that the salt bridge and the hydrogen bond are responsible for the stabilisation of the N-domain. Moreover, hydrogen-deuterium exchange studies of CLIC1 shows that the residues in these salt bridges (Arg29-Glu81, Lys37-Glu85 and Lys20-Asp225) are located in the two segments (peptide 11-31 and peptide 68-82) that display the highest exchange rate at pH 5.5 (Stoychev *et al.*, 2009). Therefore, at pH 5.5 (roughly the pH at the membrane surface), protonation of these acidic residues causes critical salt bridges and hydrogen bonds in the N-domain and in the domain interface to break, leading to structural flexibility in the N-domain. This flexibility of the N-domain is able to reduce the energy barrier for the structural transition from the soluble protein to the membrane-competent conformation and is further able to facilitate the membrane insertion of CLIC1.

4.2. Unfolding of CLIC1

The equilibrium unfolding of CLIC1 has revealed that CLIC1 unfolds via a two-state mechanism at pH 7.0 and via a three-state mechanism with an appearance of an equilibrium intermediate at pH 5.5. Therefore, in order to detect the transient intermediate species and to obtain more information on the mechanism of unfolding, CLIC1 unfolding kinetics were conducted by unfolding CLIC1 from the native state to the unfolded state and the

intermediate state, and also unfolded from the intermediate state to the unfolded state.

4.2.1. The appearance of hidden intermediates in the N→U transition

At pH 7.0, unfolding of native CLIC1 monitored by fluorescence and CD both show a single-phasic transition. The similar m_u values obtained from both probes (Table 3) further suggest that there is no detectable intermediate in the process of unfolding the native CLIC1 at pH 7.0. At pH 5.5, CLIC1 also demonstrates single-phasic unfolding kinetics traces when monitored using both probes. However, the non-coincidence of the m_u values obtained from the fit of CD- and fluorescence-monitored unfolding kinetics suggests the existence of “hidden intermediate species” along the unfolding reaction (Bhuyan and Udgaonkar, 1998). The single-phasic transition of both the CD- and fluorescence-monitored kinetic traces might result from the fact that under these strong denaturing conditions (5.5 ~ 7 M urea) the hidden transient intermediates of CLIC1 in the N→U transition are less stable than the unfolded state (Bai, 2003) and thus they cannot be significantly populated and detected by the probes used during the unfolding process. In addition, the unfolding kinetic studies of the N→U transition further show that the intermediate state (including hidden intermediates) only forms at pH 5.5, which is same as with the equilibrium unfolding studies. However, in this study, we do not have enough information to conclude that the hidden transient intermediate formed in the unfolding transition between the native and unfolded state and the intermediate formed at equilibrium under mild denaturing conditions are identical.

4.2.2. The equilibrium intermediate is more stable than the native state at pH 5.5

Unfolding of the equilibrium intermediate state (the I→U transition) monitored by fluorescence occurs in two phases: a fast phase and a slow phase. The appearance of two kinetic phases generally suggests that three species appear along this unfolding transition.

Although fluorescence-monitored unfolding of the intermediate state displays two kinetic phases, the CD-monitored unfolding only shows a single phase. Since CD is a probe used to monitor change in global secondary structure, it might not be as sensitive as fluorescence to the local structural change around Trp35 in the N-domain when the equilibrium intermediate unfolds. When comparing the $k_u(\text{H}_2\text{O})$ of the CD-monitored unfolding of the native and intermediate states, the intermediate state is shown to unfold at a slower rate than the native state in the absence of denaturant at pH 5.5 (Table 3), indicating that the intermediate appears to be more stable than the native state at this pH. The same result can be seen in the equilibrium unfolding studies where the $\Delta G(\text{H}_2\text{O})$ for the $\text{I} \rightarrow \text{U}$ transition at pH 5.5 is larger than the $\Delta G(\text{H}_2\text{O})$ for the $\text{N} \rightarrow \text{I}$ transition at pH 5.5 or the $\text{N} \rightarrow \text{U}$ transition at pH 7.0 (Table 2). This may imply that, at pH 5.5, the native state is destabilised and the intermediate of CLIC1 is more energetically favoured than the native state under this condition.

4.2.3. Formation of the equilibrium intermediate

When using fluorescence as a probe to monitor CLIC1 unfolding from the native state to the equilibrium intermediate state (the $\text{N} \rightarrow \text{I}$ transition), a hypofluorescence minimum occurs and separates the unfolding into two clear kinetic phases (Figure 19). The fluorescence-monitored unfolding traces of the $\text{N} \rightarrow \text{I}$ transition occur initially with a fast decrease in intensity followed by a gradual increase in intensity. These two kinetic phases both fit to a single exponential model. Although we cannot be certain how many species are involved in this transition, the observation of two phases suggests that there are likely three species involved in the $\text{N} \rightarrow \text{I}$ transition of CLIC1 (Utiyama and Baldwin, 1986).

The first phase in the formation of the CLIC1 intermediate displays a decrease in fluorescence intensity, indicating the likelihood of an unfolding reaction. Unfolding processes often increase the distance between the tyrosine and tryptophan residues in the same protein,

and disrupt the FRET between these residues and further cause the fluorescence intensity of the protein to decrease (Lakowicz, 2006), although it is certainly possible to get an increase in fluorescence intensity upon unfolding. After the first rapid unfolding, the second phase displays a slight increase in fluorescence intensity slower than the first phase. For the data, we are unable to state conclusively whether these two kinetic phases occur in sequence or in parallel. However, from the fractional population plot obtained from equilibrium unfolding, at 3 to 4 M urea at pH 5.5, majority of the species is in the intermediate state (Figure 13). Also, the equilibrium intermediate shows a compact tertiary structure when compared to the native state. It is likely that the enhanced fluorescence intensity in the second phase results from the fact that the unfolded structure of CLIC1 somehow refolds, recovering the FRET between the tryptophan and the tyrosine residues and thus increasing the fluorescence intensity at 345 nm. Moreover, the negative m_u values of these two phases suggest that the structure of CLIC1 in the intermediate state, especially around Trp35, becomes more compact than the native state (Table 3). This observation is consistent with the results obtained from the equilibrium unfolding studies where the spectra of the equilibrium intermediate show that Trp35 becomes more buried in the intermediate state than in the native state. Therefore, these two kinetic phases might be interpreted to be a sequential process: the increase in fluorescence intensity in the second phase represents a slow repacking or rearrangement of the protein structure after the fast unfolding reaction shown in the first phase (Steer and Merrill, 1997).

Slow reactions in unfolding processes of proteins can be caused by formation of disulfide bonds. All the unfolding kinetics experiments in this study were performed in the presence of 1 mM DTT. Under reducing conditions, CLIC1 is unable to form either intermolecular or intramolecular disulfide bonds. Therefore, it is unlikely that the slow rearrangement of CLIC1 structure after the rapid unfolding is due to disulfide bonds formation. On the other

hand, the proline isomerisation process is also a cause of slow steps in unfolding reactions but it often cannot be detected using usual spectroscopic methods. However, it can be measured using a “double-jump” assay. This method relies on the fact that proline isomerisation is a slow process and the refolding rate of the $U_f \rightarrow N$ and the $U_s \rightarrow N$ transitions are thus different (Brandts *et al.*, 1975; Schmid, 1986), where U_f and U_s represent unfolded species with native and non-native prolyl isomers, respectively. Proline isomerisation in unfolding reactions can, therefore, be detected and monitored. Generally “double-jump” assays can be performed using stopped-flow techniques. However, in this study, the unfolding kinetics studies were conducted using a manual mixing method and thus, unfortunately, “double-jump” assays were not able to be performed. Therefore, whether this slow structural rearrangement is caused by proline isomerisation or not, remains to be determined. In addition, after rapid unfolding, hydrophobic residues of partially unfolded protein are exposed to the polar solvent and thus they are prone to interact with each other and become buried again in order to get away from the solvent. Therefore, the hydrophobic interaction among residues might also be one of the possible forces that drive the repacking of the partially unfolded CLIC1. Combined with the assumptions that there are three species involved in this reaction and that the reaction occurs in sequence, a pathway of the $N \rightarrow I$ transition can thus be described as an initial rapid unfolding of native CLIC1 to a partially unfolded structure, followed by a slow rearrangement of CLIC1 structure to form the equilibrium intermediate.

4.2.4. Unfolding pathway of CLIC1

Unfortunately, from the limited data, there is no clear evidence to conclude either that the equilibrium intermediate is on- or off-pathway or that the hidden intermediate species formed in the $N \rightarrow U$ transition at pH 5.5 are the same species as the equilibrium intermediate. The overall view of the unfolding pathway that is derived from the results in this study is summarised in Figure 21. At pH 7.0, which corresponds to the pH value in the cytosol, CLIC1 unfolds from the native state to the unfolded state without any detectable intermediates. At pH 5.5, which corresponds to the pH value near the membrane surface, the unfolding of CLIC1 from the native state to the unfolded state occurs in a single phase, but this unfolding transition is accompanied by unstable hidden intermediate species.

The formation of the equilibrium intermediate occurs in two phases. Native CLIC1 unfolds rapidly in the first phase to form a partially unfolded structure. In the second phase, the partially unfolded structure of CLIC1 repacks due to unknown interactions among residues and rearranges to form the native-like equilibrium intermediate state gradually. The partially unfolded equilibrium intermediate with more exposed hydrophobic area than native CLIC1 (Figure 16) then might be able to serve as a precursor to membrane docking (Littler *et al.*, 2010). The free energy required to form the equilibrium intermediate is the least among three transitions ($N \rightarrow U$, $N \rightarrow I$ and $I \rightarrow U$) and thus, at pH 5.5 CLIC1 is prone to form the equilibrium intermediate from the native state (Table 2).

The unfolding of the intermediate state occurs in two phases: a fast and a slow phase. However, we are unable to state conclusively whether the two phases in the $I \rightarrow U$ transition are sequential or parallel. The free energy needed for this transition is the highest among three transitions (Table 2). This further confirms that the intermediate state is fairly stable at pH 5.5 when compared to the native and unfolded states at both pH.

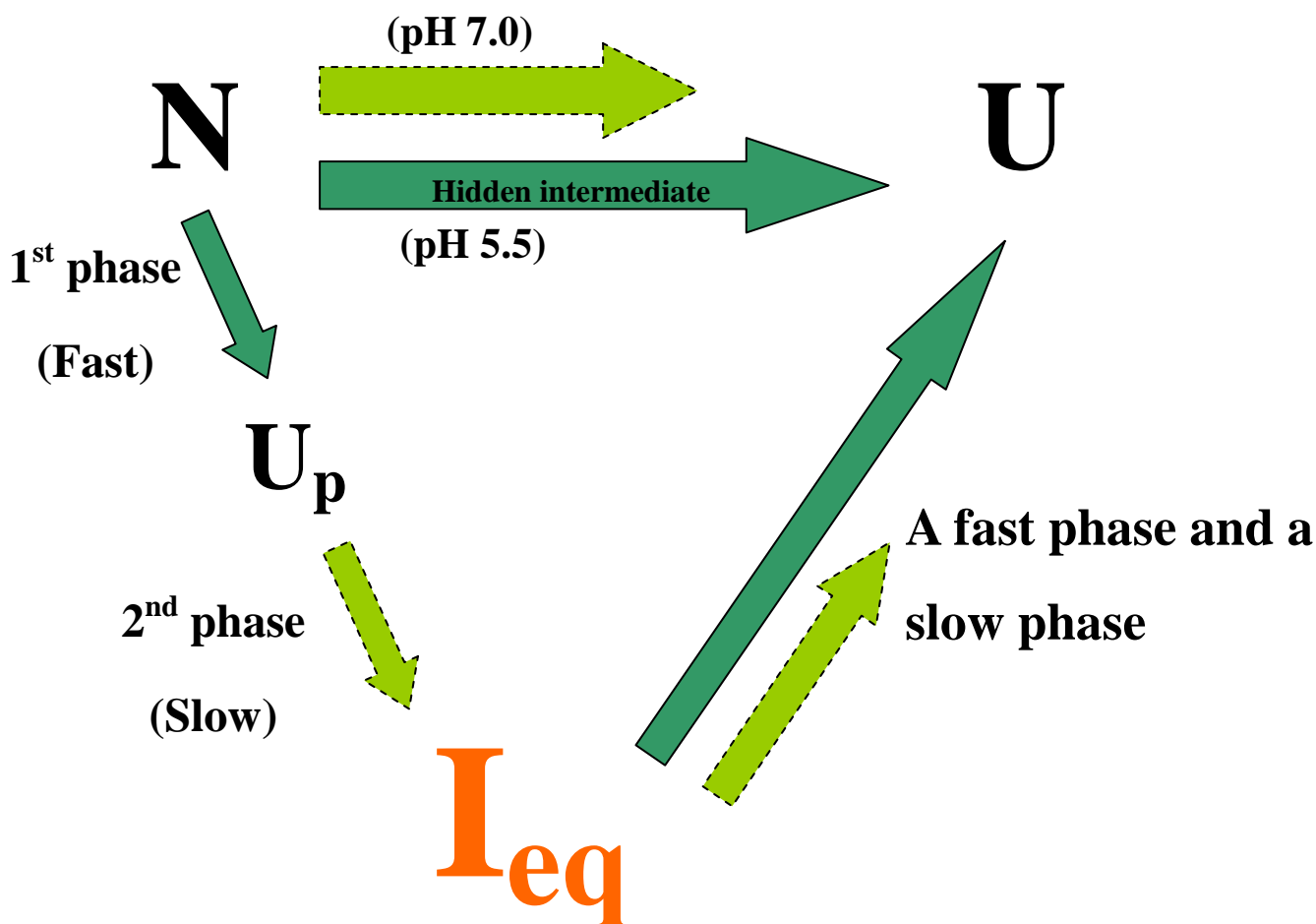


Figure 21: Proposed unfolding pathway of CLIC1

Possible unfolding scheme for CLIC1 at 20°C. The arrows with solid line and dashed line represent fast/faster and slow/slower phases, respectively. At pH 7.0, the protein unfolds from the native state (N) to the unfolded state (U) in a single-phasic transition without formation of any detectable intermediate. However, at pH 5.5, the unfolding of CLIC1 occurs in a fast phase with hidden intermediate species. In the formation of the native-like equilibrium intermediate (I_{eq}) at pH 5.5, N unfolds to a partially unfolded form (U_p) in a fast phase and then restructures to form the stable equilibrium intermediate in a slow phase. The unfolding of the intermediate state occurs in a fast and a slow phase. However, whether these two phases occur sequentially or in parallel, remains unknown.

4.3. Proposed CLIC1 insertion mechanism

The signal that triggers CLIC1 to insert into membranes is still unclear. Both oxidation and low pH have been shown to increase the channel forming activity of CLIC1 in artificial bilayers (reviewed by Singh, 2010). However, it is unlikely that either oxidation or low pH can be the only control for CLIC1 insertion (Littler *et al.*, 2010). Therefore, it is possible that the function of these two factors is cooperative. In this study, the focus is on how the different pHs, typical of the cytosol and the membrane surface, can influence the unfolding behaviour of soluble CLIC1 in the absence of the membranes.

At pH 7.0 (cytosol), the equilibrium unfolding and the unfolding kinetics of soluble CLIC1 both show that CLIC1 is relatively stable and neither equilibrium nor transient intermediates are detectable so unfolding is highly cooperative. At pH 5.5 (membrane surface), the structure of soluble CLIC1 becomes more flexible (Stoychev *et al.*, 2009), the native state is destabilised and a stable equilibrium intermediate forms. Therefore, at pH 5.5, it is likely that the energy barrier needed for the structural transition between soluble and membrane-competent form is reduced. The membrane insertion of CLIC1, therefore, becomes accessible more easily due to the reduced energy barrier.

The possible insertion mechanism of CLIC1 has been proposed previously in the literature (Littler *et al.*, 2010). Applying the results of CLIC1 differential unfolding behaviour at various pHs obtained in this study to the previously proposed CLIC1 membrane insertion mechanism, a hypothetical scheme of CLIC1 insertion is shown in Figure 22. Since there is no membrane work involved in this study, the mechanism for the membrane insertion and the pore formation of CLIC1 proposed in the following is simply a hypothesis.

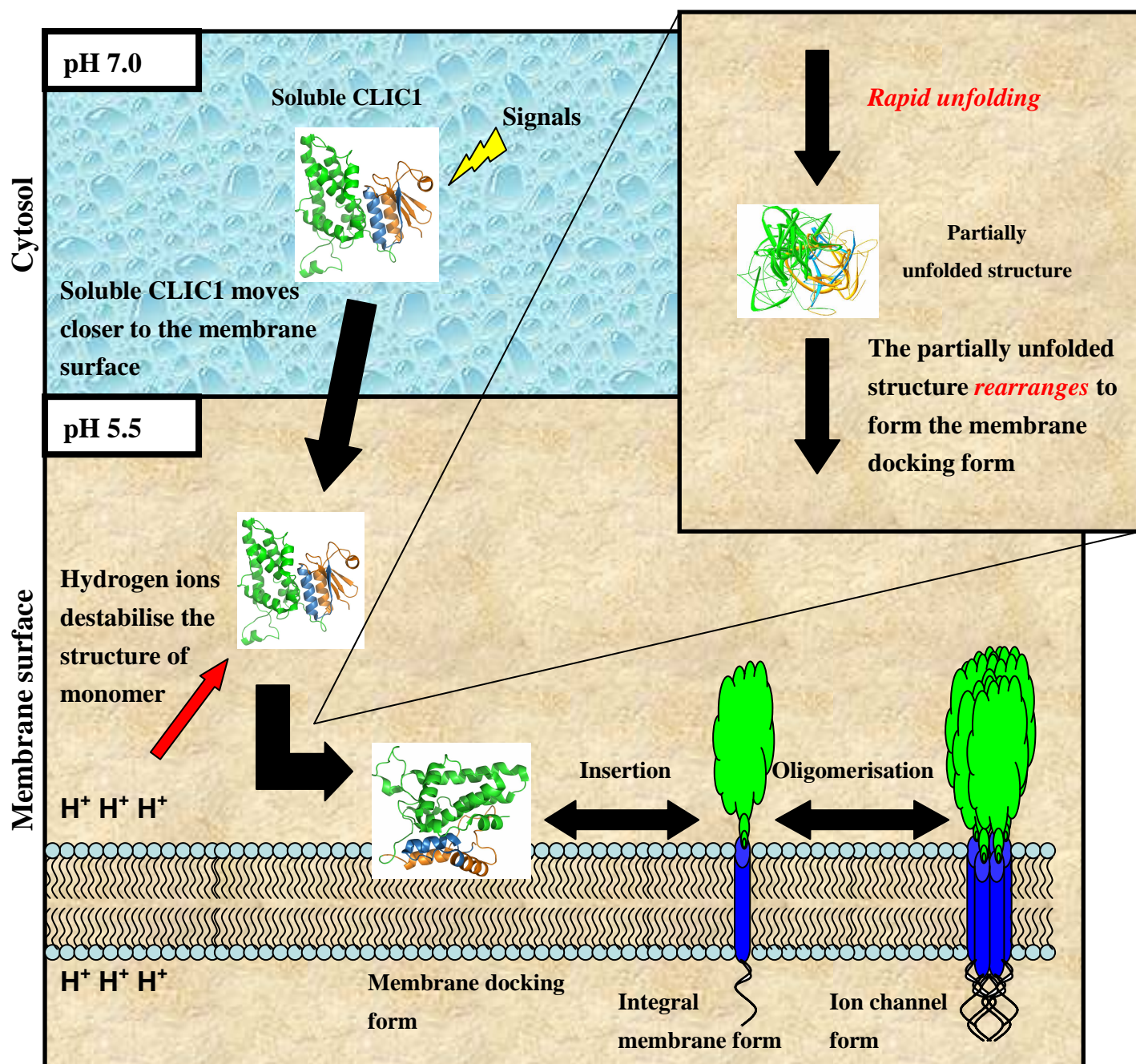


Figure 22: Proposed membrane insertion model of CLIC1

The C-domain and PTMD are indicated in green and blue, respectively. In the cytosol where the pH is close to 7.0, CLIC1 exists in its soluble form which is a monomeric conformation. Once the soluble CLIC1 is stimulated by a certain signal or stress, CLIC1 monomers move close to the membrane surface where the pH is 5.5 and are protonated by hydrogen ions on the membrane surface. The protonation destabilises the structure of the soluble CLIC1 monomer, causing a rapid unfolding of the structure followed by a restructuring to form the membrane docking form. The membrane docking structure possesses exposed hydrophobic areas on its surface and thus has the ability to interact with the membrane. After the docking process, the PTMD region inserts into the membrane. CLIC1 integral monomers then oligomerise to form a functional ion channel.

Under normal conditions, CLIC1 is in the cytosol, stable and soluble. Once there is a signal (could be oxidation or another unknown signal) to activate CLIC1 insertion, CLIC1 moves close to the membrane surface. The local low pH at the membrane surface then destabilises the structure of CLIC1 by breaking critical salt bridges, resulting in a more flexible and destabilised structure, and allowing CLIC1 to convert into the membrane-docking form (Figure 22).

The equilibrium intermediate is likely to have similar properties to the membrane-docking form of CLIC1, in terms of flexibility and hydrophobicity. The unfolding kinetics of the $N \rightarrow I$ transition shows the most significant result of this study. After destabilisation by the local low pH, CLIC1 goes through a rapid unfolding process followed by a gradual rearrangement of the structure to form the intermediate with exposed hydrophobic surface areas. The membrane-docking form has thus reduced the energy barrier to the interaction with and insertion of soluble CLIC1 into membranes.

After membrane docking, CLIC1 inserts into the membrane with the PTMD embedded in the lipid bilayer. In order to form a functional channel and to conduct the complete function of the protein, the integral CLIC1 with only one transmembrane helix is likely to form an oligomer (Singh, 2010). It has been proposed that the CLIC1 membrane-competent form might form an oligomer before insertion into membranes (McIntyre, PhD thesis). In this study, because of the exposure of the hydrophobic areas, the equilibrium intermediate has the potential to form oligomeric structure through hydrophobic interaction. However, this cannot be concluded without further experiments. Although dimeric CLIC1 is able to insert into artificial membranes, oligomerisation is still more likely to happen after monomeric CLIC1 inserts into membranes due to the fact that the pre-insertion oligomeric form of CLIC1 might cause steric hindrance to the insertion process (Littler *et al.*, 2004).

4.4 Conclusions

The focus of this study was to examine the effect of the pH typical of the cytosol and membrane surface on the unfolding mechanism of soluble CLIC1. It was found in this study that the unfolding behaviour of soluble CLIC1 is different under different conditions.

Unfolding of CLIC1 is cooperative at pH 7.0 without either equilibrium or transient intermediates detected. At pH 7.0, the unfolding of native CLIC1 occurs at a significantly slower rate than at pH 5.5. This indicates that the conformational stability of CLIC1 is reduced at low pH when compared to neutral pH. This destabilisation might result from the breakage of critical stabilising salt bridges and hydrogen bonds by protonation at low pH. The low pH also leads CLIC1 to unfold following a different pathway with the existence of intermediate species. At pH 5.5, equilibrium unfolding and unfolding kinetics studies demonstrate that both stable intermediate species and transient hidden intermediate species are populated during the transition, respectively.

It has been proposed that CLIC1 needs to unfold and refold in order to form a membrane-competent form to interact with or insert into the membrane. It can be seen in this study that at pH 5.5 CLIC1 experiences a rapid unfolding and a slow refolding to form the equilibrium intermediate state which is proposed to be a membrane-competent form of the protein. This result appears to be in agreement with the proposal that CLIC1 converts between two conformations by the unfolding and refolding process.

Although the results of this study provide some information and hypotheses toward the membrane insertion mechanism of CLIC1, a number of questions still remain unanswered. Is the equilibrium intermediate state of CLIC1 really the membrane-competent form of the

protein? All the unfolding kinetics studies in this study were conducted at 20°C. What will the unfolding kinetics be like if the experiments are performed at 37°C, the physiological temperature of human bodies? In this study, unfolding kinetics studies were performed using a manual mixing method which might not only limit the monitoring of fast events in the early stage of unfolding but also limit the detection of proline isomerisation reactions. Further unfolding kinetics studies can be conducted using a stopped-flow technique in order to detect fast events or to detect proline isomerisation using “double-jump” assays. The initial conditions tests can also be performed for more information about whether the pathways occur sequentially or in parallel to supplement the existing knowledge. Also, CLIC1 has only one tryptophan residue located in the putative transmembrane region in the N-domain. The lone tryptophan, Trp35, is advantageous because it enables us to monitor the structural changes specifically in the transmembrane region and the N-domain by using tryptophan fluorescence spectroscopy during the unfolding process. However, the lone tryptophan also restricts the observation of changes in the C-domain. What role does the C-domain play during the unfolding process? Although CD is a technique that is able to monitor a global structural change, tryptophan bears an advantage to monitor the local environment. Therefore, locating a tryptophan in the C-domain and knocking out the one in the N-domain by mutations can be done to monitor any structural changes in the C-domain to complement the current results obtained from the single tryptophan Trp35.

5. References

- Abkevich, V. I. and Shakhnovich, E. I. (2000) What can disulfide bonds tell us about protein energetics, function and folding: simulations and bioinformatics analysis. *J. Mol. Biol.* **300**, 975-985
- Anfinsen, C. B. (1973) Principles that govern the folding of protein chain. *Science* **181**, 223-230
- Arai, M. and Kuwajima, K. (2000) Role of the molten globule state in protein folding. *Adv. Protein Chem.* **53**, 209-282
- Ashley, R. H. (2003) Challenging accepted ion channel biology: p64 and the CLIC family of putative intracellular anion channel proteins. *Mol. Membr. Biol.* **20**, 1-11
- Bai, Y. (2003) Hidden intermediates and levinthal paradox in the folding of small proteins. *Biochem. Biophys. Res. Commun.* **305**, 785-788
- Banerjee, T. and Kishore, N. (2005) 2,2,2-trifluoroethanol-induced molten globule state of concanavalin A and energetics of 8-anilinoanthracene sulfonate binding: calorimetric and spectroscopic investigation. *J. Phys. Chem.* **109**, 22655-22662
- Bartlett, A. I. and Radford, S. E. (2009) An expanding arsenal of experimental methods yields an explosion of insights into protein folding mechanisms. *Nat. Struct. Mol. Biol.* **16**, 582-588
- Baumeister W., Walz, J., Zühl, F. and Seemüller, E. (1998) The proteasome: paradigm of a self-compartmentalizing protease. *Cell* **92**, 367-380
- Beecham, J. M. (1992) Global analysis of biochemical and biophysical data. *Methods Enzymol.* **210**, 37-54
- Berry, K. L., Bulow, H. E., Hall, D. H. and Hobert, O. (2003) A *C. elegans* CLIC-like protein required for intracellular tube formation and maintenance. *Science* **302**, 2134-2137

Berryman, M. A. and Bretsher, A. (2000) Identification of a novel member of the chloride intracellular gene family (CLIC5) that associates with the actin cytoskeleton of placental microvilli. *Mol. Biol. Cell* **11**, 1509-1521

Berryman, M. A. and Goldenring, J. R. (2003) CLIC4 is enriched at cell–cell junctions and colocalizes with AKAP350 at the centrosome and midbody of cultured mammalian cells. *Cell Motil. Cytoskel.* **56**,159-172

Bhuyan, A. K. and Udgaonkar, J. B. (1998) Multiple kinetic intermediates accumulate during the unfolding of horse cytochrome c in the oxidized state. *Biochemistry* **37**, 9147-9155

Bieri, O. and Kiefhaber, T. (2000) Kinetic models in protein folding in *Mechanism of protein folding*, second edition (Pain, R. H. ed.), pp. 34-64, Oxford University Press, Great Britain

Bilsel, O., Zitzewitz, J. A., Bowers, K. E. and Matthews, C. R. (1999) Folding mechanism of the α -subunit of tryptophan synthase, an α/β barrel protein: Global analysis highlights the interconversion of multiple native, intermediate, and unfolded forms through parallel channels. *Biochemistry* **38**, 1018-1029

Board, P. G., Coggan, M., Watson, S., Gage, P. W. and Dulhunty, A. F. (2004) CLIC-2 modulates cardiac ryanodine receptor Ca^{2+} release channels. *Int. J. Biochem. Cell Biol.* **36**, 1599-1612

Brandts, J. F., Halvorson, H. R. and Brennan, M. (1975) Consideration of the possibility that the slow step in protein denaturation reactions is due to *cis-trans* isomerism of proline residues. *Biochemistry* **14**, 4953-4963

Bryan, P. N. and Orban, J. (2010) Proteins that switch folds. *Curr. Opin. Struct. Biol.* **20**, 482-488

Bullough, P. A., Hughson, F. M., Skehel, J. J. and Wiley, D. C. (1994) Structure of influenza haemagglutinin at the pH of membrane fusion. *Nature* **371**, 37-43

Bychkova, V. E. and Ptitsyn, O. B. (1995). Folding intermediates are involved in genetic diseases? *FEBS Lett.* **359**, 6-8

Chan, H. S., Bromberg, S and Dill, K. A. (1995) Models of Cooperativity in protein folding. *Phil. Trans. Soc. London* **348**, 61-70

Clark, P. L. (2004) Protein folding in the cell: reshaping the folding funnel. *Trends Biochem. Sci.* **29**, 527-534

Creighton, T. (2000) Protein folding coupled to disulphide-bond formation in *Mechanisms of protein folding*, second edition (Pain, R. H., ed) pp. 250-278, Oxford University Press, Great Britain

Daggett, V. and Fersht, A. R. (2000) Transition states in protein folding in *Mechanisms of Protein Folding*, second edition (Pain, R. H., ed) pp. 175-211, Oxford University Press, Great Britain

Dill, K. A. and Chan, H. S. (1997) From Levinthal to pathways to funnels. *Nat. Struct. Biol.* **4**, 10-19

Dobson, C. M., Sali, A. and Karplus, M. (1998) Protein folding: a perspective from theory and experiment. *Angew. Chem. Int. Edit.* **37**, 868-893

Dobson, C. M. and Karplus, M. (1999) The fundamentals of protein folding: bringing together theory and experiment. *Curr. Opin. Struct. Biol.* **9**, 92-101

Dobson, C. M. (2003) Protein folding and disease: a view from the First Horizon Symposium. *Nature Rev. Drug Discov.* **2**, 154-160

Dobson, C. M. (2004) Principles of protein folding, misfolding and aggregation. *Sem. Cell Devel. Biol.* **15**, 3-16

Dulhunty, A., Gage, P., Curtis, S., Chelvanayagam, G. and Board, P. (2001) The glutathione transferase structural family includes a nuclear chloride channel and a ryanodine receptor calcium release channel modulator. *J. Biol. Chem.* **276**, 3319-3323

Duncan, R. R., Westwood, P. K., Boyd, A. and Ashley, R. H. (1997) Rat brain p64H1, expression of a new member of the p64 chloride channel protein family in endoplasmic reticulum. *J. Biol. Chem.* **272**, 23880-23886

Dunker, A. K., Lawson, J. D., Brown, C. J., Williams, R. M., Romero, P., Oh, J. S., Oldfield, C. J., Campen, A. M., Ratliff, C. M., Hipps, K. W., Ausio, J., Nissen, M. S., Reeves, R., Kang, C. H., Kissinger, C. R., Bailey, R. W., Griswold, M. D., Chiu, W., Garber, E. C. and Obradovic, A. (2001) Intrinsically disordered protein. *J. Mol. Graph. Model.* **19**, 26-59

Ecroyd, H. and Carver, J. A. (2008) Unraveling the mysteries of protein folding and misfolding. *IUBMB Life* **60**, 769-774

Edwards, J. C. (1999) A novel p64-related Cl-channel: subcellular distribution and nephron segment-specific expression. *Am. J. Physiol.* **276**, F398-F408

Eftink, M. R. and Maity, H. (2000) Use of optical spectroscopic methods to study the thermodynamic stability of proteins in *Spectrophotometry and Spectrofluorimetry: A Practical Approach*, second edition (Gore, M. G., ed) pp. 307-328, Oxford University Press, USA

Ellison, P. A. and Cavagnero, S. (2006) Role of unfolded state heterogeneity and en-route ruggedness in protein folding kinetics. *Protein Sci.* **15**, 564-582

Elter, A., Hartel, A., Sieben, C., Hertel, B., Fischer-Schliebs, E., Luttge, U., Moroni, A. and Thiel, G. (2007) A plant homolog of animal chloride intracellular channels (CLICs) generates an ion conductance in heterologous systems. *J. Biol. Chem.* **282**, 8786-8792

Evans, M. S., Clarke, T. F. and Clark, P. L. (2005) Conformations of cotranslational folding intermediates. *Protein Pept. Lett.* **12**, 189-195

Fanucchi, S., Adamson, R. J. and Dirr, H. W. (2008) Formation of an unfolding intermediate state of soluble chloride intracellular channel protein CLIC1 at acidic pH. *Biochemistry* **47**, 11674-11681

Fenton, J. W., Fasco, M. J. and Stackrow, A. B. (1977) Human thrombins. Production, evaluation, and properties of alpha-thrombin. *J. Biol. Chem.* **252**, 3587-3598

Fernandez-Salas, E., Sagar, M., Cheng, C., Yuspa, S. H. and Weinberg, W. C. (1999) p53 and tumour necrosis factor alpha regulate the expression of a mitochondrial chloride channel protein. *J. Biol. Chem.* **274**, 36488-36497

Fernandez-Salas, E., Suh, K. S., Speransky, V. V., Bowers, W. L., Levy, J. M., Adams, T., Pathak, K. R., Edwards, L. E., Hayes, D. D., Cheng, C., Steven, A. C., Weinberg, W. C. and Yuspa, S. H. (2002) mtCLIC/CLIC4, an organellar chloride channel protein is increased by DNA damage and participates in the apoptotic response to p53. *Mol. Cell Biol.* **22**, 3610-3620

Fersht, A. R. (1999) Structure and mechanism in protein science: a guide to enzyme catalysis and protein folding. WH Freeman, New York

Fersht, A. R. and Daggett, V. (2002) Protein folding and unfolding at atomic resolution. *Cell* **108**, 573-582

García-Sáez, A. J., Mingarro, I., Pérez-Payá, E. and Salgado, J. (2004) Membrane-insertion fragments of Bcl-xL, Bax and Bid. *Biochemistry* **43**, 10930-10943

Garel, J. R. and Baldwin, R. L. (1973) Both the fast and slow refolding reactions of ribonuclease A yield native enzyme. *Proc. Natl. Acad. Sci. USA* **70**, 3347-3351

Goodchild, S. C., Howell, M. W., Cordina, N. M., Littler, D. R., Breit, S. N., Curmi, P. M. and Brown, L. J. (2009) Oxidation promotes insertion of the CLIC1 chloride intracellular channel into the membrane. *Eur. Biophys. J.* **39**, 129-138

Greene, R. F. Jr. and Pace, C. N. (1974) Urea and guanidine hydrochloride denaturation of ribonuclease, lysozyme, α -chymotrypsin and β -lactoglobulin. *J. Biol. Chem.* **249**, 5388-5393

Harrop, S. J., De Maere, M. Z., Fairlie, W. D., Rezstsova, T., Valenzuela, S. M., Mazzanti, M., Tonini, R., Qiu, M. R., Jankova, L., Warton, K., Bauskin, A. R., Wu, W. M., Pankhurst, S., Campbell, T. J., Breit, S. N. and Curmi, P. M. G. (2001) Crystal structure of a soluble form of the intracellular chloride ion channel CLIC1 (NCC27) at 1.4Å resolution. *J. Biol. Chem.* **276**, 44993-45000

Hagerman, P. J. and Baldwin, R. L. (1976) A quantitative treatment of the kinetics of the folding transition of ribonuclease A. *Biochemistry* **15**, 1462-1473

Hartl, F. U., Hlodan, R. and Langer, T. (1994) Molecular chaperones in protein folding: the art of avoiding sticky situations. *Trends Biochem. Sci.* **19**, 20-25

Herczenik, E. and Gebbink, M. F. B. G. (2008) Molecular and cellular aspects of protein misfolding and disease. *FASEB J.* **22**, 2115-2133

Ikeguchi, M., Kuwajima, K., Mitani, M. and Sugai, S. (1986) Evidence for identity between the equilibrium unfolding intermediate and a transient folding intermediate: A comparative study of the folding reactions of α -lactalbumin and lysozyme. *Biochemistry* **25**, 6965-6972

- Jackson, S. E. (1998) How do small single-domain proteins fold? *Fold. Des.* **3**, R81-R91
- Jaenicke, R. and Rudolph, R. (1989) Folding proteins in *Protein structure: a practical approach*, first edition (Creighton, T. E. ed.), pp. 191-224, IRL Press, Oxford University Press, Oxford
- Kelly, S. M. and Price, N. C. (1997) The application of circular dichroism to studies of protein folding and unfolding. *Biochim. Biophys. Acta* **1338**, 161-185
- Kuwajima, K., Hiraoka, Y., Ikeguchi, M. and Sugai, S. (1985) Comparison of the transient folding intermediates in lysozyme and α -lactalbumin. *Biochemistry* **24**, 874-881
- Kuwajima, K. (1989) The molten globule state as a clue for understanding the folding and cooperativity of globular-protein structure. *Proteins* **6**, 87-103
- Kuwajima, K., Garvey, E. P., Finn, B. E. Mathews, C. R. and Sugai, S. (1991) Transient intermediates in the folding of dihydrofolate reductase as detected by far-ultraviolet circular dichroism spectroscopy. *Biochemistry* **30**, 7693-7703
- Kuwajima, K. and Arai, M. (2000) The molten globule state: the physical picture and biological significance in *Mechanisms of Protein Folding*, second edition (Pain, R. H., ed) pp. 138-174, Oxford University Press, Great Britain
- Laemmli, U. K. (1970) Cleavage of structural proteins during the assembly of the head of bacteriophage T4. *Nature* **227**, 680-685
- Laidman, J., Forse, G. J. and Yeates, T. O. (2006) Conformational change and assembly through edge β strands in transthyretin and other amyloid proteins. *Acc. Chem. Res.* **39**, 576-583
- Lakowicz, J. R. (2006) *Principles of fluorescence spectroscopy*. Plenum Press, New York
- Lepock, J. R., Ritchie, K. P., Kolios, M. C., Rodahl, A. M., Heinz, K. A. and Kruuv, J. (1992) Influence of transition rates and scan rate on kinetic simulations of differential scanning calorimetry profiles of reversible and irreversible protein denaturation. *Biochemistry* **31**, 12706-12712

- Lehtovaara, P. (1978) Anomalous migration of leghaemoglobin on sodium dodecyl sulphate/polyacrylamide-gel electrophoresis. *Biochem. J.* **169**, 251-253
- Linding, R., Schymkowitz, J., Rousseau, F., Diella, F. and Serrano, L. (2004) A comparative study of the relationship between protein structure and β -aggregation in globular and intrinsically disordered proteins. *J. Mol. Biol.* **342**, 345-353
- Littler, D. R., Harrop, S. J., Fairlie, W. D., Louise J. Brown, L. J., Pankhurst, G. J., Pankhurst, S., DeMaere, M. Z., Campbell, T. J., Bauskin, A. R., Tonini, R., Mazzanti, M., Breit, S. N. and Curmi, P. M. G. (2004) The intracellular chloride ion channel protein CLIC1 undergoes a redox-controlled structural transition. *J. Biol. Chem.* **279**, 9298-9305
- Littler, D. R., Harrop, S. J., Brown, L. J., Pankhurst, G. J., Mynott, A. V., Luciani, P., Mandyam, R. A., Mazzanti, M., Tanda, S., Berryman, M. A., Breit, S. N. and Curmi, P. M. G. (2008) Comparison of vertebrate and invertebrate CLIC proteins: the crystal structures of *Caenorhabditis elegans* EXC-4 and *Drosophila melanogaster* DmCLIC. *Proteins* **71**, 364-378.
- Littler, D. R., Harrop, S. J., Goodchild, S. C., Phang, J. M., Mynott, A. V., Jiang, L., Valenzuela, S. M., Mazzanti, M., Brown, L. J., Breit, S. N. and Curmi, P. M. G. (2010) The enigma of the CLIC proteins: Ion channels, redox proteins, enzymes, scaffolding proteins? *FEBS. Lett.* **584**, 2093-2101
- Luo, X., Tang, Z., Xia, G., Wassmann, K., Matsumoto, T., Rizo, J. and Yu, H. (2004) The Mad2 spindle checkpoint protein has two distinct natively folded states. *Nat. Struct. Mol. Biol.* **11**, 338-345
- Makowski, G. S. and Ramsby, M. L. (1997) Protein molecular weight determination by sodium dodecyl sulfate polyacrylamide gel electrophoresis in *Protein structure, a practical approach*, second edition (Creighton, T.E. ed.), pp 3-4, Oxford University Press, UK
- Mamathambika, B. S. and Bardwell, J. C. (2008) Disulfide-linked protein folding pathways. *Annu. Rev. Cell Dev. Biol.* **24**, 211-235
- Matouschek, A. (2003) Protein unfolding - an important process in vivo? *Curr. Opin. Struct. Biol.* **13**, 98-109

- Matulis, D. and Lovrien, R. E. (1998) 1-Anilino-8-Naphthalene sulfonate anion-protein binding depends primarily on ion pair formation. *Biophys. J.* **74**, 422-429
- McLaughlin, S. (1989) The electrostatic properties of membranes. *Annu. Rev. Biophys. Biophys. Chem.* **18**, 113-136
- Meredith, S. C. (2005) Protein denaturation and aggregation: cellular responses to denatured and aggregated proteins. *Ann. N. Y. Acad. Sci.* **1066**, 181-221
- Merrill, A. R., Cohen, F. S. and Cramer, W. A. (1990) On the nature of the structural change of the colicin E1 channel peptide necessary for its translocation-competent state. *Biochemistry* **29**, 5829-5836
- Merrill, A. R., Palmer, L. R. and Szabo, A. G. (1993) Acrylamide quenching of the intrinsic fluorescence of tryptophan residues genetically engineered into the soluble colicin E1 channel peptide. Structural characterization of the insertion-competent state. *Biochemistry* **32**, 6974-6981
- Milton, R. H., Abeti, R., Averaimo, S., DeBiasi, S., Vitellaro, L., Jiang, L., Curmi, P. M., Breit, S. N., Duchen, M. R. and Mazzanti, M. (2008) CLIC1 function is required for beta-amyloid-induced generation of reactive oxygen species by microglia. *J. Neurosci.* **28**, 11488-11499
- Mottonen, J., Strand, A., Symersky, J., Sweet, R. M., Danley, D. E., Geoghegan, K. F., Gerard, R. D. and Goldsmith, E. J. (1992) Structural basis of latency in plasminogen activator inhibitor-1. *Nature* **355**, 270-273
- Murzin, A. G. (2008) Metamorphic proteins. *Science* **320**, 1725-1726
- Musse, A. A. and Merrill, A. R. (2003) The molecular basis for the pH-activation mechanism in the channel-forming bacterial colicin E1. *J. Biol. Chem.* **278**, 24491-24499
- Myers, J. K., Pace, C. N. and Scholtz, J. M. (1995) Denaturant *m* values and heat capacity changes: Relation to changes in accessible surface areas of protein unfolding. *Prot. Sci.* **4**, 2138-2148

- Novarino, G., Fabrizi, C., Tonini, R., Denti, M. A., Malchiodi-Albedi, F., Lauro, G. M., Sacchetti, B., Paradisi, S., Ferroni, A., Curmi, P. M., Breit, S. N. and Mazzanti, M. (2004) Involvement of the intracellular ion channel CLIC1 in microglia-mediated beta-amyloid-induced neurotoxicity. *J. Neurosci.* **24**, 5322-5330
- Ohgushi, M. and Wada, A. (1983) ‘‘Molten-globule state’’: A compact form of globular proteins with mobile side-chains. *FEBS Lett.* **164**, 21-24
- Onuchic, J. N., Socci, N. D., Luthey-Schulten, Z. and Wolynes, P. G. (1996) Protein folding funnels: the nature of the transition state ensemble. *Fold Des.* **1**, 441-450
- Onuchic, J. N., Luthey-Schulten, Z. and Wolynes, P. G. (1997) Theory of protein folding: the energy landscape perspective. *Annu. Rev. Phys. Chem.* **48**, 545-600
- Onuchic, J. N. and Wolynes, P. G. (2004) Theory of protein folding. *Curr. Opin. Struct. Biol.* **14**, 70-75
- Pace, C. N. (1986) Determination and analysis of urea and guanidine hydrochloride denaturation curves. *Methods Enzymol.* **131**, 266-280
- Pace, C. N., Shirley, B. A. and Thomson, J. A. (1989) Measuring the conformational stability of a protein in *Protein Structure: a practical approach*, first edition (Creighton, T. E. ed.), pp. 311-330, IRL Press, Oxford University Press, Oxford
- Parker, M. W. and Pattus, F. (1993) Rendering a membrane protein soluble in water: a common packing motif in bacterial protein toxins. *Trends Biochem. Sci.* **18**, 391-395
- Parker, M. W. and Feil, S. C. (2005) Pore-forming protein toxin: from structure to function. *Prog. Biophys. Mol. Biol.* **88**, 91-142
- Perkins, S. J. (1986) Protein volumes and hydration effects. *Eur. J. Biochem.* **157**, 169-180
- Ptitsyn, O. B. (1995) Molten globule and protein folding. *Adv. Protein Chem.* **47**, 83-229
- Ptitsyn, O. B., Bychkova, V. E. and Uversky, V. N. (1995). Kinetic and equilibrium folding intermediates. *Phil. Trans. R. Soc. B* **348**, 35-41

Qian, Z., Okuhara, D., Abe, M. K. and Rosner, M. R. (1999) Molecular cloning and characterization of a mitogen-activated protein kinase-associated intracellular chloride channel. *J. Biol. Chem.* **274**, 1621-1627

Rami B. R. and Udgaonkar, J. B. (2002) Mechanism of formation of a productive molten globule form of barstar. *Biochemistry* **41**, 1710-1716

Reed, R., Holmes, D., Weyers, J. and Jones, A. (2003) Practical skills in biomolecular sciences (2nd ed.), pp. 131 Pearson Education Ltd., UK

Roder, H., Elöve, G. A. and Shastry, M. C. R. (2000) Early stages of protein folding in *Mechanisms of protein folding*, second edition (Pain, R. H., ed.) pp. 65-104, Oxford University Press, Great Britain

Royer, C. A., Mann, C. J. and Matthews, R. (1993) Resolution of the fluorescence equilibrium unfolding profile of trp aporepressor using single tryptophan mutants. *Protein Sci.* **2**, 1844-1852

Rumbley, J., Hoang, L., Mayne, L. and Englander, S. W. (2001) An amino acid code for protein folding. *Proc. Natl. Acad. Sci.* **98**, 105-112

Rumfeldt, J. A., Galvagnion, C., Vassall, K. A. and Meiering, E. M. (2008) Conformational stability and folding mechanisms of dimeric proteins. *Prog. Biophys. Mol. Biol.* **98**, 61-84

Sakai, H. and Tsukihara, T. (1998) Structures of membrane proteins determined at atomic resolution. *J. Biochem.* **124**, 1051-1059

Santucci, R., Sinibaldi, F. and Fiorucci, L. (2008) Protein folding, unfolding and misfolding: role played by intermediate states. *Mini Rev. Med. Chem.* **8**, 57-62

Schendel, S. L. and Cramer, W. A. (1994) On the nature of the unfolded intermediate in the in vitro transition of the colicin E1 channel domain from the aqueous to the membrane phase. *Protein Sci.* **3**, 2272-2279

Schendel, S. L., Xie, Z., Montal, M. O., Matsyama, S., Montal, M. and Reed, J. C. (1997) Channel formation by antiapoptotic protein Bcl-2. *Proc. Natl. Acad. Sci.* **94**, 5113-5118

- Schlesinger, P. H., Blair, H. C., Teitelbaum, S. T. and Edwards, J. C. (1997) Characterization of the osteoclast ruffled border chloride channel and its role in bone resorption. *J. Biol. Chem.* **272**, 18636-18643
- Schmid, F. X. (1986) Fast-folding and slow-folding forms of unfolded proteins. *Methods Enzymol.* **131**, 70-82
- Semisotnov, G. V., Rodionova, N. A., Razgulyaev, O. I., Uversky, V. N., Gripas, A. F. and Gilmanshin, R. I. (1991) Study of the “molten globule” intermediate state in protein folding by a hydrophobic fluorescence probe. *Biopolymers* **31**, 119-128.
- Shao, S. and Hegde, R. S. (2010) Membrane protein insertion at the endoplasmic reticulum. *Annu. Rev. Cell Dev. Biol.* 2010 Oct 29. [Epub ahead of print]
- Singh, H. and Ashley, R. H. (2006) Redox regulation of CLIC1 by cysteine residues associated with the putative channel pore. *Biophys. J.* **90**, 1628-1638
- Singh, H., Cousin, M. A. and Ashley, R. H. (2007) Functional reconstitution of mammalian ‘chloride intracellular channels’ CLIC1, CLIC4 and CLIC5 reveals differential regulation by cytoskeletal actin. *FEBS J.* **274**, 6306-6316
- Singh, H. (2010) Two decades with dimorphic Chloride Intracellular Channels (CLICs). *FEBS Lett.* **584**, 2112-2121
- Steer, B. A. and Merrill, A. R. (1997) Characterization of an unfolding intermediate and kinetic analysis of guanidine hydrochloride-induced denaturation of the colicin E1 channel peptide. *Biochemistry* **36**, 3037-3046
- Stix, B., Kahne, T., Sletten, K., Raynes, J., Roessner, A. and Rocken, C. (2001) Proteolysis of AA amyloid fibril proteins by matrix metalloproteinases-1, -2, and -3. *Am. J. Pathol.* **159**, 561-570
- Stoychev, S. H., Nathaniel, C., Fanucchi, S., Brock, M., Li, S., Asmus, K., Woods, V. L. Jr. and Dirr, H. W. (2009) Structural dynamics of soluble chloride intracellular channel protein CLIC1 examined by amide hydrogen-deuterium exchange mass spectrometry. *Biochemistry* **48**, 8413-8421

Stryer, L. (1965) The interaction of a naphthalene dye with apomyoglobin and apohemoglobin. A fluorescent probe of nonpolar binding sites. *J. Mol. Biol.* **13**, 482-495

Suh, K. S., Mutoh, M., Nagashima, K., Fernandez-Salas, E., Edwards, L. E., Hayes, D. D., Crutchley, J. M., Marin, K. G., Dumont, R. A., Levy, J. M., Cheng, C., Garfield, S. and Yuspa, S. H. (2004) The organellular chloride channel protein CLIC4/mtCLIC translocates to the nucleus in response to cellular stress and accelerates apoptosis. *J. Biol. Chem.* **279**, 4632-4641

Suh, K. S., Mutoh, M., Gerdes, M. and Yuspa, S. H. (2005) CLIC4, an intracellular chloride channel protein, is a novel molecular target for cancer therapy. *J. Investig. Dermatol. Symp. Proc.* **10**, 105-109

Suh, K. S., Mutoh, M., Mutoh, T., Li, L., Ryscavage, A., Crutchley, J. M., Dumont, R. A., Cheng, C. and Yuspa, S. H. (2007) CLIC4 mediates and is required for Ca²⁺-induced keratinocyte differentiation. *J. Cell Sci.* **120**, 2631-2640

Szilágyi, A., Kardos, J., Osvath, Sz., Barna, L. and Zavodszky, P. (2007) Protein folding in *Handbook of Neurochemistry and Molecular Neurobiology* (Lajtha, A. and Banik, N. ed.) volume 7, pp. 303-344, Springer

Tanford, C. (1970) Protein denaturation: Part C. Theoretical models for the mechanism of denaturation. *Adv. Protein Chem.* **24**, 1-95

Thuduppathy, G. R. and Hill, R. B. (2005) Acid destabilisation of the solution conformation of Bcl-XL does not drive its pH-dependent insertion into membranes. *Protein Sci.* **15**, 1-10

Thuduppathy, G. R., Craig, J. W., Kholodenko, V., Schon, A. and Hill, B. (2006) Evidence that membrane insertion of the cytosolic domain of Bcl-XL is governed by an electrostatic mechanism. *J. Mol. Biol.* **359**, 1045-1058

Tonini, R., Ferroni, A., Valenzuela, S. M., Warton, K., Campbell, T. J., Breit, S. N. and Mazzanti, M. (2000) Functional characterization of the NCC27 nuclear protein in stable transfected CHO-K1 cells. *FASEB J.* **14**, 1171-1178

Tuinstra, R. L., Peterson, F. C., Kutlesa, S., Elgin, E. S., Kron, M. A. and Volkman, B. F. (2008) Interconversion between two unrelated protein folds in the lymphotactin native state. *Proc. Natl. Acad. Sci. USA* **105**, 5057-5062

- Tulk, B. M. and Edwards, J. C. (1998) NCC27, a homolog of intracellular Cl channel p64, is expressed in brush border of renal proximal tubule. *Am. J. Physiol.* **274**, F1140-F1149
- Tulk B. M., Schlesinger, P. H. and Edwards, J. C. (2000) CLIC1 functions as a chloride channel when expressed and purified from bacteria. *J. Biol. Chem.* **275**, 26986-26993
- Tulk, B. M., Kapadia, S. and Edwards, J. C. (2002) CLIC1 inserts from the aqueous phase into phospholipid membranes, where it functions as an anion channel. *Am. J. Physiol. Cell Physiol.* **282**, 1103-1112
- Tung, J. J., Hobert, O., Berryman, M. and Kitajewski, J. (2009) Chloride intracellular channel 4 is involved in endothelial proliferation and morphogenesis *in vitro*. *Angiogenesis* **12**, 209-220.
- Tung, J. J. and Kitajewski, J. (2010) Chloride intracellular channel 1 functions in endothelial cell growth and migration. *J. Angiogenes. Res.* **2**, 23
- Udgaonkar, J. B. (2008) Multiple routes and structural heterogeneity in Protein Folding. *Annu. Rev. Biophys.* **37**, 489-510
- Ulmasov, B., Bruno, J., Woost, P. G., and Edwards, J. C. (2007) Tissue and subcellular distribution of CLIC1. *BMC Cell Biol.* **8**, 8
- Utiyama, H. and Baldwin, R. (1986) Kinetics mechanisms of protein folding. *Methods Enzymol.* **131**, 51-70
- Uversky, V. N. (2002) What does it mean to be natively unfolded? *Eur. J. Biochem.* **269**, 2-12
- Uversky, V. N. and Fink, A. L. (2004) Conformational constraints for amyloid fibrillation: the importance of being unfolded. *Biochim. Biophys. Acta* **1698**, 131-153.
- Valenzuela, S. M., Martin, D. K., Por, S. B., Robbins, J. M., Warton, K., Bootcov, M. R., Schofield, P. R., Campbell, T. J. and Breit, S. N. (1997) Molecular cloning and expression of a chloride channel of cell nuclei. *J. Biol. Chem.* **272**, 12575-12582

- Valenzuela, S. M., Mazzanti, M., Tonini, R., Ru, Q. M., Warton, K., Musgrove, E., Campbell, T. J. and Breit, S. N. (2000) The nuclear chloride ion channel NCC27 is involved in regulation of the cell cycle. *J. Physiol.* **529**, 541-552
- Van der Goot, F. G., González-Mañas, J. M., Lakey, J. H. and Pattus, F. (1991) A “molten-globule” membrane-insertion intermediate of the pore-forming domain of colicin A. *Nature* **354**, 408-410
- Wallace, L. A. and Matthews, C. R. (2002) Sequential vs. parallel protein-folding mechanisms: experimental tests for complex folding reactions. *Biophys. Chem.* **101-102**, 113-131
- Walters, J., Milam, S. L. and Clark A. C. (2009) Practical approaches to protein folding and assembly: spectroscopic strategies in thermodynamics and kinetics. *Methods Enzymol.* **455**, 1-39
- Warton, K., Tonini, R., Fairlie, W. D. and Matthews, J. M. (2002) Recombinant CLIC1 (NCC27) assembles in lipid bilayers via a pH-dependent two-state process to form chloride ion channels with identical characteristics to those observed in Chinese hamster ovary cells expressing CLIC1. *J. Biol. Chem.* **277**, 26003-26011
- Wilce, M. C., and Parker, M. W. (1994) Structure and function of glutathione *S*-transferases. *Biochim. Biophys. Acta* **1205**, 1-18
- Wildegger, G. and Kiefhaber, T. (1997) Three-state model for lysozyme folding: triangular folding mechanism with an energetically trapped intermediate. *J. Mol. Biol.* **270**, 294-304.
- Woody, R. W. (1995) Circular dichroism. *Methods Enzymol.* **246**, 34-71
- Wright, P. E. and Dyson, H. J. (1999) Intrinsically unstructured proteins: re-assessing the protein structure-function paradigm. *J. Mol. Biol.* **293**, 321-331
- Zakharov, S. D. and Cramer, W. A. (2002) Colicin crystal structures: pathways and mechanisms for colicin insertion into membranes. *Biochim. Biophys. Acta* **1565**, 333-346
- Zimmerman, S. S. and Scheraga, H. A. (1976) Stability of *cis*, *trans*, and nonplanar peptide groups. *Macromolecules* **9**, 408-416

Zitzewitz, J. A., Bilsel, O., Luo, J., Jones, B. E. and Matthews, C. R. (1995) Probing the folding mechanism of a leucine zipper peptide by stopped-flow circular dichroism spectroscopy. *Biochemistry* **34**, 12812-12819